The Abdus Salam
International Centre for Theoretical Physics

United Nations
Educational, Scientific and
Cultural Organization

IAEA
International Atomic Energy Agency

2132-8

Winter College on Optics and Energy

8 - 19 February 2010

Dye-SensitizedSolarCells: fundamentals

A. Li Bassi
CNST-IIT@PoliMI
Milano
Italy

POLITECNICO DI MILANO

Dye-Sensitized Solar Cells: fundamentals

Andrea Li Bassi
CNST (Center for NanoScience and Technology) - IIT@PoliMI
Department of Energy
POLITECNICO DI MILANO

andrea.libassi@polimi.it
www.nanolab.polimi.it

Excitonic solar cells (ESC)

- **Organic solar cells (e.g. bulk heterojunctions, BHJ)**
- **Hybrid solar cells**
- **Dye-sensitized solar cells**
- **QD-sensitized solar cells**

B.A. Gregg, MRS Bull 30, 20 (2005)

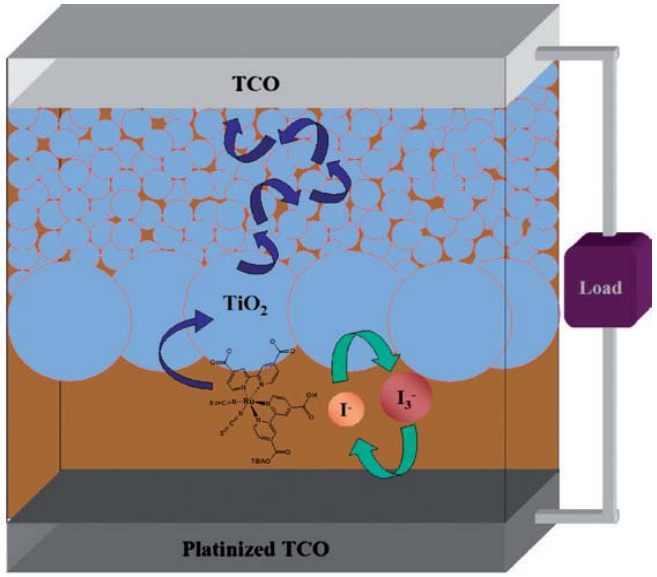

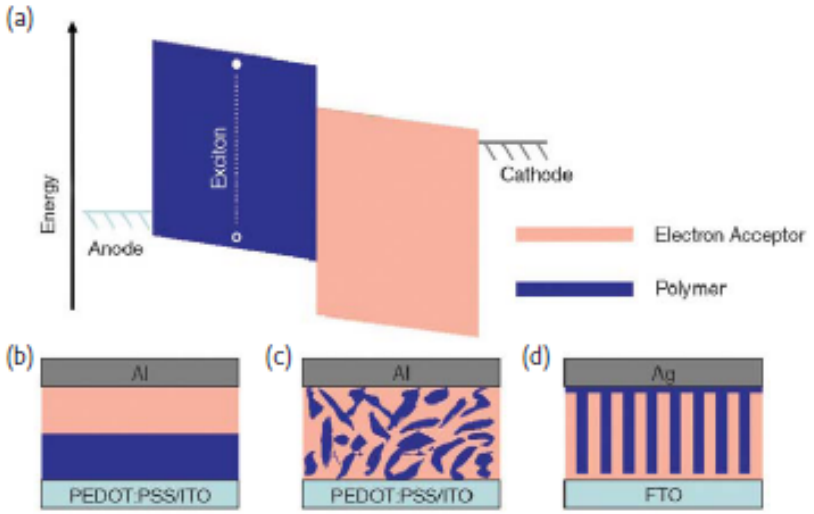

A.C. Meyer et al., Mater. Today 10, 28 (2007)

Excitonic solar cells (ESC)

p-n junctions PV

- light absorption
- creation of free e^-
- charges accelerated by in-built electric field in the junction
- photovoltage = difference in quasi-Fermi levels of *n*- and *p*-type regions

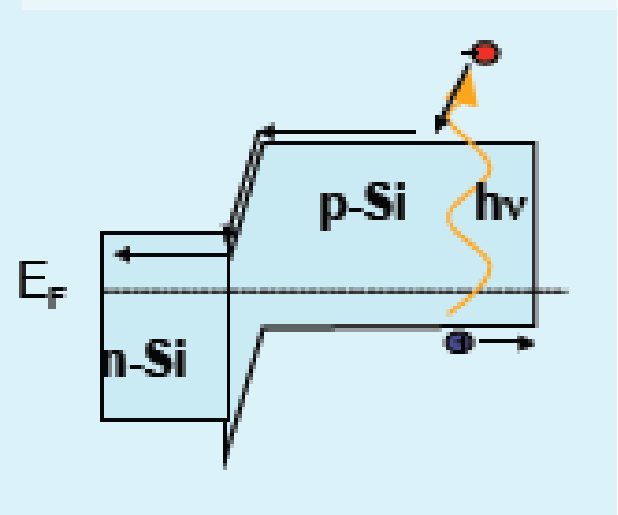

ESC

- light absorption
- generation of a transiently localized excited state (exciton), i.e. e^- in C.B. (or LUMO), h^+ in V.B. (or HOMO);
- system anchored to material with lower C.B. (LUMO)
- exciton dissociation into mobile carriers at the interface

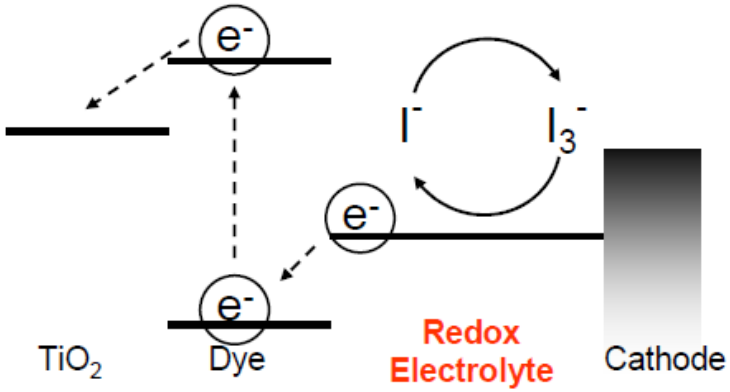

Excitonic solar cells (ESC)

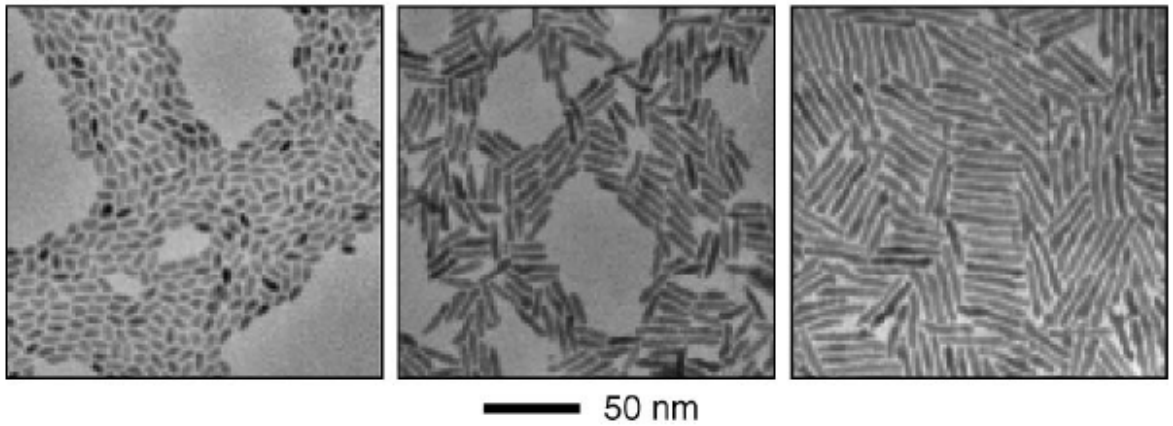

Hybrid organic-nanocrystals (e.g. CdSe)

D.J. Milliron, I. Gur, A.P. Alivisatos, MRS Bull 30, 41 (2005)

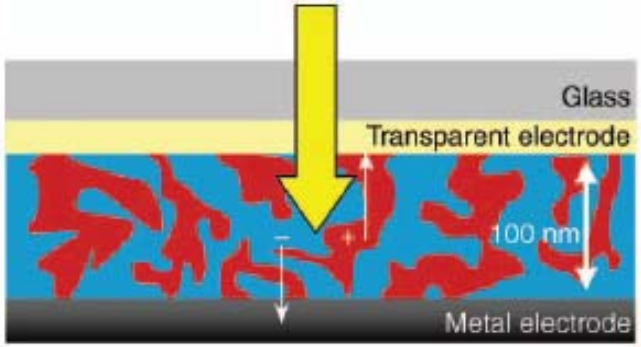

Polymer-fullerene bulk heterojunction (BHJ)

R.A.J. Janssen, MRS Bull 30, 33 (2005)

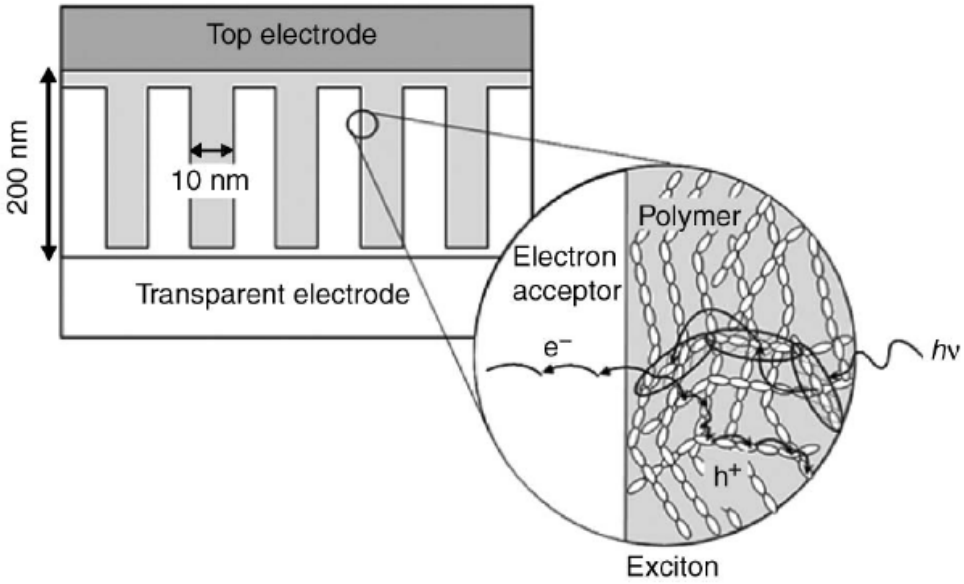

Ordered organic-inorganic BHJ

K.M. Coakley, MRS Bull 30, 37 (2005)

Dye-sensitized solar cells (DSSC): principle

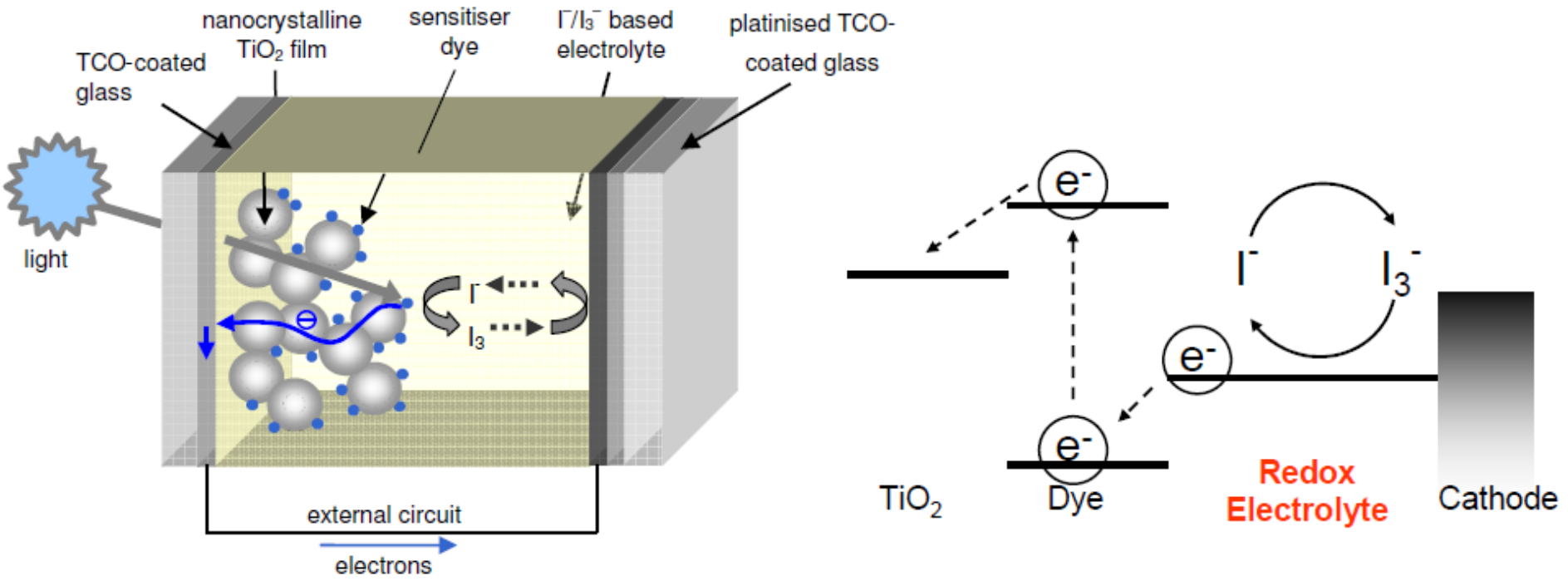

M. Graetzel and J.R. Durrant, 'Dye-sensitized mesoscopic solar cells', in 'Nanostructured and photoelectrochemical systems for solar photon conversion', ed. M.D. Archer, A.J. Nozik, World Scientific 2008

Exciton generation separated from charge transport

History

1991: O'Regan-Gratzel, 7% efficiency for a Dye-Sensitized Solar Cell (DSSC) based on nanocrystalline TiO_2

B. O'Regan and M. Gratzel, Nature, 1991, 353, 737–740

1993: reached efficiency of 10%

M. K. Nazeeruddin et al., J. Am. Chem. Soc., 1993, 115, 6382–6390

Today: record refficency > 11%

e.g. Y. Chiba, A. Islam, Y. Watanabe, R. Komiya, N. Koide and L. Y. Han, Jpn. J. Appl. Phys., Part 2, 2006, 45, L638–L640

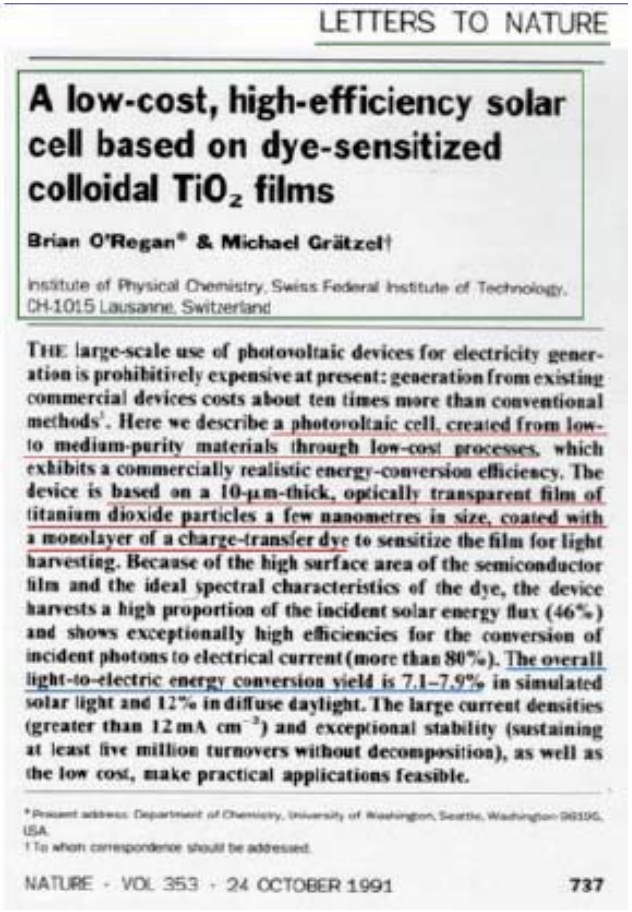

LETTERS TO NATURE

A low-cost, high-efficiency solar cell based on dye-sensitized colloidal TiO_2 films

Brian O'Regan* & Michael Grätzel†

Institute of Physical Chemistry, Swiss Federal Institute of Technology, CH-1015 Lausanne, Switzerland

THE large-scale use of photovoltaic devices for electricity generation is prohibitively expensive at present: generation from existing commercial devices costs about ten times more than conventional methods[1]. Here we describe a photovoltaic cell, created from low- to medium-purity materials through low-cost processes, which exhibits a commercially realistic energy-conversion efficiency. The device is based on a 10-μm-thick, optically transparent film of titanium dioxide particles a few nanometres in size, coated with a monolayer of a charge-transfer dye to sensitize the film for light harvesting. Because of the high surface area of the semiconductor film and the ideal spectral characteristics of the dye, the device harvests a high proportion of the incident solar energy flux (46%) and shows exceptionally high efficiencies for the conversion of incident photons to electrical current (more than 80%). The overall light-to-electric energy conversion yield is 7.1–7.9% in simulated solar light and 12% in diffuse daylight. The large current densities (greater than 12 mA cm^{-2}) and exceptional stability (sustaining at least five million turnovers without decomposition), as well as the low cost, make practical applications feasible.

* Present address: Department of Chemistry, University of Washington, Seattle, Washington 98195, USA.
† To whom correspondence should be addressed.

Unique characteristics

- High energy conversion efficiency (> 10%)
- Low-cost fabrication (estimated 0.60 $/W at 10%)
- Supply of materials
- Potential for colorful consumer products (varying the dye, for PV integrated buildings, windowpanes; plastic substrates if TiO_2 preparation at < 250°C)
- Low environmental pollution (except for organic solvents in electrolyte, see development of solid-state electrolytes)
- Good recyclability

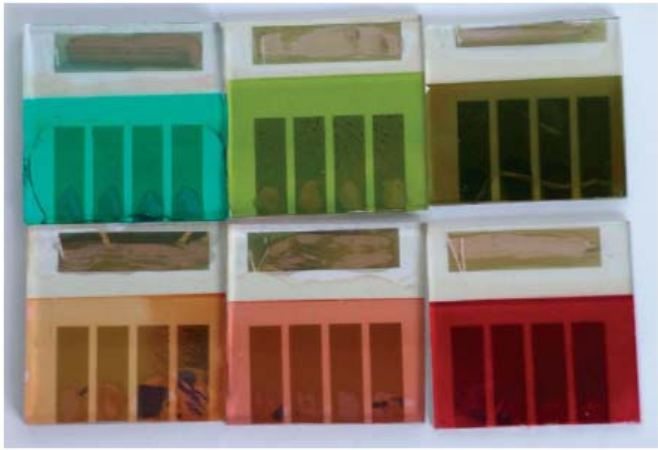

DSSC characterization

I-V measurements

Standard: 25 °C, 1000 W/m^2, AM1.5 spectral power distribution

Main parameters: V_{OC}, J_{SC}, *ff* , η , IPCE

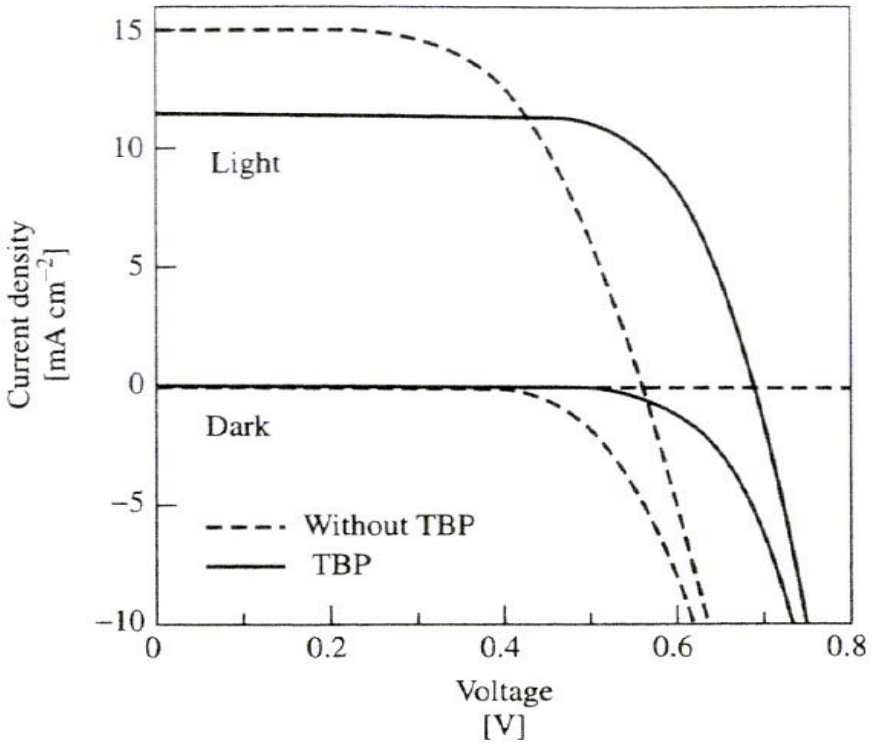

I-V curve for solar cells

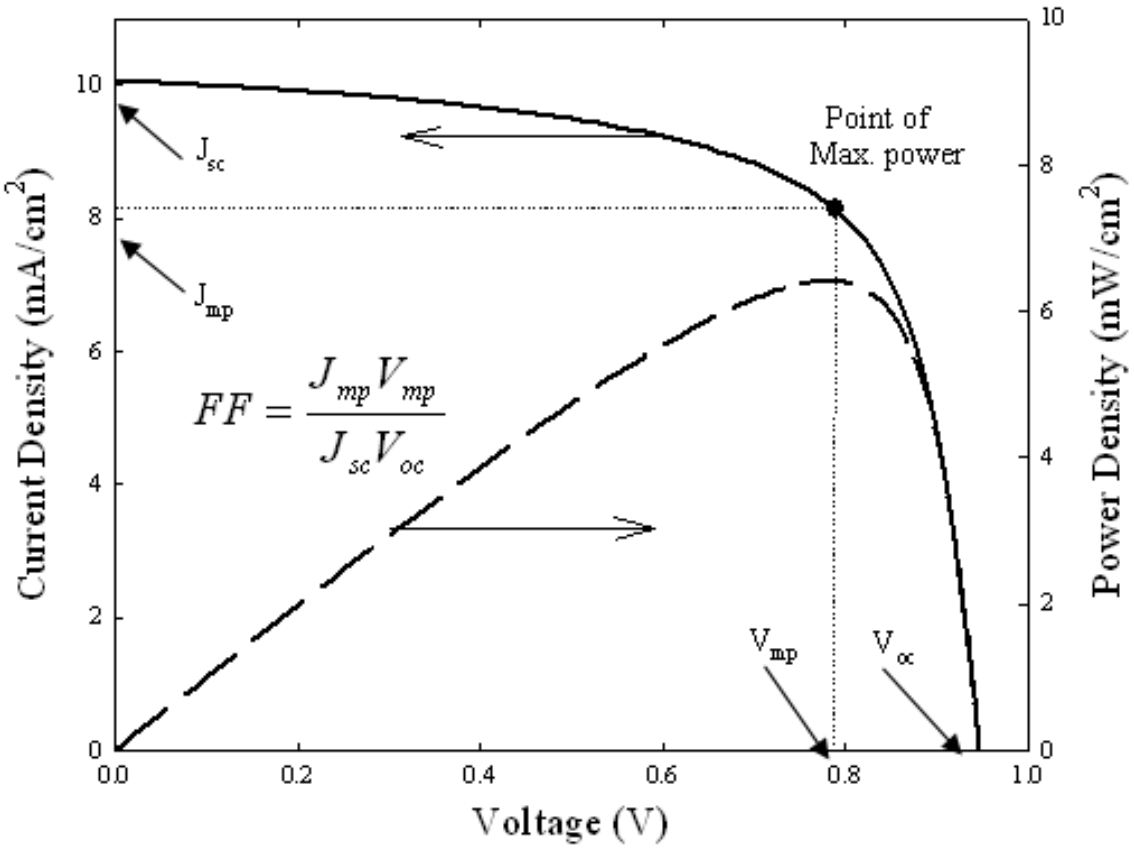

PV performance

Solar energy-to-electricity conversion efficiency: $\eta = \frac{J_{SC} \times V_{OC} \times ff \times 100}{I_0}$

$$ff = \frac{I_m V_m}{I_{SC} V_{OC}} = \frac{P_{\max}}{I_{SC} V_{OC}}$$

I_0: photon flux (about 100 mW/cm^2 for AM1.5)

Typical for DSSC: J_{SC} = 20 mA/cm^2; V_{OC} > 0.7 V, *ff* = 0.7

ff: depends on squareness of *J-V* characteristic.

Ideal cell: high resistance to paraller currents (charge recombination, e$^-$ back transfer); low series resistances (FTO, FTO-TiO_2 junction)

PV performance

Incident photon-to-current conversion efficiency (IPCE)

$$\mathrm{IPCE}\,[\%] = \frac{1240\,[eV\cdot nm]\times J_{SC}\,[\mu A\cdot cm^{-2}]}{\lambda\,[nm]\times\Phi\,[\mu W\cdot cm^{-2}]}\times 100$$

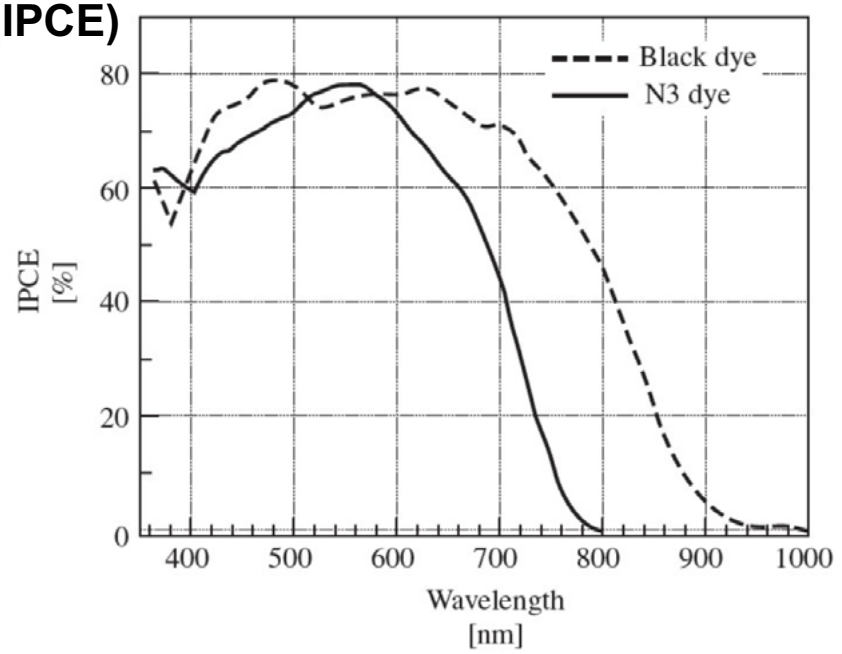

J_{SC}: short circuit photocurrent density for monochromatic irradiation

Φ: monochromatic light intensity

N3: IPCE up to 80% at 550 nm and > 70% at 400-650 nm

→ considering losses due to light reflection and absorption by TCO, internal photon-to-current conversion efficiency is 90-100%

$$\mathrm{IPCE} = \mathrm{LHE}\cdot\phi_{\mathrm{inj}}\cdot\eta_C \qquad (\mathrm{LHE} = 1 - \mathrm{T})$$

LHE: light harvesting efficiency

Mechanism

1. Ru complex photosensitizers absorb incident photon flux

2. Dye molecules are excited form ground state (S) to excited state (S*) due to MLCT (metal to ligand charge transfer) transition

3. e^- injection in TiO_2 C.B., photosensitizer oxidation

$$S + h\nu \rightarrow S^*$$

$$S^* \rightarrow S^+ + e^- (TiO_2)$$

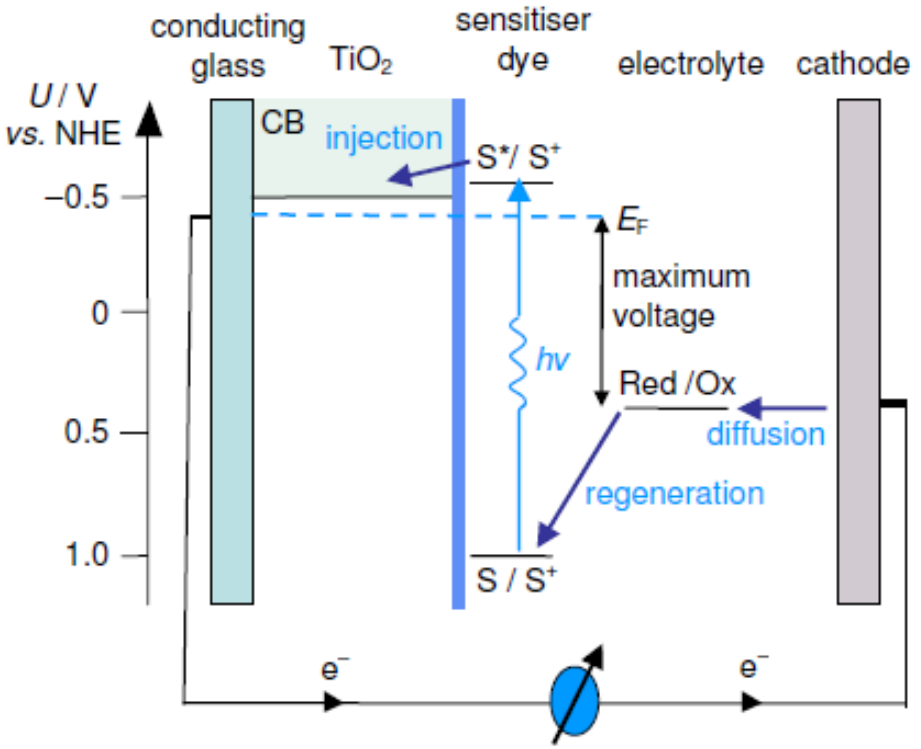

Mechanism

4. Diffusion transport of e^- through TiO_2 to back contact (TCO)

5. S^+ reduced by e^- from I^- ion redox mediator and I^- oxidized to I_3^-

$$S^+ + e^- \rightarrow S$$

6. Redox mediator I_3^- diffuses towards counter electrode and re-reduces to I^-

$$I_3^- + 2e^- \rightarrow 3I^-$$

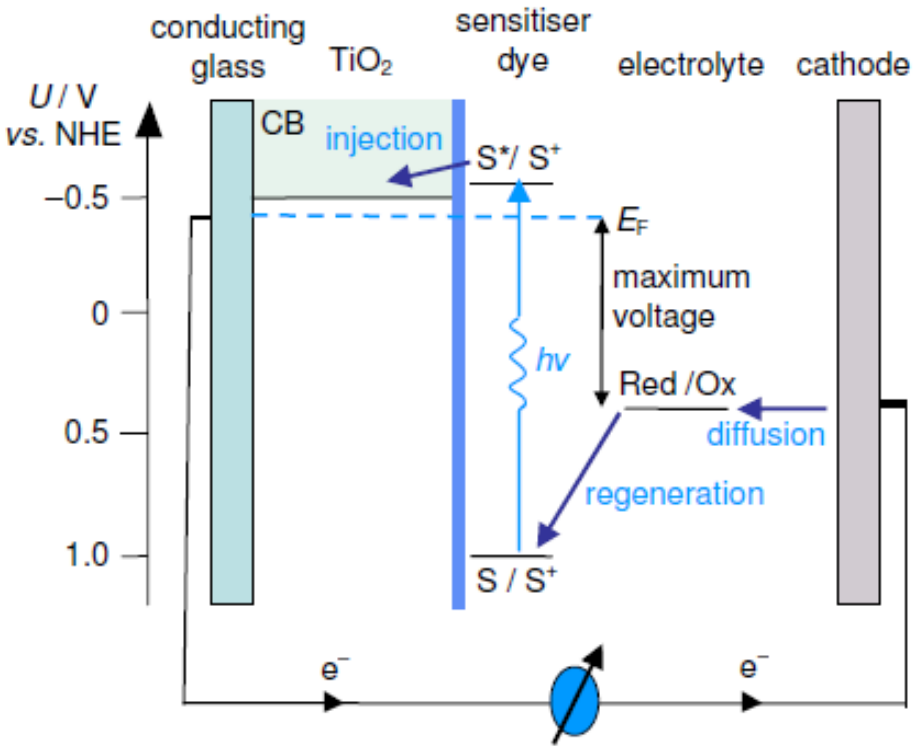

Electric power generated without permanent chemical transformation

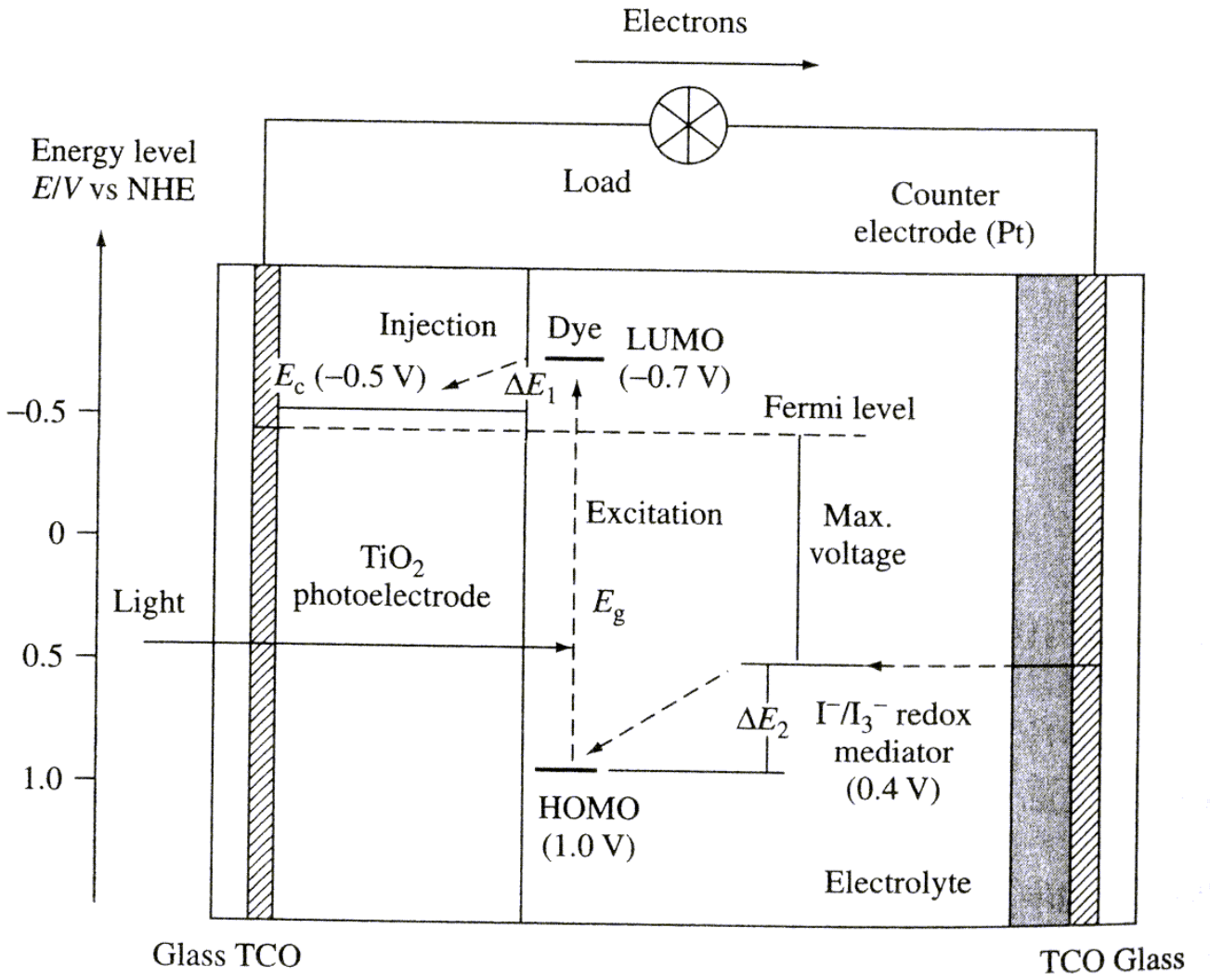
Electrons
Load
Counter electrode (Pt)
Energy level E/V vs NHE
−0.5
0
0.5
1.0
Injection
Dye
LUMO (−0.7 V)
E_c (−0.5 V)
ΔE_1
Fermi level
Excitation
Max. voltage
TiO_2 photoelectrode
Light
E_g
ΔE_2
I^-/I_3^- redox mediator (0.4 V)
HOMO (1.0 V)
Electrolyte
Glass TCO
TCO Glass

Mechanism

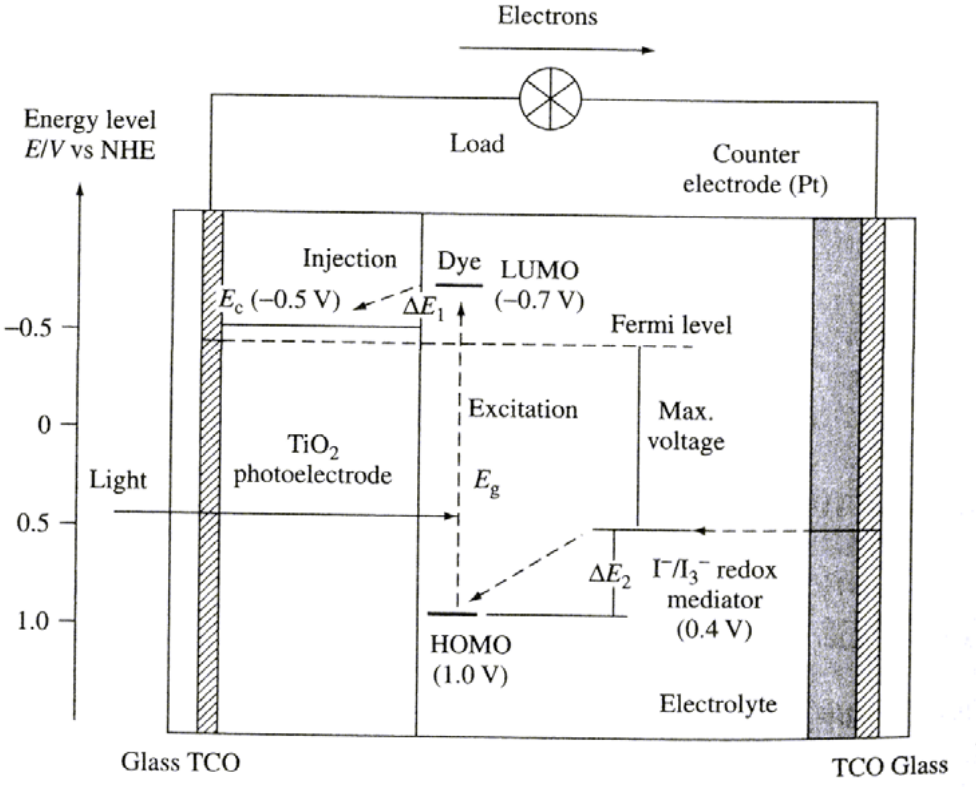

- **HOMO-LUMO dye**
- **quasi Fermi level E_F of TiO_2 (near C.B.):**
  - 0.5 V vs. NHE
- **I^-/I_3^- redox potential: 0.4 V vs. NHE**

Photocurrent determined by LUMO-HOMO energy difference

LUMO - C.B. > 0 (~ 200 meV): injection (need substantial electronic coupling)

[I^-/I_3^- redox] – HOMO > 0 (~ 200 meV): dye reduction

Voltage: TiO_2 E_F – I^-/I_3^- redox potential: max voltage ~ 0.9 V

- Depends on electrolyte because E_F depends on electrolyte components

Mechanism

In contrast with conventional *p-n* type PV cells:

- DSSC does not involve charge-recombination between e^- and h^+ (no holes in the semiconductor)

- Majority carrier device

- Charge transport in TiO_2 separated from photon absorption site

→ effective charge separation expected

• conventional *p-n* type PV cells:

junction and equilibrium between charge carriers leads to space charge formation → photogenerated charges separated by electric field in space charge layer

• DSSC: small particles

→ charge separation due to dipole formed upon adsorption of H^+ or Li^+ (from dye or electrolyte) on TiO_2 surface

→ charge separation and reduced recombination [A. Zaban et al., J. Phys. Chem. B 102, 452 (1998)]

Light harvestng: effect of incresed TiO_2 surface area

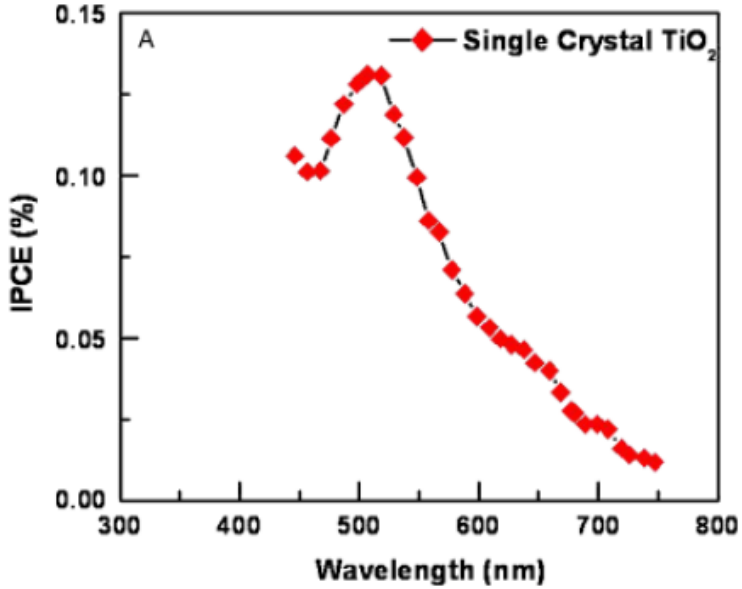

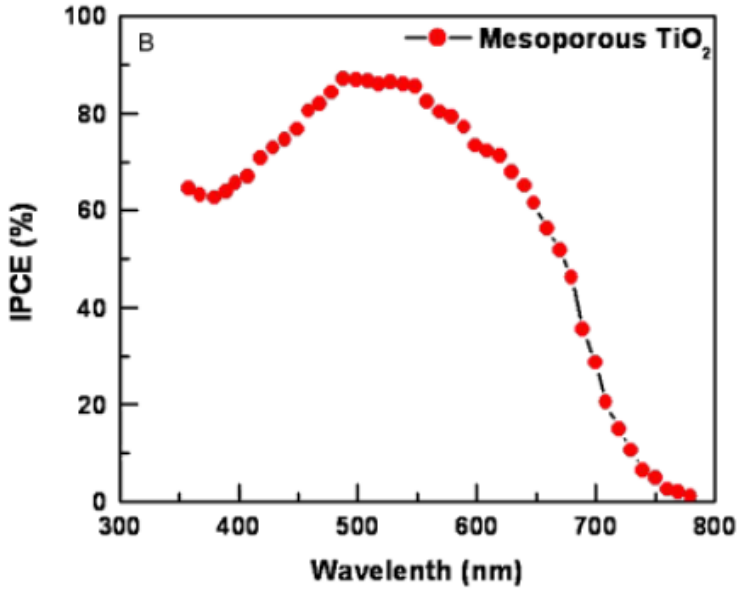

M. Graetzel, Nature 414, 339 (2001)

Materials

TiO_2 photoelectrode

- Si, GaAs, InP, CdS decompose under irradiation in solution (photocorrosion)

- oxide semiconductor materials, especially TiO_2:

good chemical stability under visible irradiation in solution; nontoxic; inexpensive

Preparation:

- TiO_2 colloidal solution (or paste) coated on TCO substrate
- sintering at 450-500 °C
- typical particle size: 10-30 nm
- thickness: ~ 10 μm

Materials

TiO_2 photoelectrode

TiO_2: cheap,abundant, nontoxic, biocompatible

Phases:

- Rutile, tetragonal, E_g = 3.05 eV
- Anatase, tetragonal, E_g = 3.23 eV
- Brookite, orthorombic, E_g = 3.26 eV

n-type semiconductor, donor-type defects, i.e. O vacancies and Ti interstitials

E_F rutile < E_F anatase (difference ~ 0.1 eV)
→ anatase preferred for DSSC
(rutile: similar V_{OC}, smaller current, smaller surface area)

Materials

TiO_2 photoelectrode

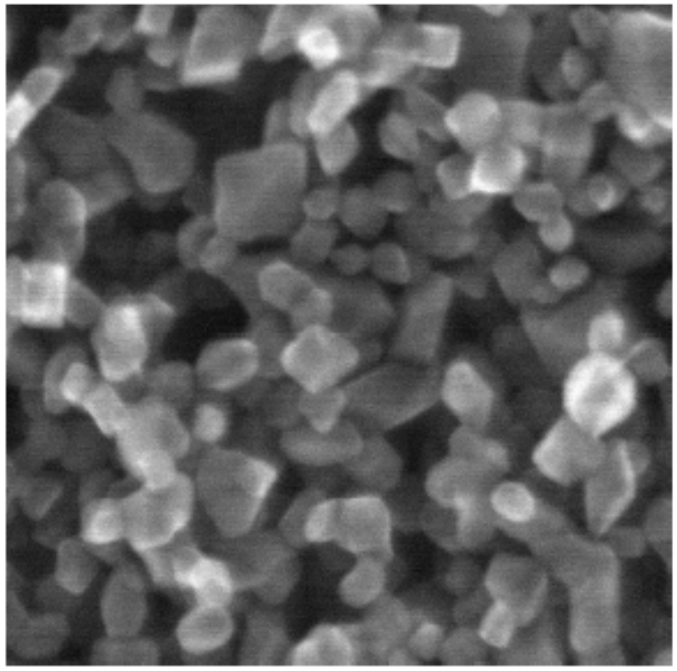

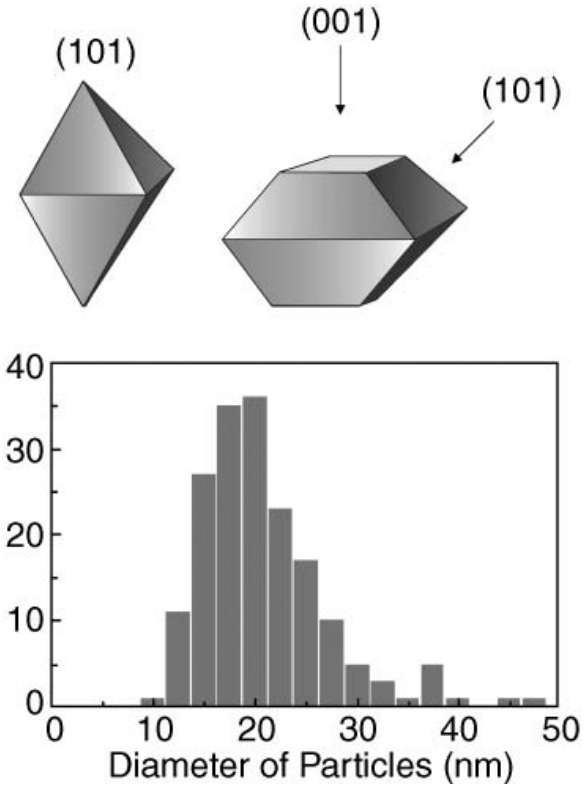

bipyramidal shape of the particles,
with (101) oriented facets exposed

M. Graetzel, MRS Bull 30, 23 (2005)

Materials

TiO_2 photoelectrode

- Nanoporous structure (porosity up to 50-70%)

- porosity can be controlled by addition of polymers (e.g. PEG, polyethylene glycol and EC, ethyl cellulose) to permit efficient penetration of electrolyte and permit diffusion of redox ions into the film

- Roughness factor (i.e. surface area/geometrical area) > 1000

(i.e. 1 cm^2 TiO_2 film 10 μm thick has > 1000 cm^2 surface area)

- contains large particles (250-300 nm) to scatter incident photons efficiently

Materials

Tipical photoanode structure:

(a) compact TiO_2 layer (thickness ~100–200 nm) coating by immersing the FTO plate in precursors such as $TiCl_4$ and subsequent sintering to prevent the electrolyte to reach the FTO plate

(b) a thick layer (thickness ~ 12–14 μm) of mesoporous TiO_2 of particle size 20–25 nm over the first monolayer

(c) a thin layer (thickness ~ 2–5 μm) of TiO_2 of particle size ~300-400 nm to improve light scattering on the top of the mesoporous particle film

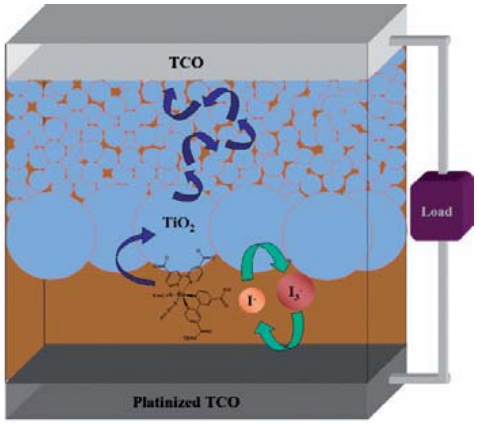

Q. Wang et al., ‘‘Characteristics of High Efficiency Dye-Sensitized Solar Cells,’’ J. Phys. Chem. B **110**, 25210–21 (2006)

Materials

Dye: Ru complex photosensitizer

- Photon absorption; electron injection

- Dye is considered to be absorbed in a monolayer, amount ~ 10^{-7} mol·cm^{-2}; coverage almost 100%

→ increase of LHE (Light Harvesting Efficiency) near 100% (1% for TiO_2 single crystals or polycrystals)

N3

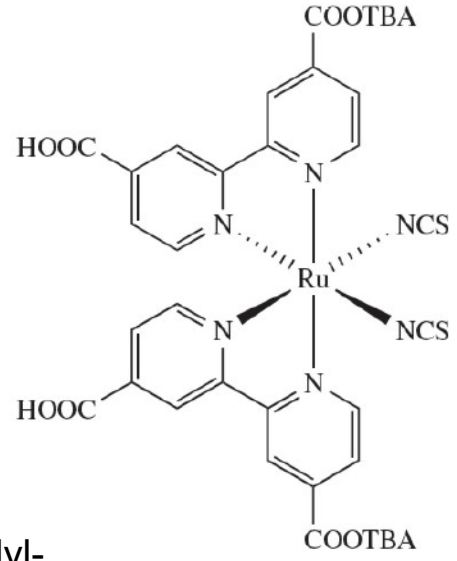

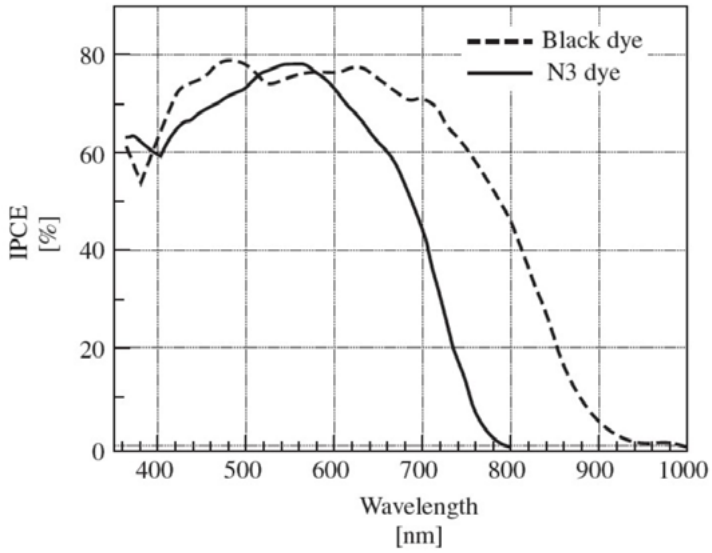

ruthenium (II) bipyridyl dye

cis-bis(isothiocyanato)-bis(2,2-bipyridyl-4,4-dicarboxylato)-ruthenium(II)

400-800 nm

Materials

Dye: Ru complex photosensitizer

N719

N3 partially deprotonated form (a di-tetra butylammonium salt)

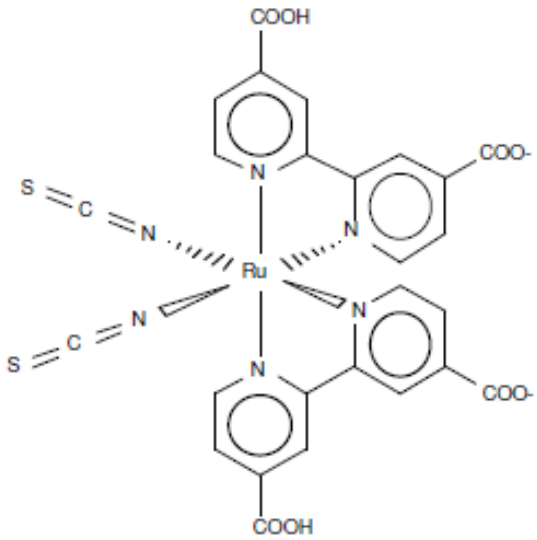

M.K. Nazeeruddin et al., *J. Am. Chem. Soc*. **115**, 6382 (1993)

Materials

Dye: Ru complex photosensitizer

‘Black dye’

tri(cyanato)-2,22-terpyridyl-4,44-tricarboxylate)Ru(II)

absorbs in near IR up to 950 nm

Nazeeruddin M. K., Pechy P., Renouard T., Zakeeruddin S. M., Humphry-Baker R.
and Comte P. (2001) *J. Am. Chem. Soc.* **123**, 1613–1624.

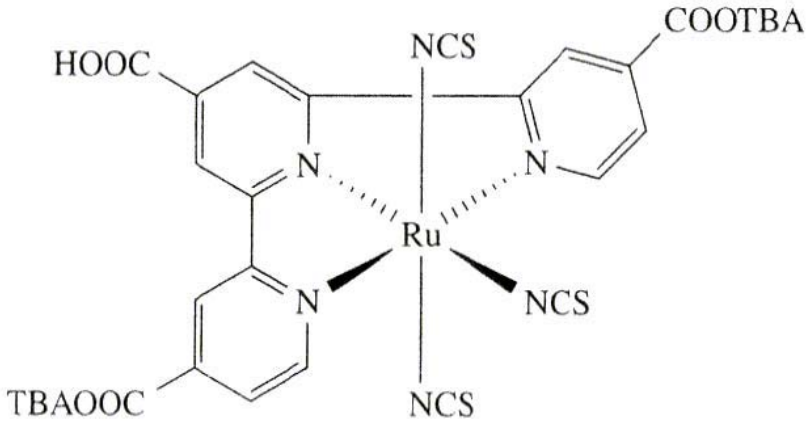

$RuL'(NCS)_3$
(Black dye)

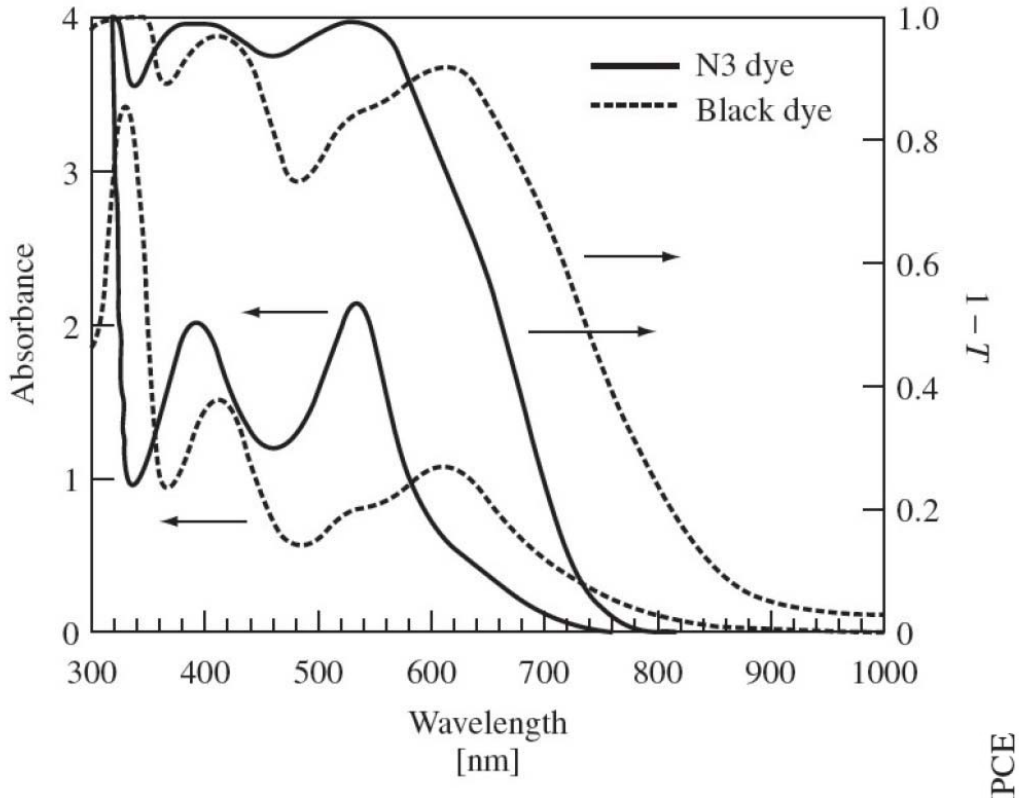
N3 dye
Black dye
Absorbance
1 − T
Wavelength
[nm]
0
1
2
3
4
0
0.2
0.4
0.6
0.8
1.0
300
400
500
600
700
800
900
1000

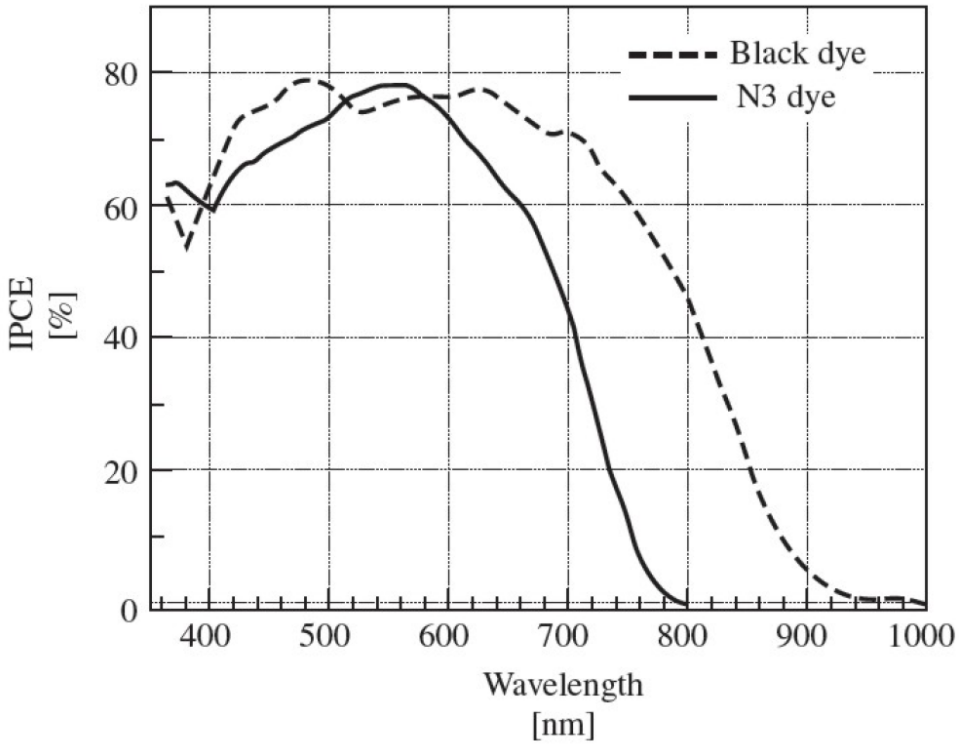
Black dye
N3 dye
IPCE
[%]
Wavelength
[nm]
0
20
40
60
80
400
500
600
700
800
900
1000

Dye anchoring to TiO_2 surface

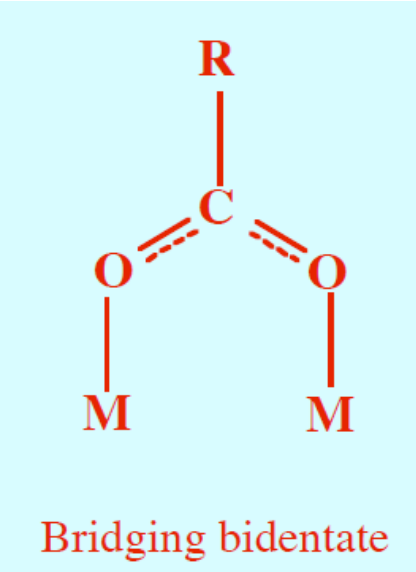

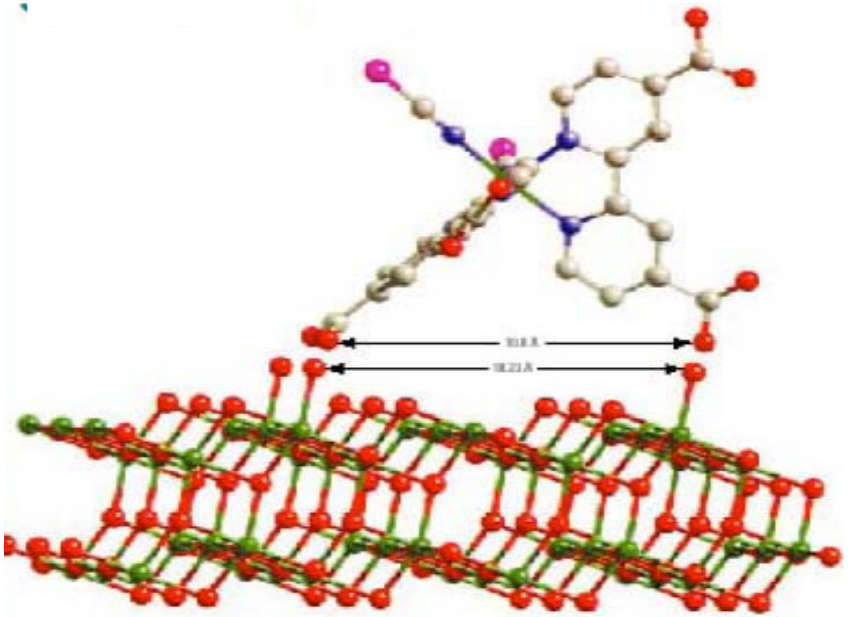

RuL2(NCS)2 sensitizer anchored to the (101) TiO_2 anatase surface through coordinative binding of two carboxyl groups to surface Ti ions

Materials

Dye: Ru complex photosensitizer

Photon absorption attributed to metal-to-ligand charge-transfer (MLCT) transition

HOMO and LUMO mainly derived from the *d* orbitals of Ru and π^* orbital of ligand, respectively

NCS ligand shifts HOMO negative → red shift in aborption; also contributes to e^- acceptance from reduced redox ions (I^-)

Carboxyl groups for anchoring to TiO_2 surface; large electronic interaction between ligand and TiO_2 C.B., resulting in effective e^- injection

Carboxylate bidentate coordination or ester bonding (-C(=O)O-) as measured by FT-IR absorption

Dye anchoring to TiO_2 surface

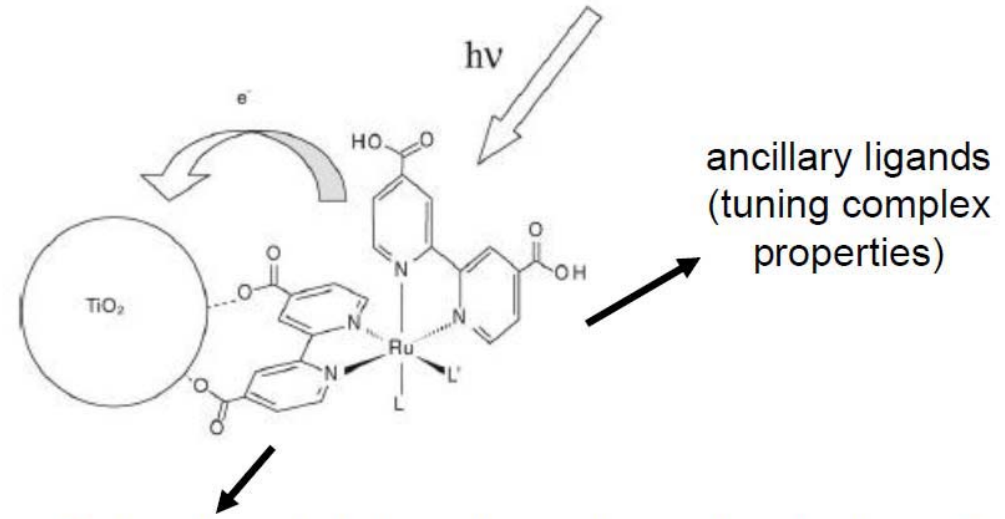

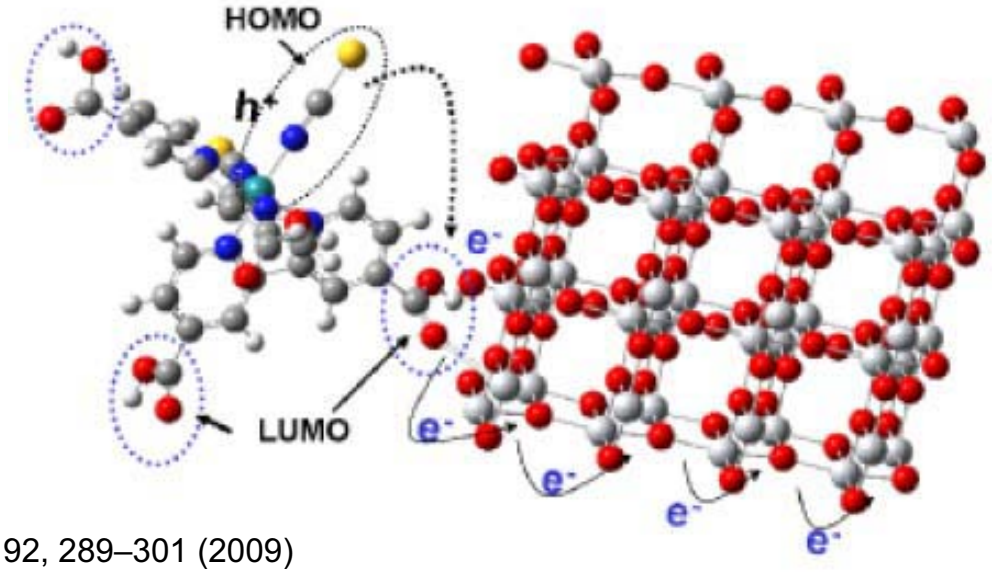

R. Jose et al., J. Am. Ceram. Soc. 92, 289–301 (2009)

DFT calculations

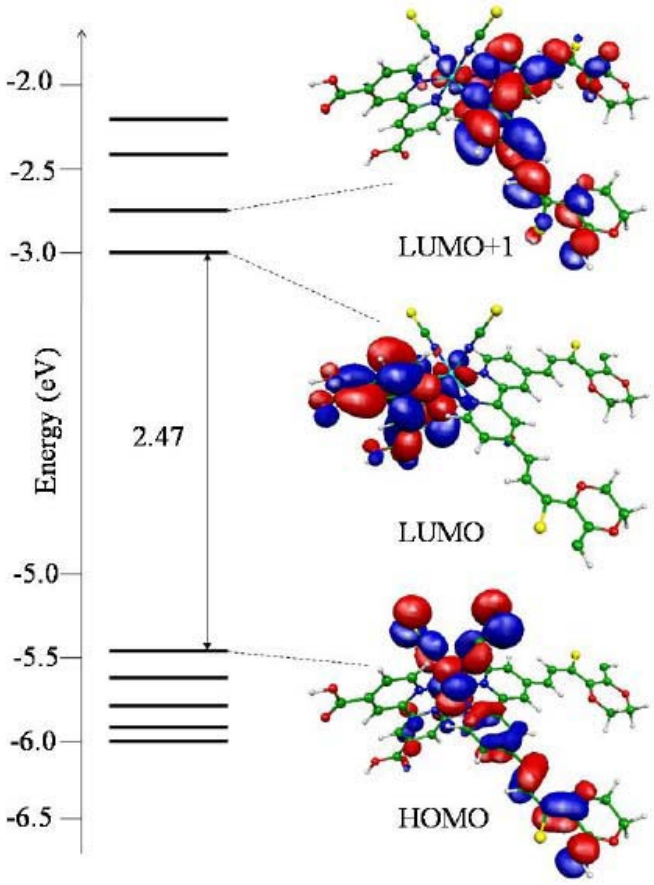

1. Absorption to LUMO+1
2. Energy transfer to LUMO localized in anchoring ligand
3. e^- injection into TiO_2 C.B.

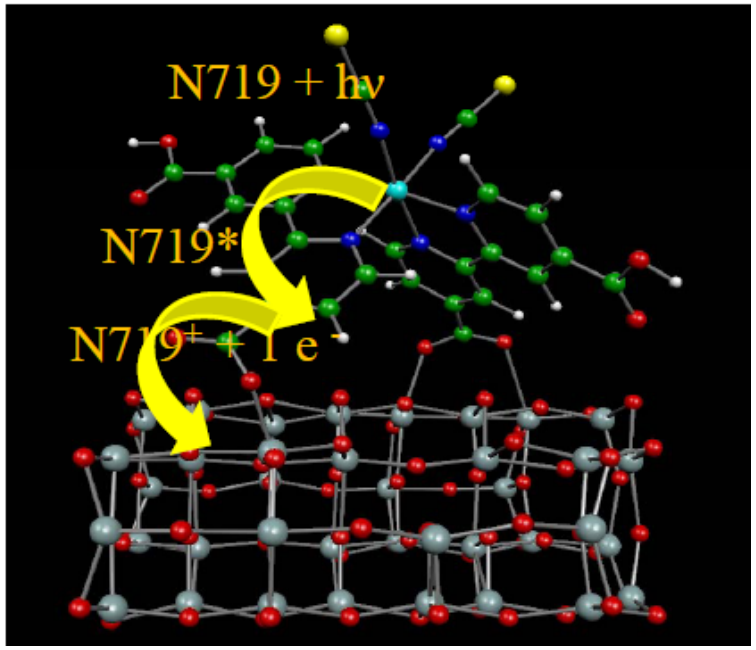

M.K. Nazeeruddin et al., Journal of Photochemistry and Photobiology A: Chemistry 185 (2007) 331–337
F. De Angelis, J. Am. Chem. Soc. **2007**, 129, 14156

Dye structure and properties

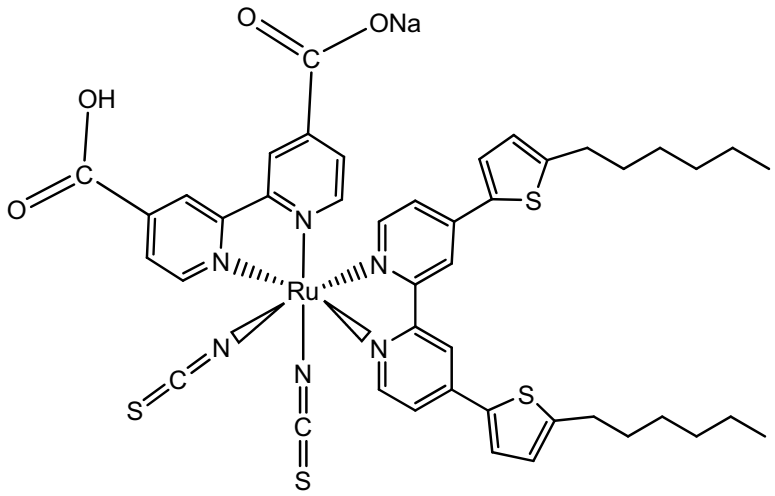

C101

Na-Ru(4,4'-(5-hexyltiophen-2-yl)-2,2'-bipyridine)(4-carboxylic-acid-4'-carboxylate-2,2'-bipyridine) (thiocyanate)$_2$

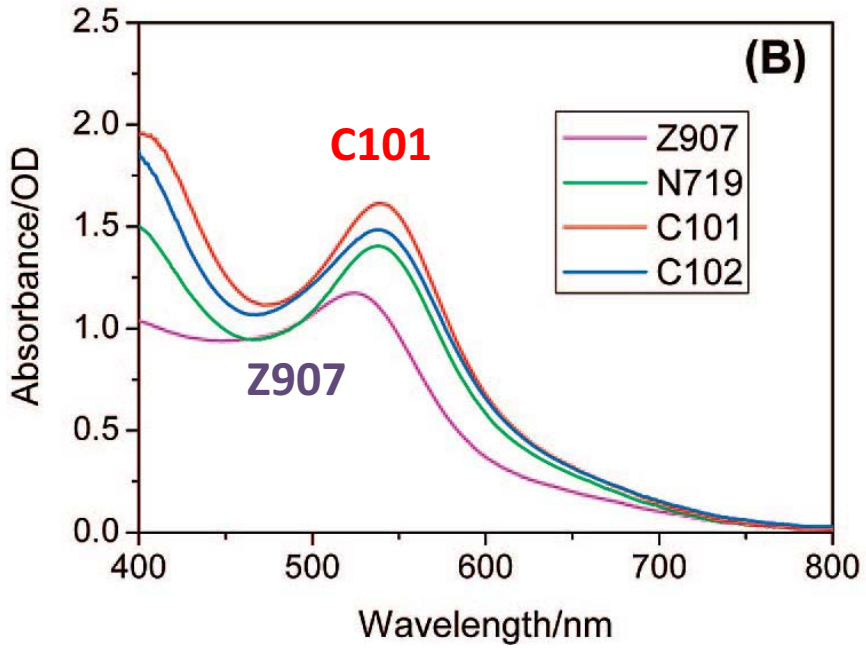

high molar extinction coefficients by extending the π-conjugation of spectator ligands; red shift of the MLCT

efficiencies > 11%

F. Gao et al., JACS, 130 (2008), 10720

Materials

Redox electrolyte

- Contains I^-/I_3^- redox ions, which mediate electrons between TiO_2 photoelectrode and counter electrode

Iodide/triiodide redox couple dissolved in a liquid organic solvent:

- mixture of iodides (LiI, NaI, KI, tetraalkylammonium iodide, 0.1-0.5 M and 0.005-0.1 M I_2 dissolved in nonprotonic solvents, i.e. acetonitrile, proprionitrile, methoxyacetonitrile, propylene carbonate, etc.)
- counter cations influence cell performance due to different ion conductivity in electrolyte and adsorption-induced shift of TiO_2 C.B.
- low viscosity solvents are desired
- also used Br^-/Br_2 but iodine redox electrolyte gives best performance

Materials

Transparent conductive oxide (TCO)-coated glass substrate

- low sheet resistance, independent of temperature up to 500 °C
- high transparency

Indium-tin oxide (ITO) resistance increases significantly at high T in air

Better **FTO** for DSSC (fluorine-doped SnO_2): R = 8-10 Ω/sq.

Materials

Counter electrode

Tri-iodide ions, formed by reduction of dye cations with I^- ions, are re-reduced to I^- ions at the counter electrode:

- High electrocatalytic activity: Pt-coated TCO substrate (5-10 $\mu g \cdot cm^{-2}$, ~ 200 nm), or carbon

DSSC characterization

Electrochemical Impedance Spectroscopy (EIS)

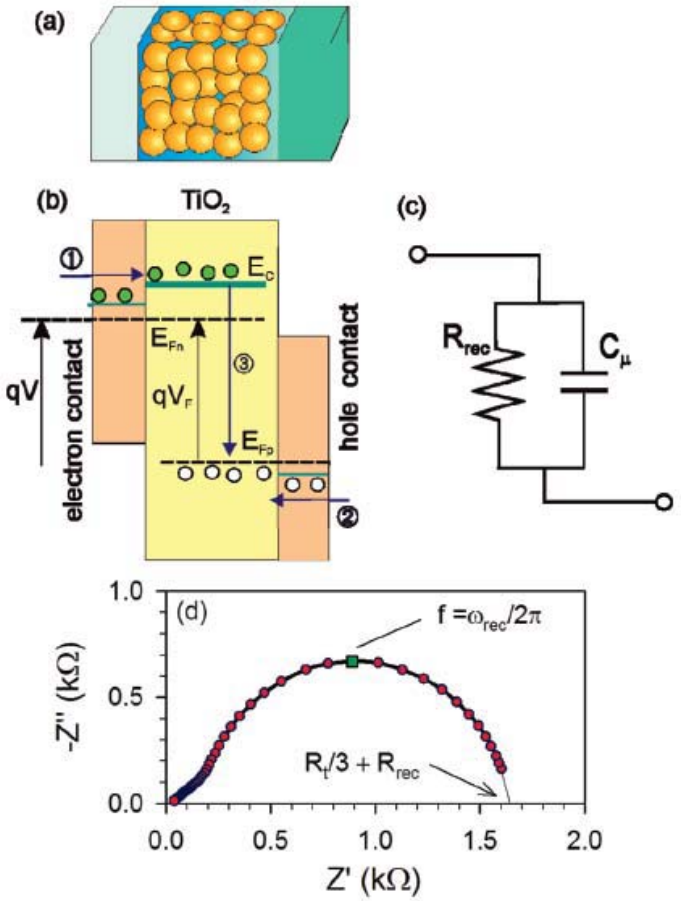

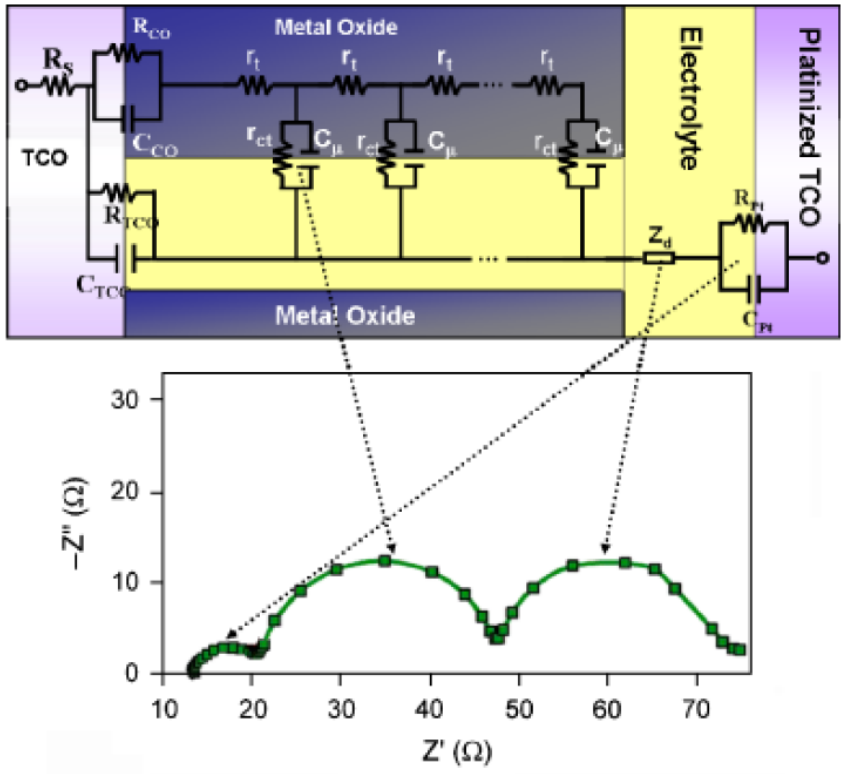

R. Jose et al., J. Am. Ceram. Soc. **92**, 289–301 (2009)

J. Bisquert, J. Phys. Chem. B **2002,** 106, 325-333

J. Bisquert et al., J. Phys. Chem. C **2009,** 113, 17278–17290

EIS spectra in dark on DSSC

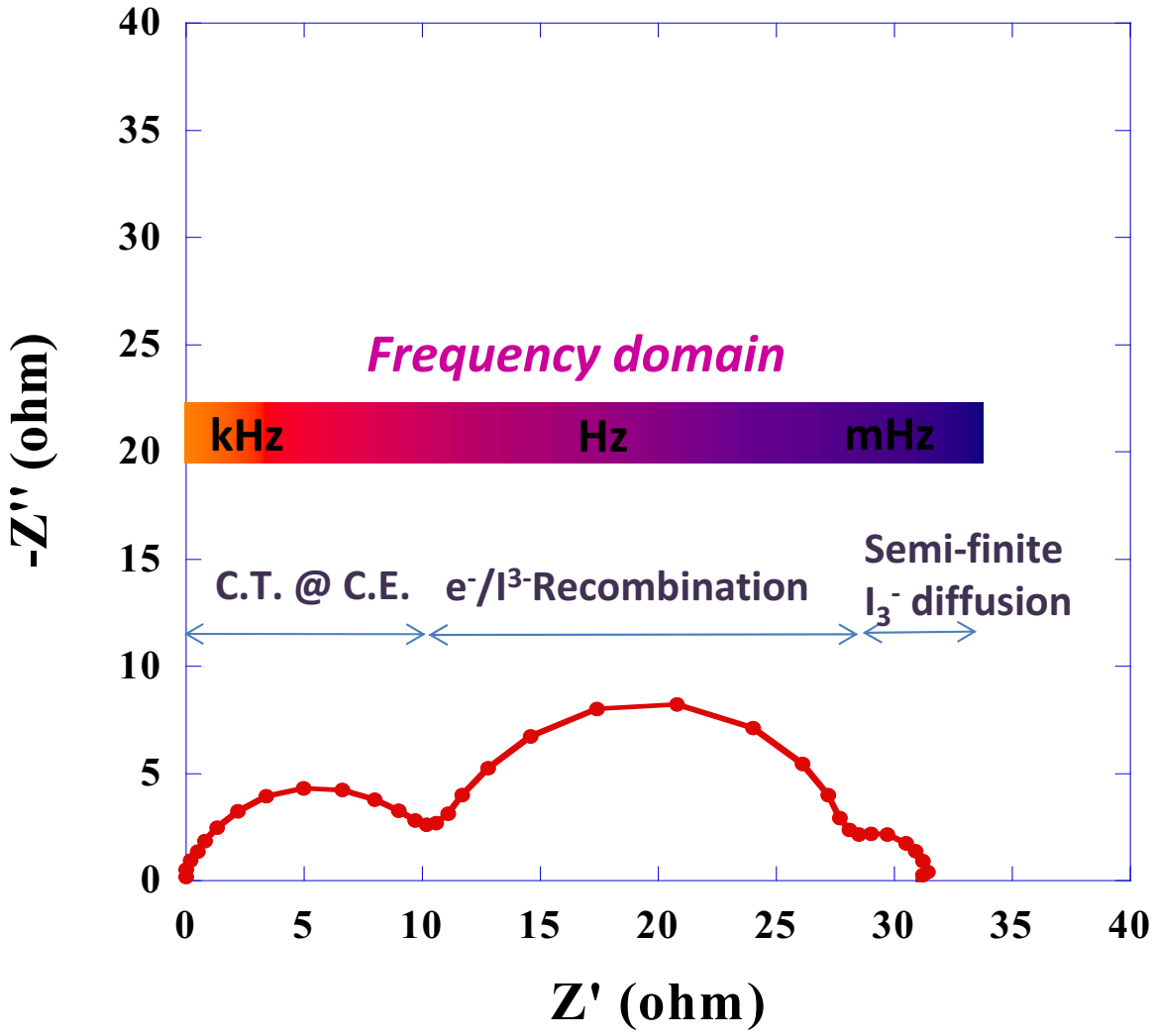

equivalent electrical circuit used to extract the kinetic constant of the device

Charge-transfer kinetics

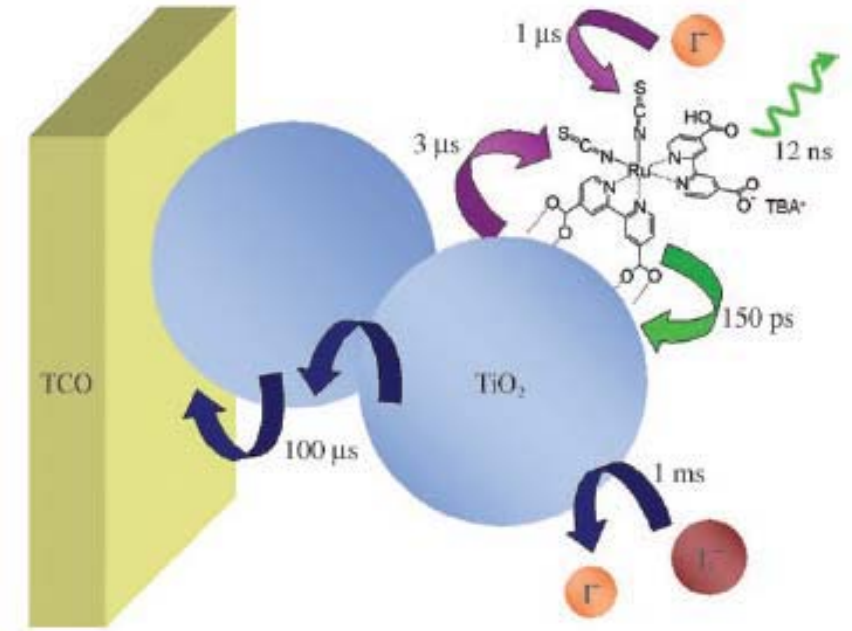

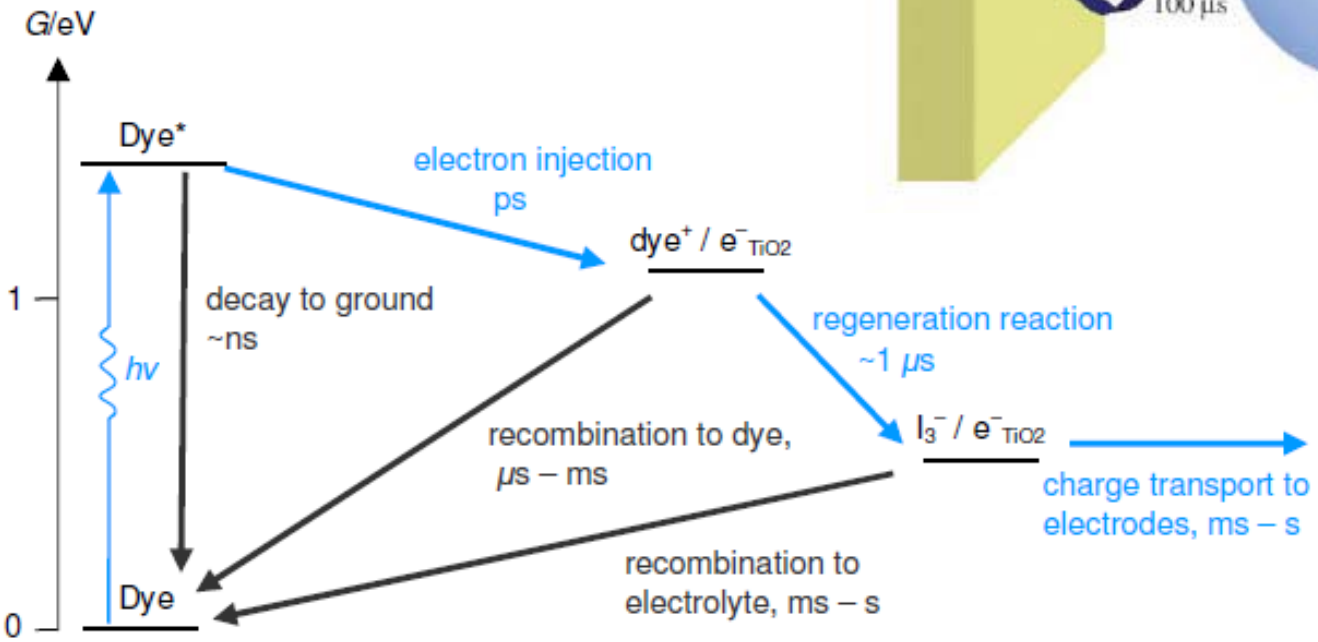

Charge-transfer kinetics

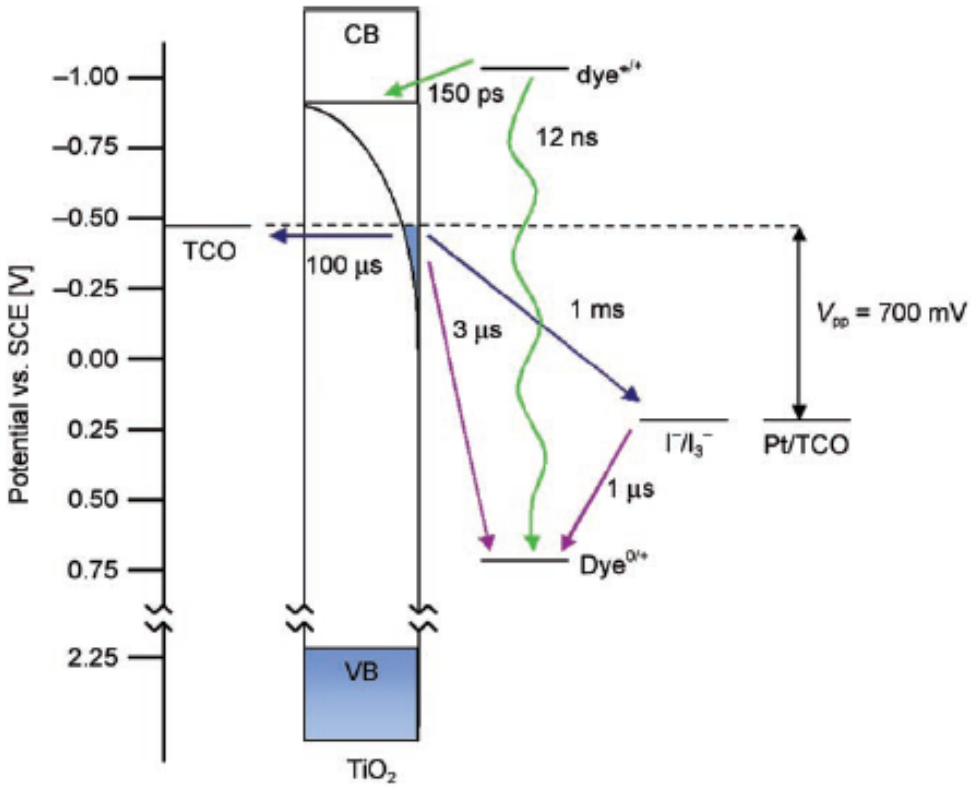

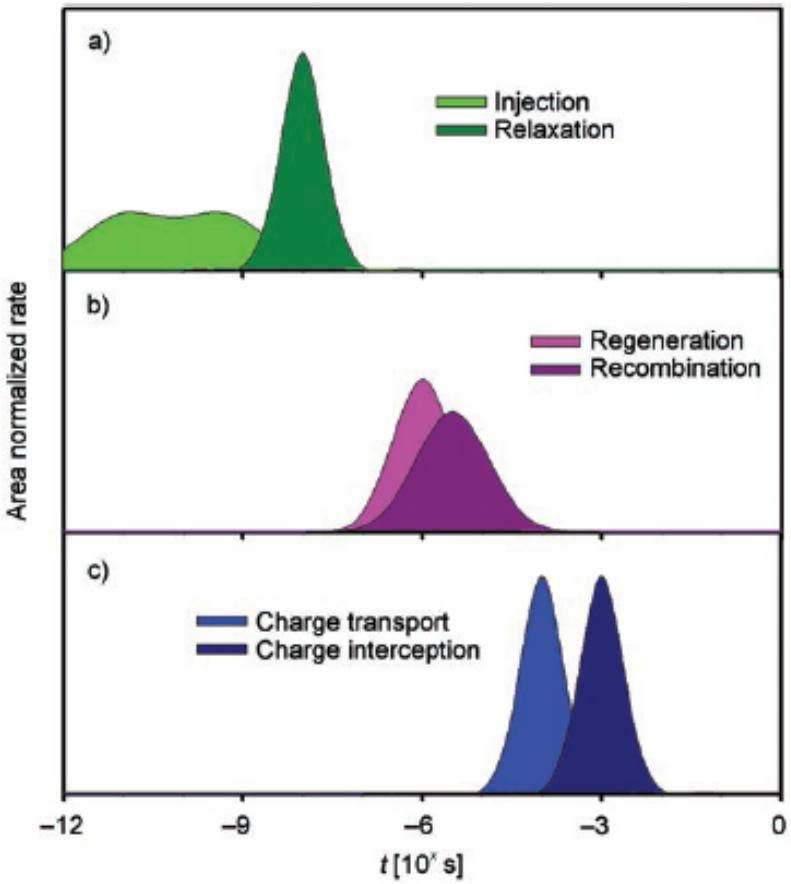

Dispersion in charge injection time distribution:
this limits possibility for C.B. energy shift and thus V_{OC}

A.B.F. Martinson et al., Chem. Eur. J. 2008, 14, 4458 – 4467

Charge-transfer kinetics

e^- injection: (measured e.g. by time-resolved absorption spectroscopy)

Depends on LUMO – (C.B TiO_2) and configuration of adsorbed photosensitizer

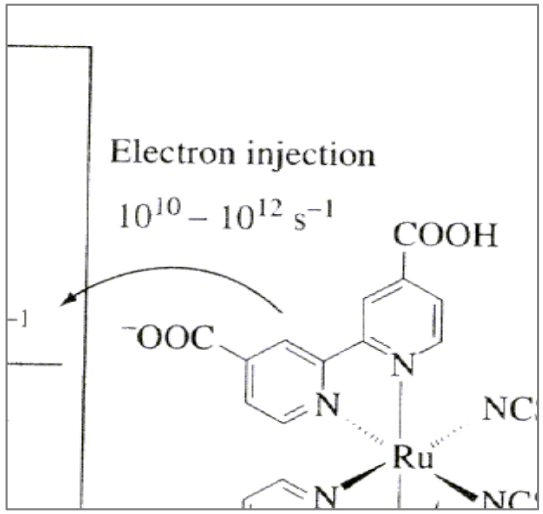

rate $k_{inj} = \left(\frac{4\pi^2}{h}\right)|V|^2 \rho(E)$

ρ(E): DOS of C.B.

$|V|^2$: electronic coupling between dye and TiO_2 (overlap between excited states of dye and C.B., depends on *distance*)

Carboxyl anchoring groups: overlap between π* states and C.B. (unoccupied 3*d* orbitals of Ti^{4+})

C.B. continuum DOS, injection faster than relaxation to HOMO

- Slower rate with ZnO (4*s* orbitals of Zn^{2+}) than TiO_2

Charge-transfer kinetics

Charge recombination between injected e^- and oxidized dye

- must be slower than e^- injection and e^- transfer from I^- to S^+ (i.e. regeneration of dye) to have effective charge separation

- usually of the order of μs-ms

In N3-TiO_2 system, charge recombination is to Ru(III) (long distance compared to ligand-TiO_2)

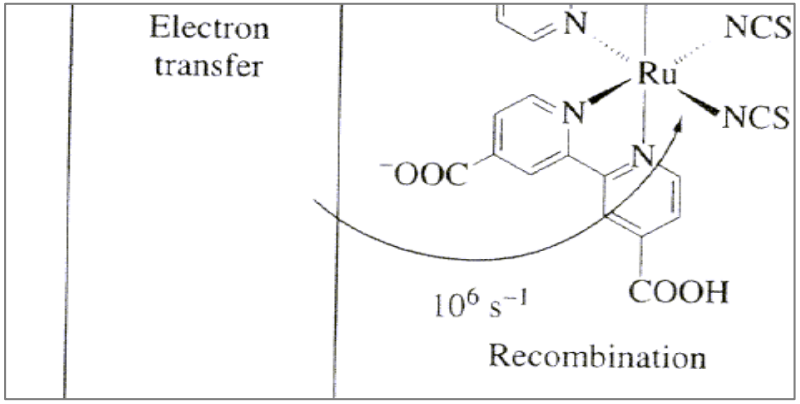

Charge-transfer kinetics

Dye (photosensitizer) regeneration

- of the order of 100 ns, faster than recombination

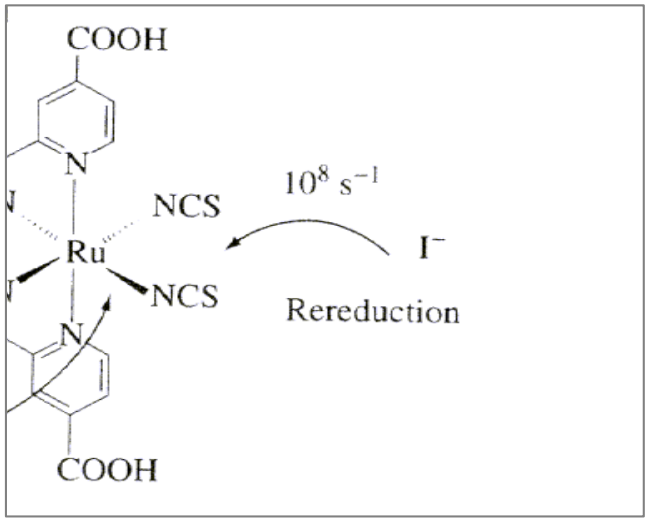

Charge-transfer kinetics

Recombination between injected e^- and tri-iodide ions **(dark current)**

$$I_3^- + 2e^- \rightarrow 3I^-$$

It can occur also on the SnO_2 surface (TiO_2 does not completely cover TCO)

- leads to loss of PV performance analogous to forward-bias injection in p-n junctions
- for each order of magnitude decrease in dark current, 59 meV gain in V_{OC} at room T

As in standard *p-n* junctions:

$$V_{OC} = \frac{mkT}{q} \ln\left(\frac{I_{inj}}{I_0} + 1\right)$$

$$I_{inj} = q\eta\Phi_0$$

$$I_0 = qn_0k_{et}[I_3^-]$$

I_0: reverse saturation current
η: photogenerated e- quantum yield
Φ_0: incident photon flux
n_0: electron density of C.B. in dark
k_{et}: rate constant for recombination
$[I_3^-]$: I_3^- concentration
m: ideality factor (1-2)

$\eta\,\Phi_0 >> n_0\,k_{et} \rightarrow$

$$V_{OC} = \frac{kT}{q} \ln\left(\frac{\eta\Phi_0}{n_0k_{et}[I_3^-]}\right)$$

Charge-transfer kinetics

Dark current is considered to occur at TiO_2/electrolyte interface where dye is not absorbed

- to suppress dark current, pyridine derivatives (*tert*-butylpyridine, TBP) → increase in photovoltage (but decrease of J_{SC})

Recombination very slow, 0.1 s to several s

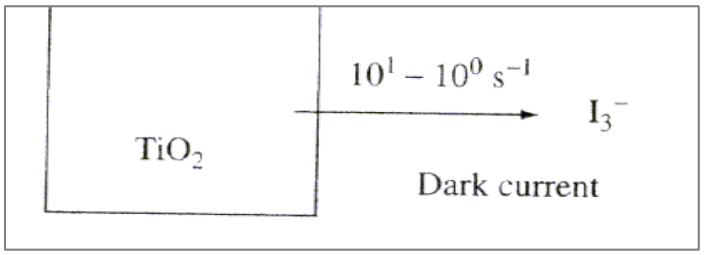

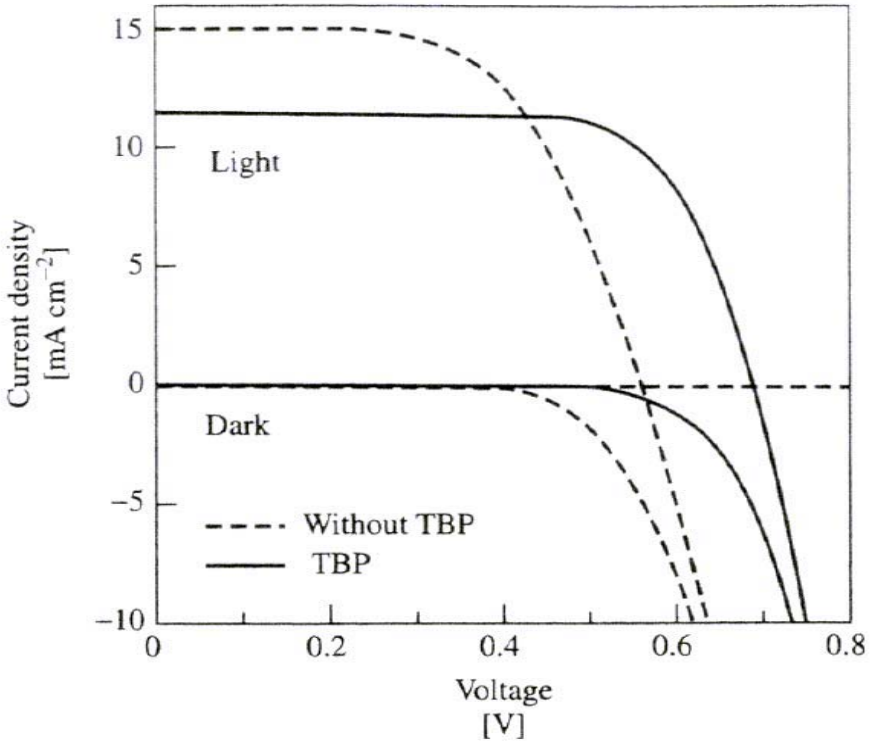

Charge-transfer kinetics

e^- transport in TiO_2 nanocrystalline film

Discussed with respect to different mechanisms:

- diffusion model (mainly diffusion and not drift)
- tunneling through potential barriers between nanoparticles
- trapping-detrapping mechanism (surface or grain boundaries)

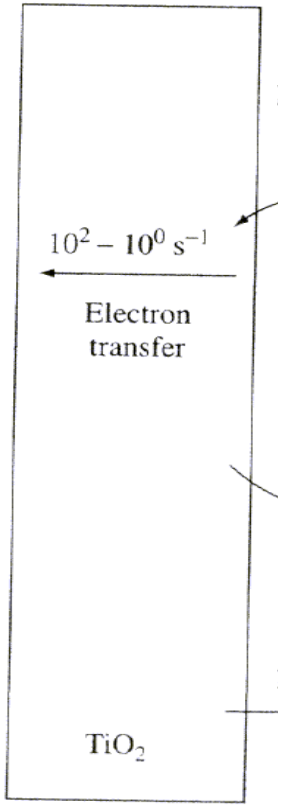

- e^- conductivity very small in TiO_2 (→ slow response of the photocurrent)
- Diffusion coefficients for nc-TiO_2 estimated $10^{-4} – 10^{-7}\ cm^2\ s^{-1}$
- DSSC: e^- conductivity increased due to e^- injection; it has been suggested that when e^- fill trap site or surface levels → diffusion increases

Transport in TiO_2

e^- transport typically through thermally activated hopping

exciton Bohr diameter for TiO_2 = 1.5 nm (below: quantum size effects)

Particles in DSSC have bulk electronic properties, but:

- Surface states in the band gap (unsaturated bons, bond angle-length distortions, impurities)
- Multiple trapping mechanism (trapping-detrapping)

	D (cm^2/s)	Mobility (cm^2/Vs)
Single crystal	0.5	20
1 μm crystalline film	0.1	4
Degussa 25	$3x10^{-4}$	0.01
Colloidal TiO_2 (9 nm)	$9x10^{-4}$	0.034

Transport in TiO_2

kinetic competition between charge transport and recombination analyzed in terms of an effective carrier diffusion length

$$L_n = \sqrt{D_{\text{eff}}\,\tau}$$

D_{eff} = effective e^- diffusion length

τ electron lifetime due to recombination

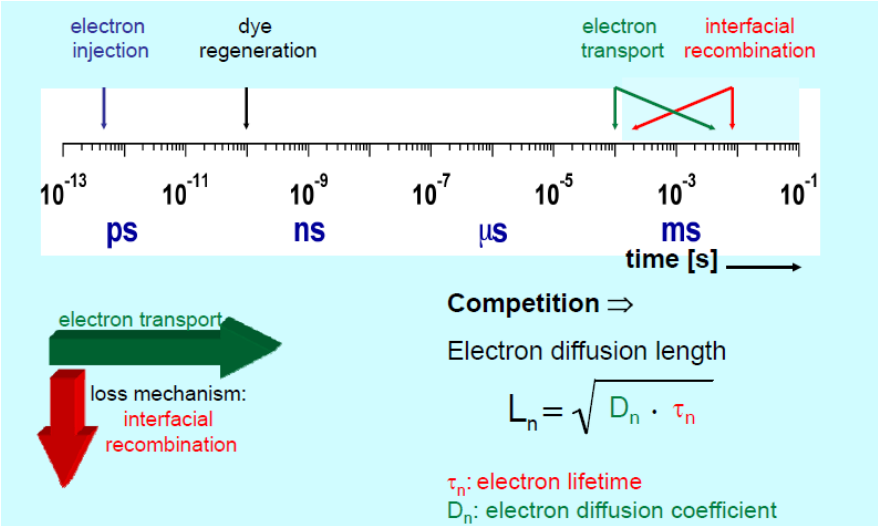

M. Graetzel

- D_{eff} increases with light intensity (due to the increased electron density in the TiO_2 film), about 10^{-4} cm^2/s
- τ shows a proportional decrease (about 1 s)
- L_n largely independent of light intensity (typical values 5–20 µm, even 100 µm near the optimum power point for cells with >10% conversion efficiency)

DSSC fabrication

TiO_2 colloid

Hydrolysis of Ti(IV) alkoxides (isopropoxide and butoxide)

TiO_2 electrode

- doctor blade technique; TiO_2 + PEG, followed by sintering at 450 °C for 30 min in air
- screen printing; TiO_2 + EC, printing, then sintering at 500 °C for 1 h in air
- sometimes: $TiCl_4$ treatment at 450°C: improves connection between particles

DSSC fabrication

Dye fixation

- Immersion in dye solution (e.g. 0.2-0.3 mM in ethanol) + storage at room T for 12 h + washing with alcohol or acetonitrile to remove excess nonadsorbed dyes

Counter electrode

- Sputtered Pt on TCO substrate (200 nm), also induces light reflection and increase in photocurrent
- Affects fill factor

Stability

extensive accelerated light-soaking tests carried out over the last decade

sensitisers employed in current DSSC embodiments can sustain 20 years of outdoor service without significant degradation

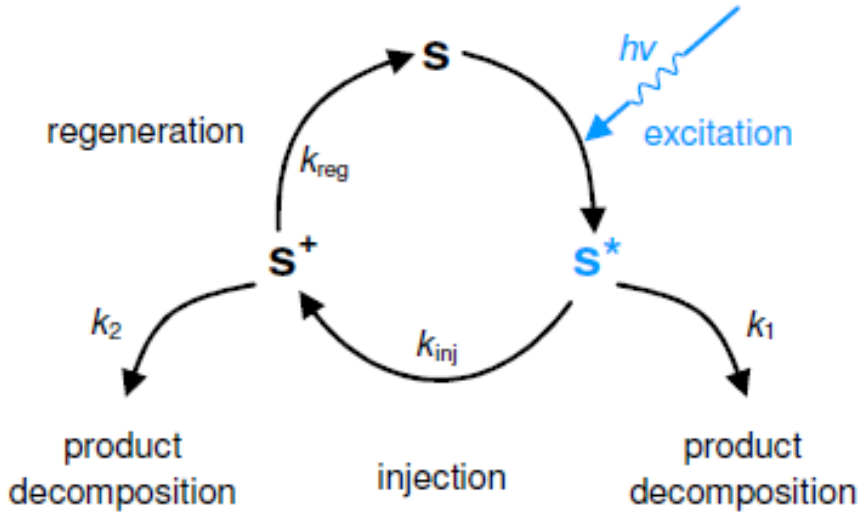

Critical for stability: side reactions from the excited state (S*) or the oxidized state of the dye (S+), competing with electron injection and sensitizer regeneration

the sum of the branching ratios for the bleeding channels is estimated to be < 1×10^{-8}, ensuring the sensitiser to reach at least 20 years

(turnover frequency of the dye is about 0.16 s^{-1})

M. Graetzel and J.R. Durrant, 'Dye-sensitized mesoscopic solar cells', in 'Nanostructured and photoelectrochemical systems for solar photon conversion', ed. M.D. Archer, A.J. Nozik, World Scientific 2008

Developments

New dye photosensitizers

• try to change absorption properties

- metal centers different from Ru (Fe, Os, Re, Pt complexes) but efficiencies with Ru complexes not attained; it is believed that HOMO of Ru complexes is best matched to iodine redox potential

- **organic dyes**: porphyrin and phtalocyanine derivatives (e.g. with Cu; but porphyrin: lack of red light or near IR absorption; phthalocyanines: too low LUMO level and problems of aggregation

• research for developing a blocking monolayer to reduce dark current (engineering of surface interaction with TiO_2)

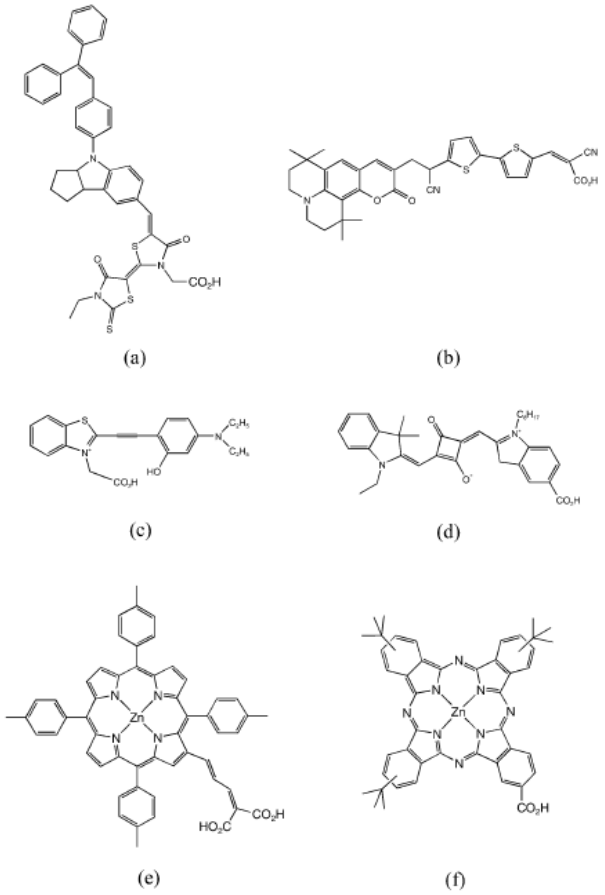

Fig. 5 Organic dyes utilized in (a) 9% efficient indoline,[40] (b) 6.5% efficient coumarin,[41] (c) 5.2% efficient hemicyanine,[42] (d) 4.5% efficient squarine,[43] (e) 7.1% efficient porphyrin,[44] and (f) 3.5% efficient phthalocyanine-based DSSCs.[45]

coumarin or polyene-type sensitisers, reported to have strikingly high solar-to-electric power conversion efficiencies, reaching up to 9.2% in full sunlight (Ito *et al.*, 2006)

New dyes development

Metal free dipolar dyes

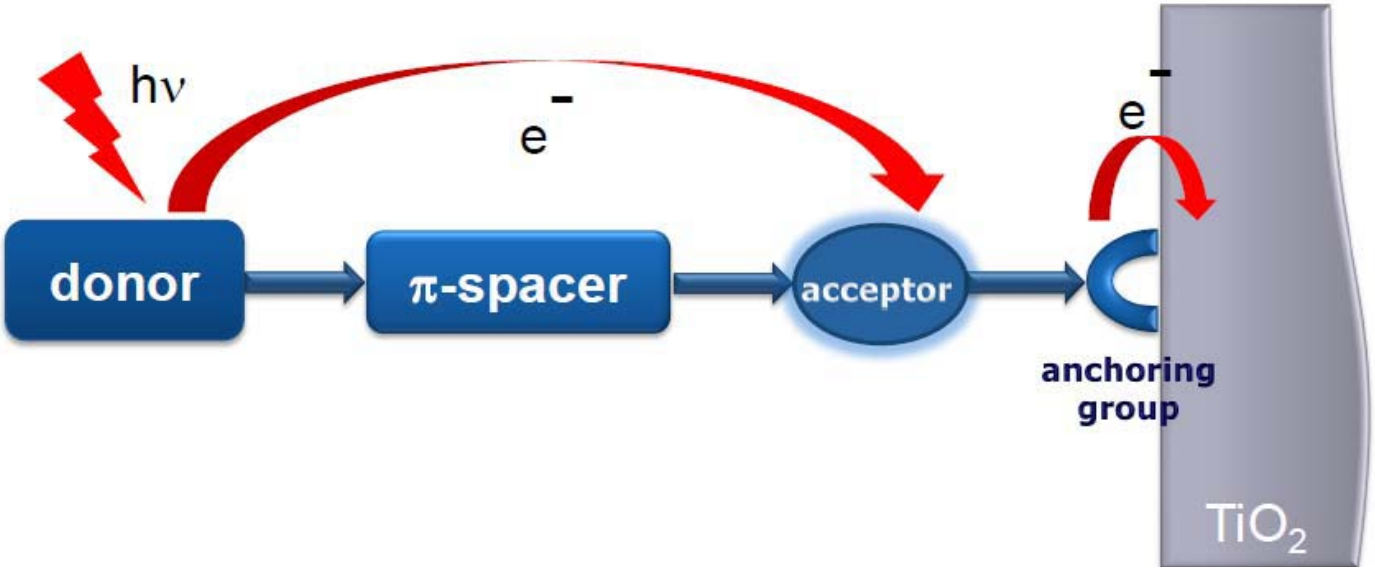

Advantages over organometallic dyes:

- Ru expensive
- structural variety
- tunable and more intense spectral absorption
- low cost manufacturing

push-pull structures

Developments

New electrolytes

attention increasingly focusing on alternatives for the solvent:
ionic liquids, gelled electrolytes and polymer electrolytes

LETTERS

High-performance dye-sensitized solar cells based on solvent-free electrolytes produced from eutectic melts

→ efficiency 8.2%

YU BAI[1]*, YIMING CAO[1]*, JING ZHANG[1], MINGKUI WANG[2], RENZHI LI[1], PENG WANG[1]†, SHAIK M. ZAKEERUDDIN[2] AND MICHAEL GRÄTZEL[2]†

[1]State Key Laboratory of Polymer Physics and Chemistry, Changchun Institute of Applied Chemistry, Chinese Academy of Sciences, Changchun 130022, China
[2]Laboratory for Photonics and Interfaces, Swiss Federal Institute of Technology, CH 1015, Lausanne, Switzerland
*These authors contributed equally to this work
†e-mail: peng.wang@ciac.jl.cn; michael.graetzel@epfl.ch

Y. Bai et al., Nature Mat. 7, 626 (2008)

Developments

New electrolytes

Solid-state DSSC

hole-trasnport material (HTM)

p-type organic conductor

hole mobility 2×10^{-4} $cm^2V^{-1}s^{-1}$

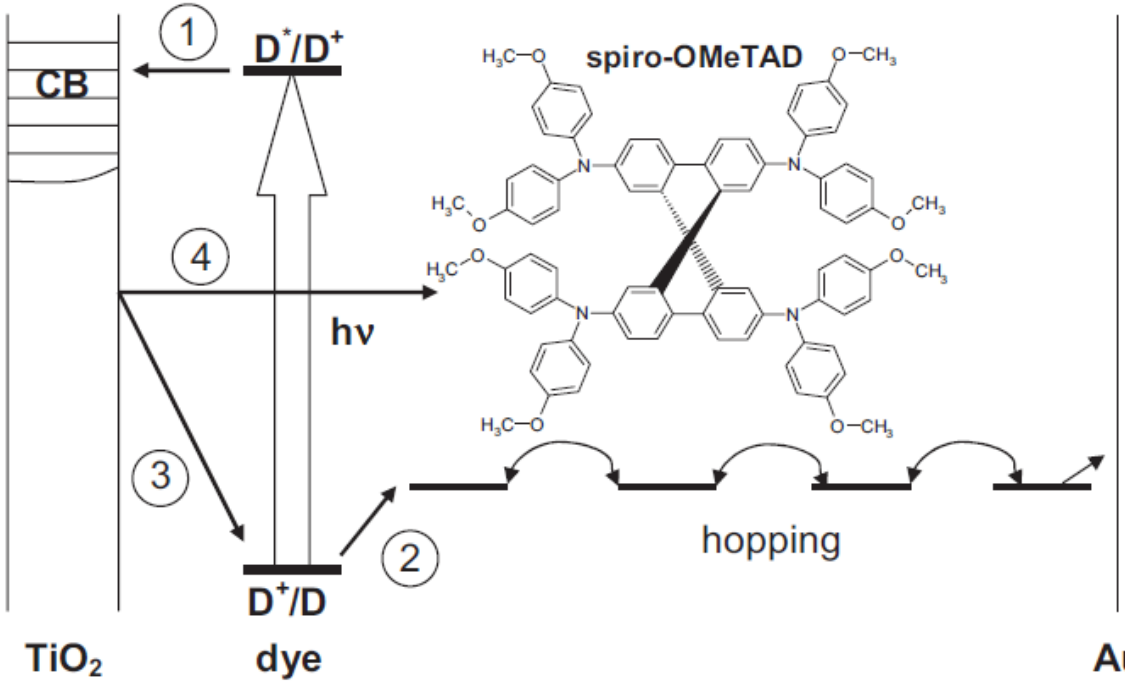

2,2′,7,7′-tetrakis(*N*,*N*-di-*p*-methoxypheny-amine)-9,9′-spirobi-fluorene (spiro- OMeTAD)

Optimal thickness: 2 μm

- poor polymer infiltration → **need for new mesoporous oxide semiconductors, with perpendicular channels!**
- interfacial e/h recombination
- efficiency > 4%

H. J. Snaith and L. Schmidt-Mende, Adv. Mater. **2007**, 19, 3187–3200

H. J. Snaith, S. M. Zakeeruddin, Q. Wang, P. Péchy, M. Grätzel, *Nano Lett.* **2006**, *6*, 2000

Solid state DSSC

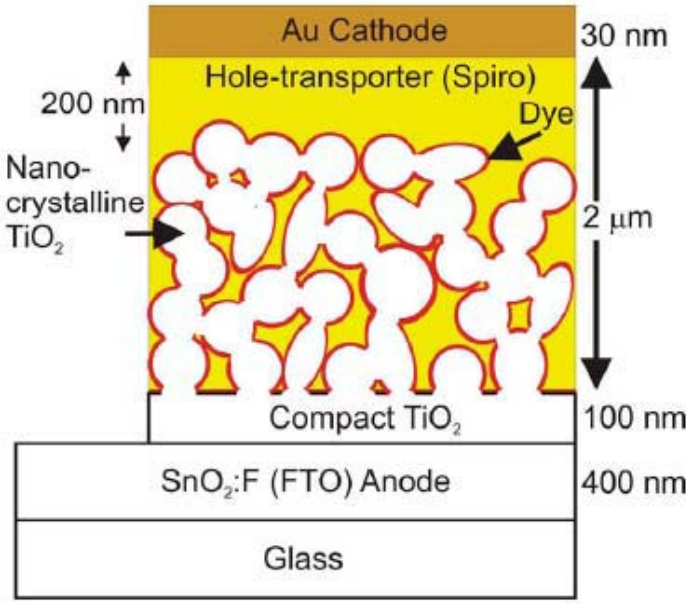

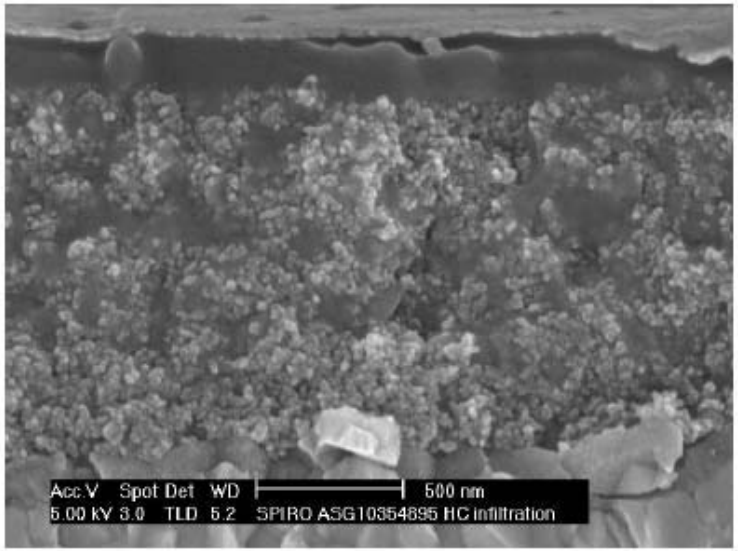

H. Snaith

Developments

New electrolytes
inorganic p-type HTM

- CuI, CuSCN (from solution or vacuum deposition), nearly 100% pore filing
- 4.7% with additional MgO ‘blocking layer’
- low stability (hole trapping by adsorbed iodine)

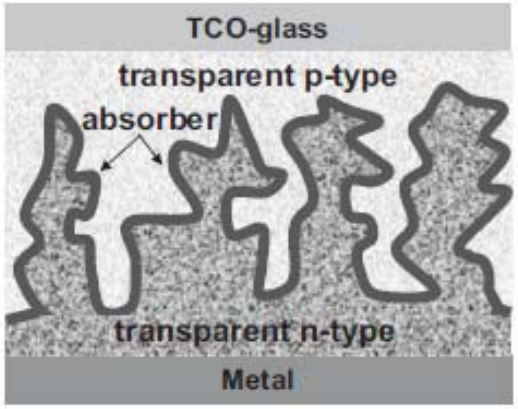

Figure 7. Schematic of an extremely thin absorber solar cell.

H.J. Snaith and L. Schmidt-Mende, *Adv. Mater.* **2007**, *19*, 3187–3200

ETA (extremely thin absorber)

e.g.

TiO_2 / CdS / CdSe / polysulphide - 2.8%

ZnO / CdTe / CuSCN - 2.3%

POLITECNICO DI MILANO

Advanced nanostructured inorganic photoanodes for DSSC and hybrid cells

Andrea Li Bassi
CNST (Center for NanoScience and Technology) - IIT@PoliMI
Department of Energy
POLITECNICO DI MILANO

andrea.libassi@polimi.it
www.nanolab.polimi.it

Advanced semiconductor photoanodes

Other oxide semiconductor film photoelectrodes

Characteristics:

- **wide bandgap**
- **energy level matching with dye**
- **high charge carrier mobility when mesoporous**
- **high surface area**

- ZnO, SnO_2, Nb_2O_5, In_2O_3, $SrTiO_3$, NiO; but TiO_2 best performance

performance affected by conductivity, C.B. level, etc.

- also combined oxides (small particle SnO_2 for dye absorption + large particle ZnO for transport)
- also TiO_2 coated with ZnO or Nb_2O_5 (reduction of dark current, modification of C.B. level)

ZnO performances similar to TiO_2, but efficiency 5% [e.g. K. Keis et al. *Sol. Energy Mater. Sol. Cells* **2002**, *73*, 51]; careful with dye (instability vs. acid)

OR: new architectures (new morphologies, e.g. hierarchical)

TiO_2 np good enough in conventional DSSC, but new photoanode architecture may provide improvements with new components (especially fast redox shuttles)

Oxide nanowires / nanotubes

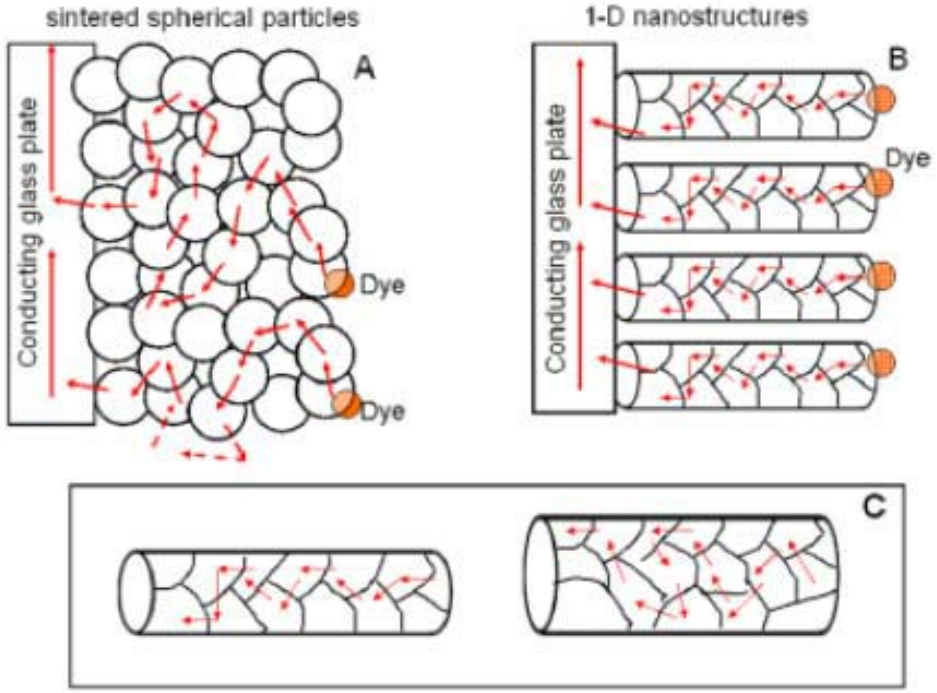

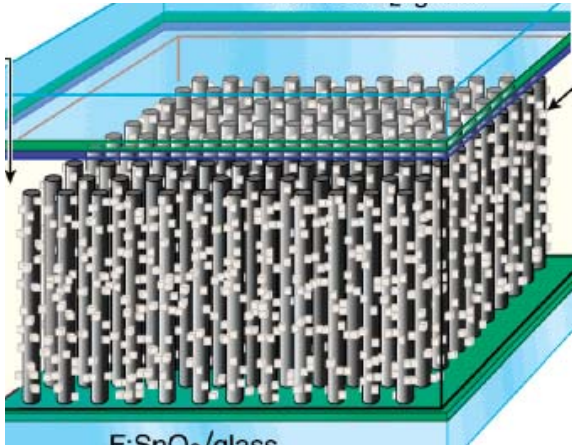

‘channeled’ conduction

R. Jose et al., J. Am. Ceram. Soc. 92, 289–301 (2009)

Advanced semiconductor photoanodes

1D TiO_2 nanostructures

Nanotubes, nanorods, nanofibers

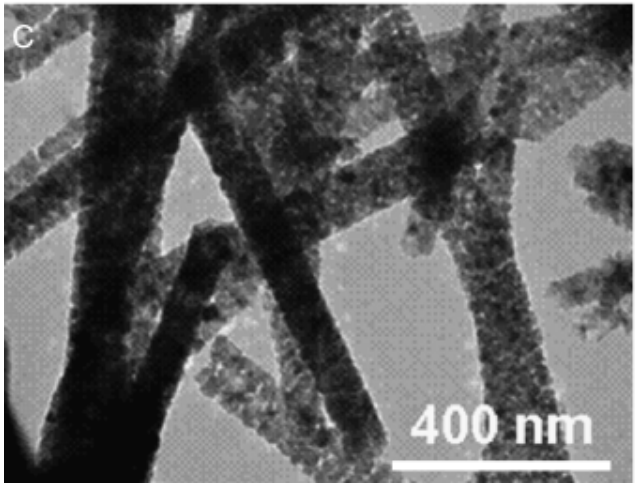

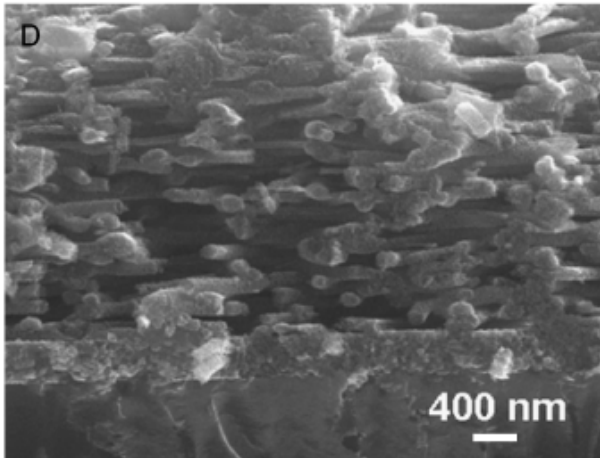

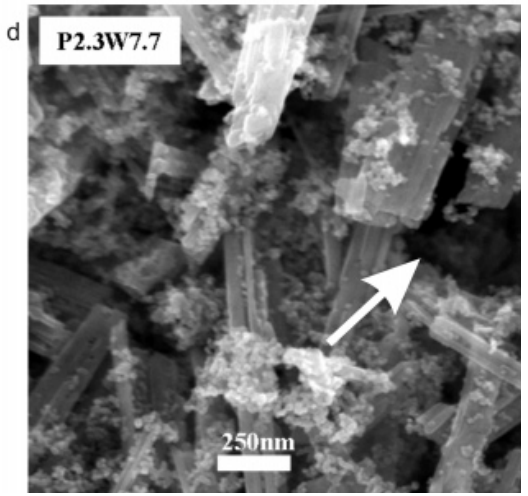

J. Phys. Chem. B **2006,** *110,* 15932-15938

- also electrospinning, need improved adhesion on substrate

G. K. Mor et al., Sol. Energy Mater. Sol. Cells 90, 2011–75 (2006).
V. Thavasi et al., Energy Environ. Sci. 1, 205–21 (2008)

TiO_2 nanowires

Single crystal TiO_2 nanowires

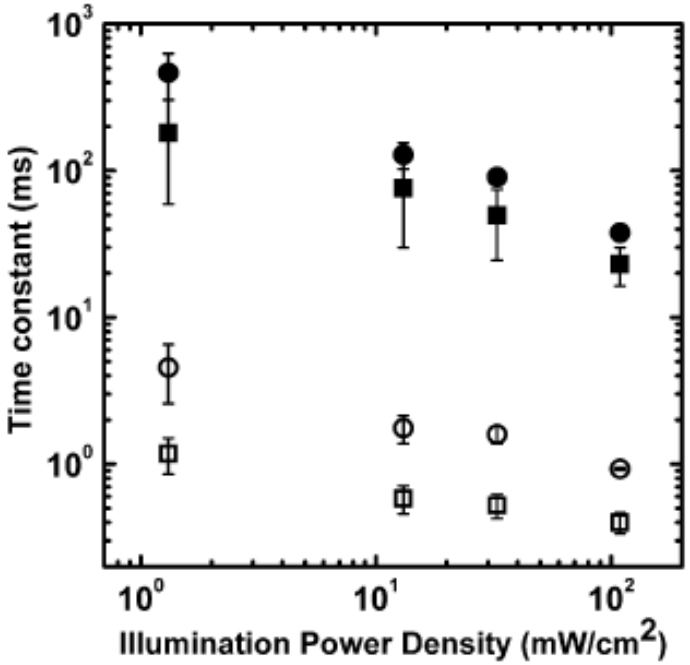

Fig. 7 (a) Recombination (●, ■) and transport (○, □) time constants for TiO_2 nanowire (circles) and nanoparticle (squares) DSSCs as a function of light intensity. Error bars represent standard deviations and illustrate reproducibility for DSSCs from three different batches (nanowires) and four different batches (nanoparticles).

surface trapping-detrapping

hydrothermal growth, from titanium isopropoxide

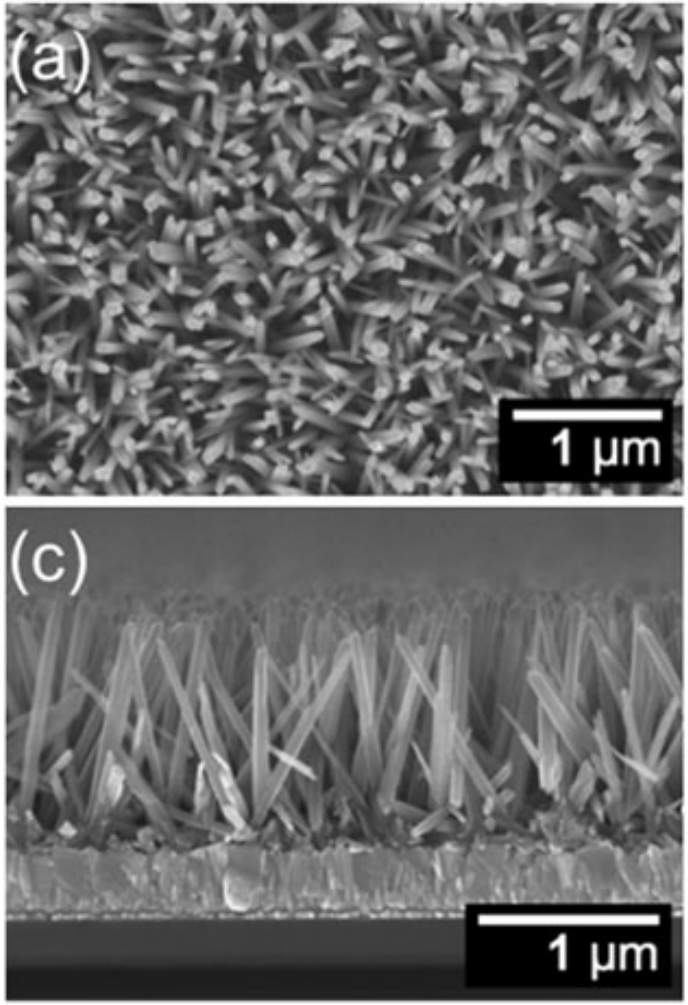

E. Enache-Pommer et al., Phys. Chem. Chem. Phys., 2009, 11, 9648–9652

TiO_2 nanotubes

Titania nanotube arrays

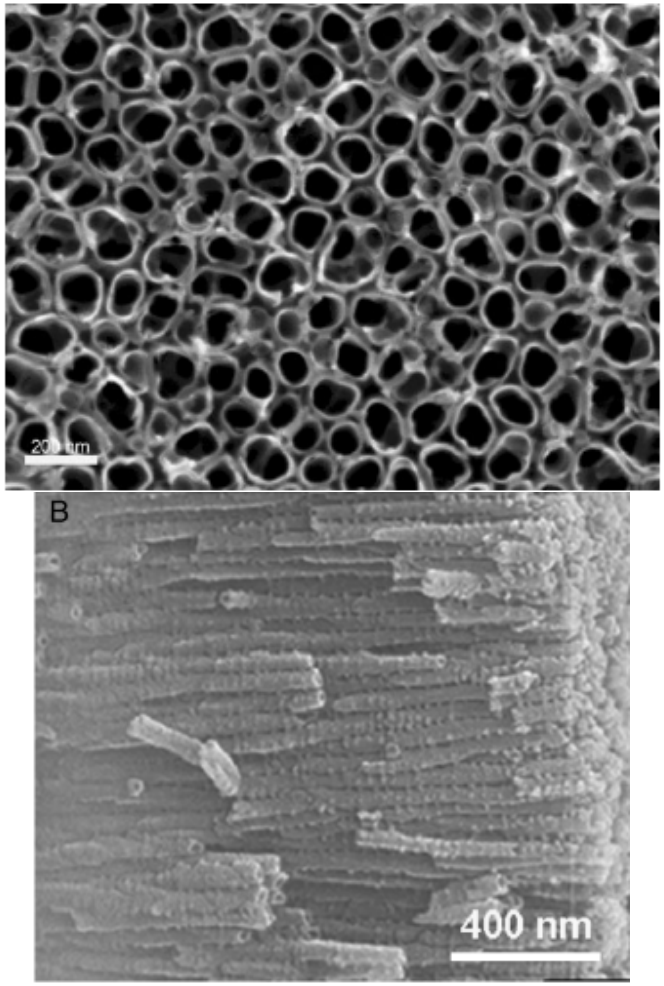

Anodization of Ti foils + annealing to > 450 °C

- need for improved e^- transport pathways
- less grain boundaries, but still surface trapping and intergrain e^- transfer
- diameter about 30 nm
- transport times comparable to np-TiO_2, but fewer recombination centers
- reduced surface area, but allows higher roughness than nanowires
- efficiency > 4% with I^-/I_3^- ; V_{OC} up to 860 mV

Drawback: usually illumination only from back side (reflection from Pt)

M. Paulose et al., *Nanotechnology* **2006**, *17*, 1446
K. Zhu et al., Nano Letters 7, 69 (2007)

H. J. Snaith and L. Schmidt-Mende, Adv. Mater. **2007**, *19*, 3187–3200

TiO_2 nanotubes

Ti films by dc or rf sputtering + anodization + thermal treatment

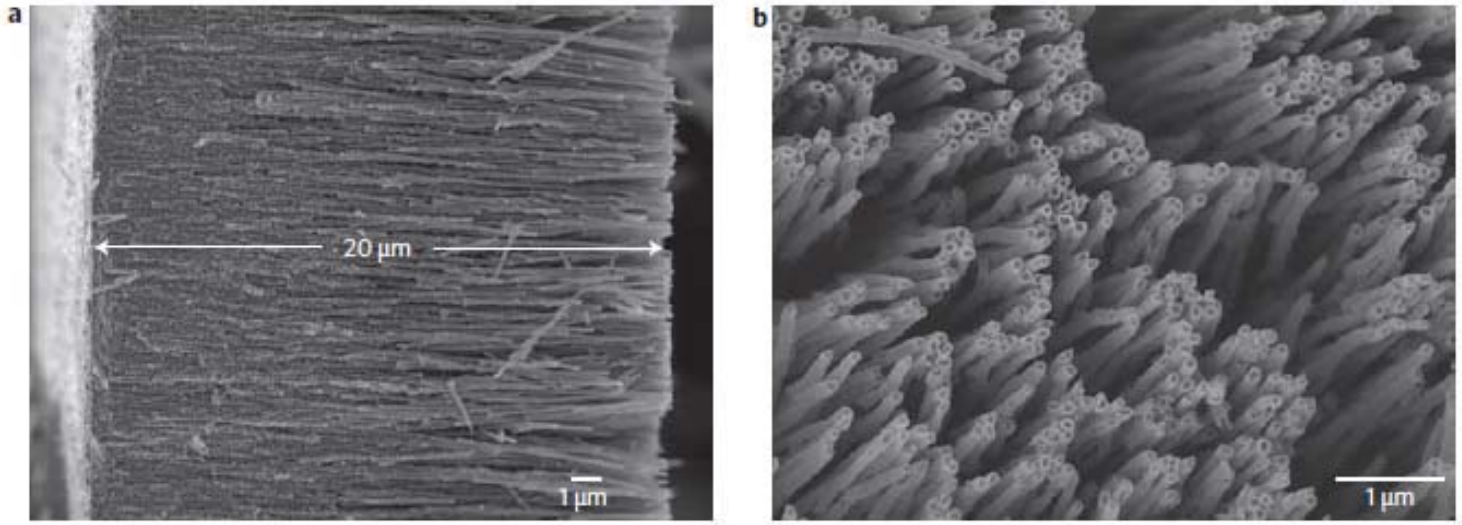

Efficiency up to 6.9%

N719 dye

O.K. Varghese et al., Nature Nanotech. 4, 592 (2009)

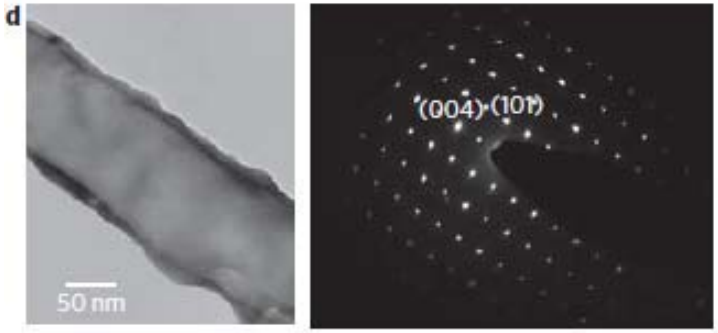

Also TiO_2 nanotubes/dye/P3HT/PEDOT:PSS
Efficiency > 3%
Mor et al., Nano Lett.9, 4251 (2009)

Advanced semiconductor photoanodes

ZnO nanorod arrays

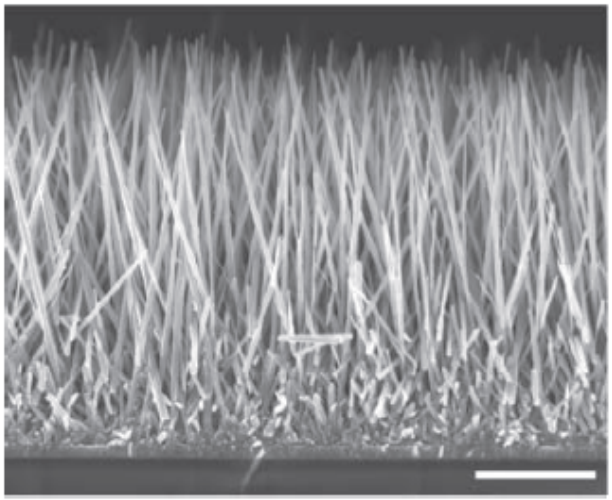

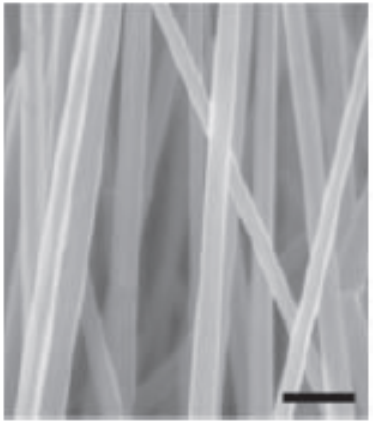

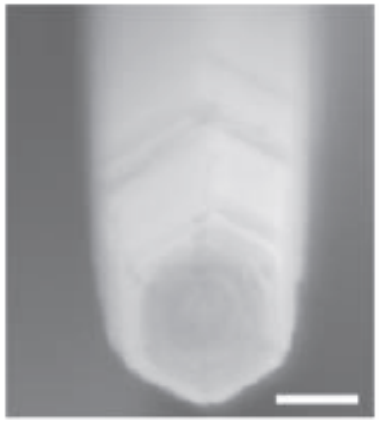

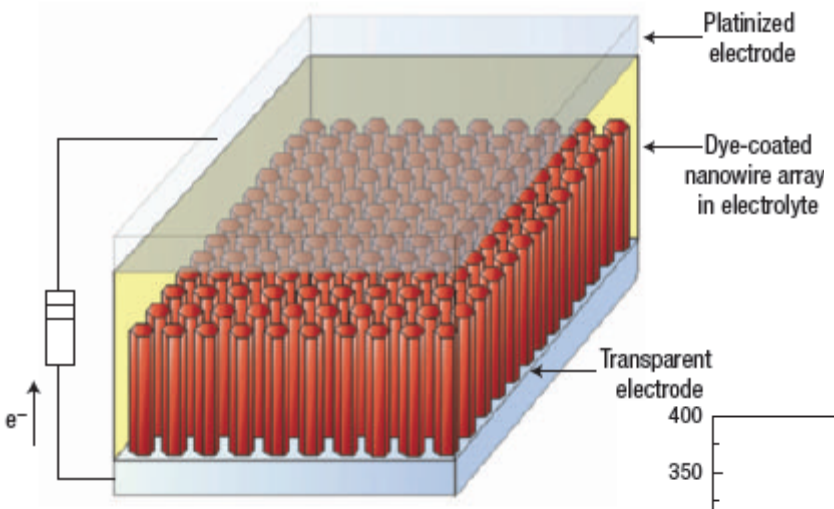

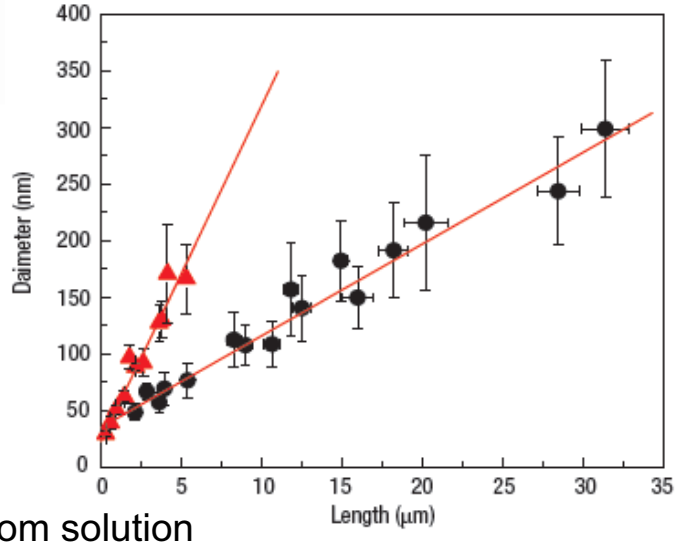

- QD-seeded growth from solution
- efficiency < 2%
- roughness factor < 200
- to enhance light absorption with reduced surface area, **need for organic HTM absorbing in visible**!

M. Law et al., *Nat. Mater.* **2005**, *4*, 455

Advanced semiconductor photoanodes

ALD (Atomic Layer Deposition) coating of templates

(e.g. anodic alumina oxide templates, or silica aerogel templates)

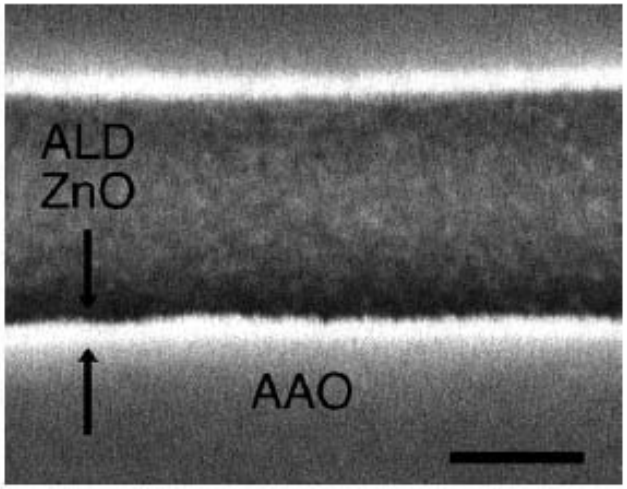

Fig. 6 Cross-sectional SEM image of ZnO tubes grown on commercial AAO *via* ALD (scale bar = 100 nm).

efficiency 1.6 %

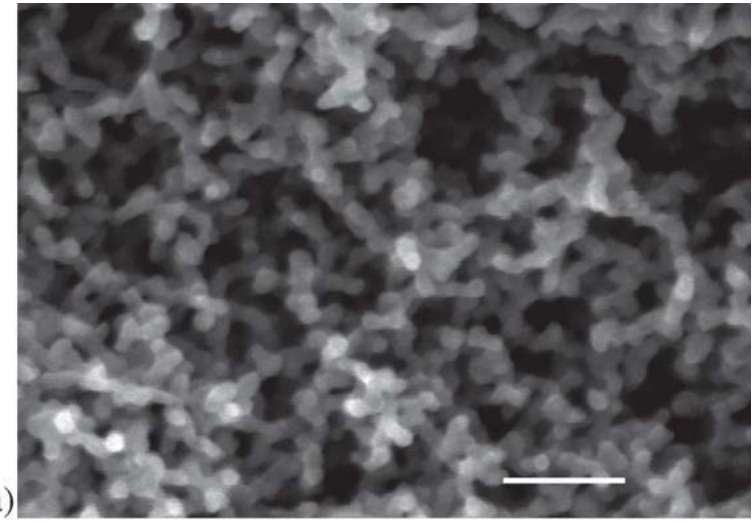

Pseudo-1D aerogel coated with TiO_2

efficiency > 5%

T.W. Hamann et al., Energy Environ. Sci., 2008, 1, 66–78

Advanced semiconductor photoanodes

ZnO nanostructures

see review by Q. Zhang et al., Adv. Mater. 2009, 21, 1–22

	ZnO	TiO_2
Crystal structure	rocksalt, zinc blende, and wurtzite	rutile, anatase, and brookite
Energy band gap [eV]	3.2–3.3	3.0–3.2
Electron mobility [$cm^2 V s^{-1}$]	205–300 (bulk ZnO), 1000 (single nanowire)	0.1–4
Refractive index	2.0	2.5
Electron effective mass [m_e]	0.26	9
Relative dielectric constant	8.5	170
Electron diffusion coefficient [$cm^2 s^{-1}$]	5.2 (bulk ZnO), 1.7×10^{-4} (nanoparticulate film)	0.5 (bulk TiO_2), $\approx 10^{-8}$–10^{-4} (nanoparticulate film)

TiO_2: V.B. from O 2*p* – Ti 3*d* hybridized orbitals, C.B. from Ti 3*d* orbitals

Decreased transition probability

ZnO: V.B. from *d* orbitals, C.B. from Zn *s*-*p* orbitals

ZnO: instability in acid dyes, formation of complexes with dyes

ZnO nanostructures

electrochemical deposition

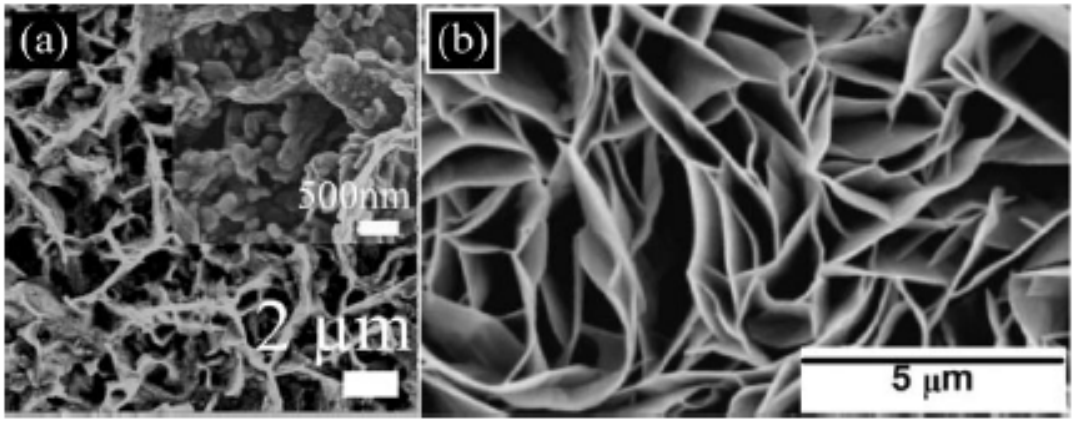

see review by Q. Zhang et al., Adv. Mater. 2009, 21, 1–22

Nanosheets, tetrapods, …
(electrodeposition, vapor deposition, hydrothermal growth…)

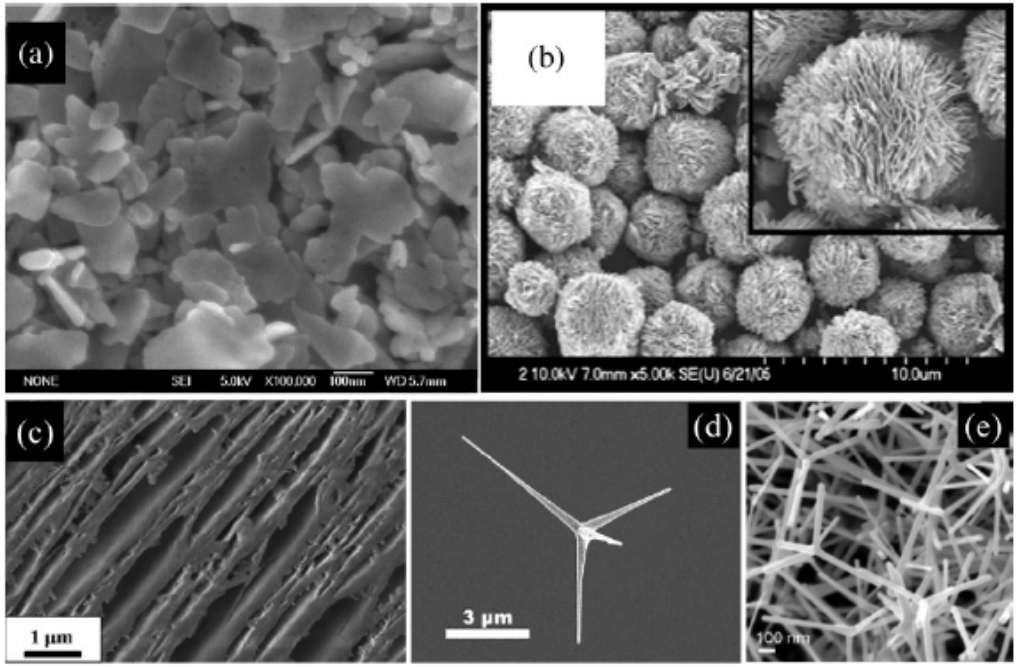

ZnO nanostructures

see review by Q. Zhang et al., Adv. Mater. 2009, 21, 1–22

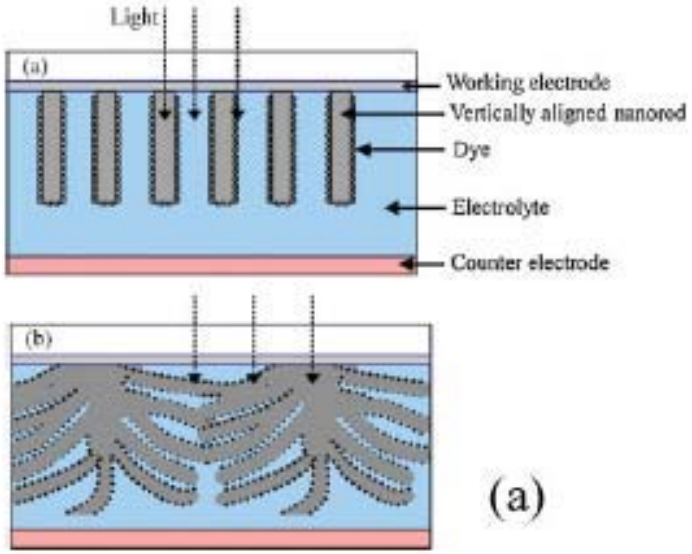

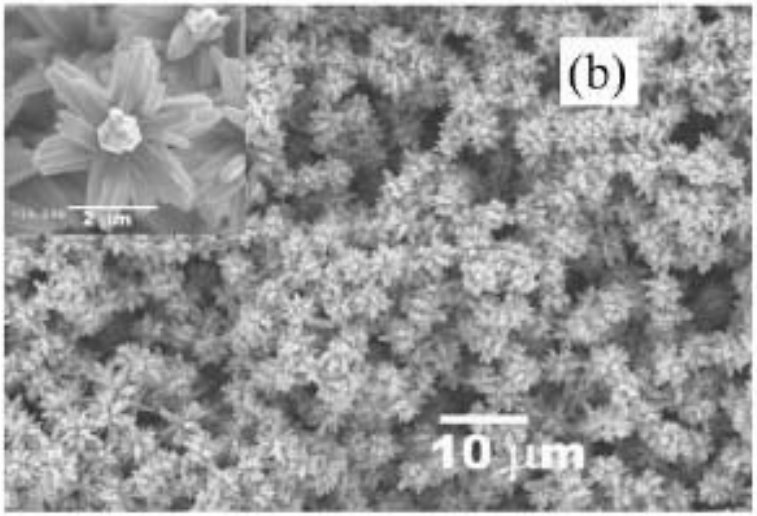

nanoflowers, hydrothermal growth

dendritic nanowires, MOCVD

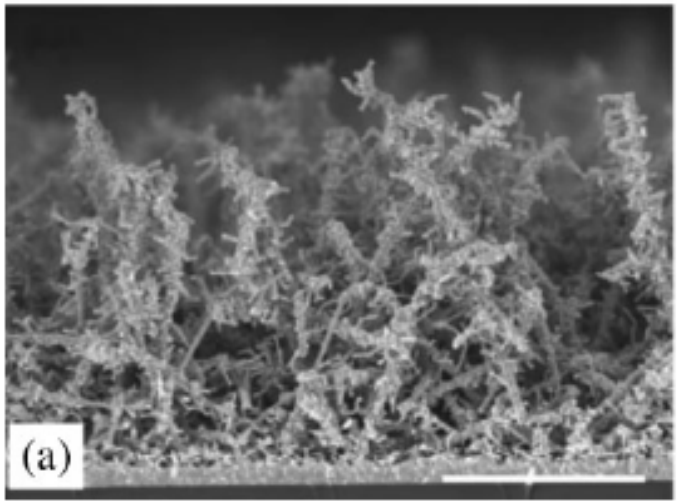

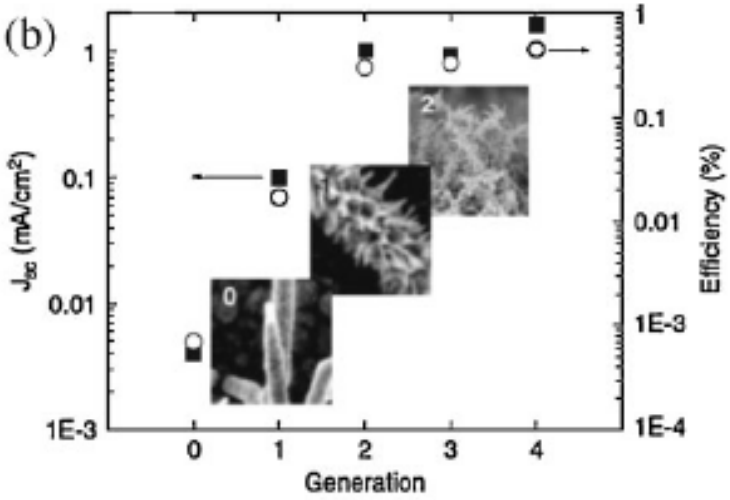

Hierarchical structures

Hierarchical structures:

see review by Q. Zhang et al., Adv. Mater. 2009, 21, 1–22

- increased surface area
- mesoporosity / light scattering enhancement

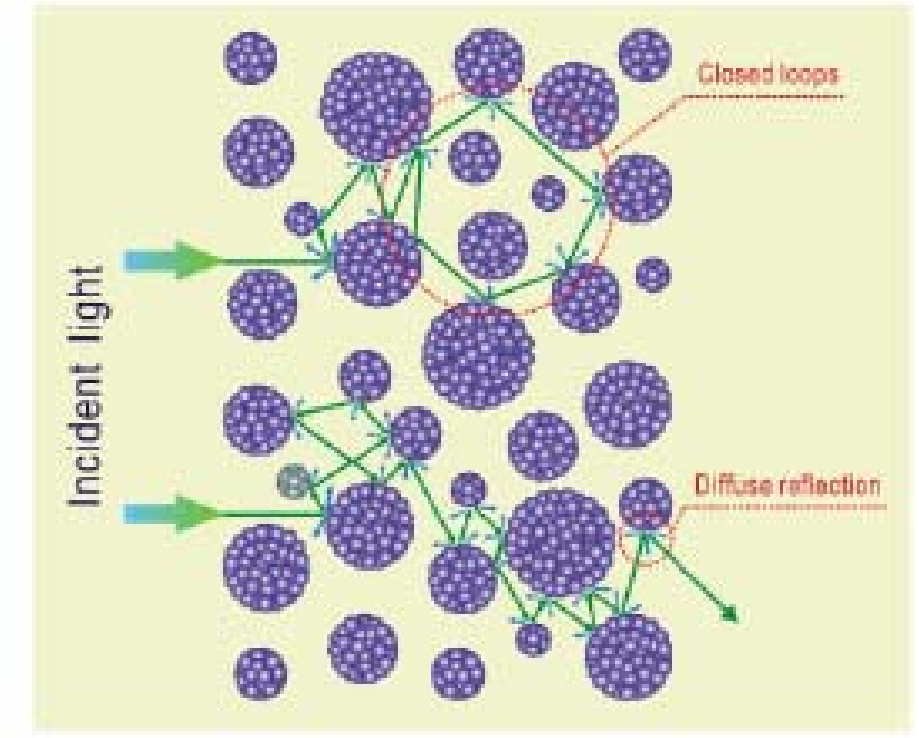

Hierarchical TiO_2 structures

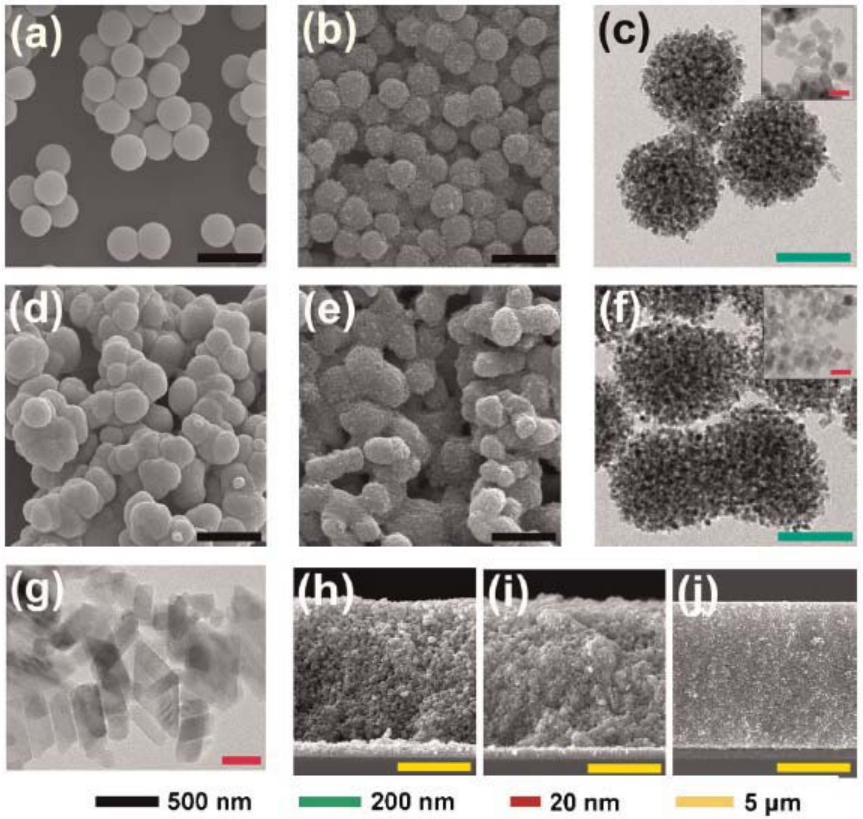

Figure 1. SEM images of the synthesized Sphere-1 a) before and b) after hydrothermal treatment at 240 °C, and Sphere-2d) before and e) after hydrothermal treatment at 240 °C. TEM images of c) Sphere-1, f) Sphere-2, and g) TiO_2 NPs. Cross-sectional SEM images for the nanoporous TiO_2 layers prepared from h) Sphere-1, i) Sphere-2, and j) TiO_2 NPs. TiO_2 layers were formed by doctor-blade method, and subsequently heat-treated at 500 °C for 15 min.

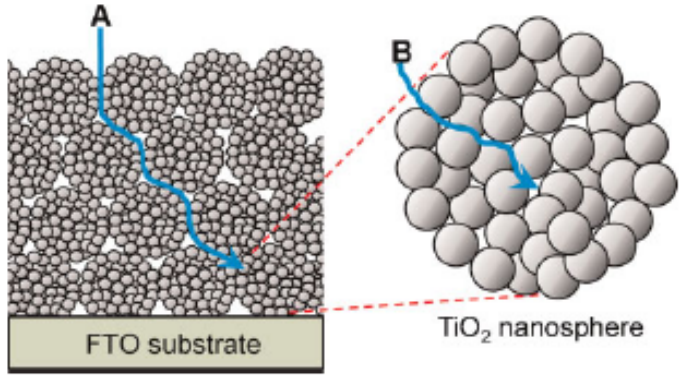

Scheme 1. Diagram for the electrolyte diffusion through the external (A) and internal (B) pores in the titania film fabricated from the nanoporous TiO_2 spheres.

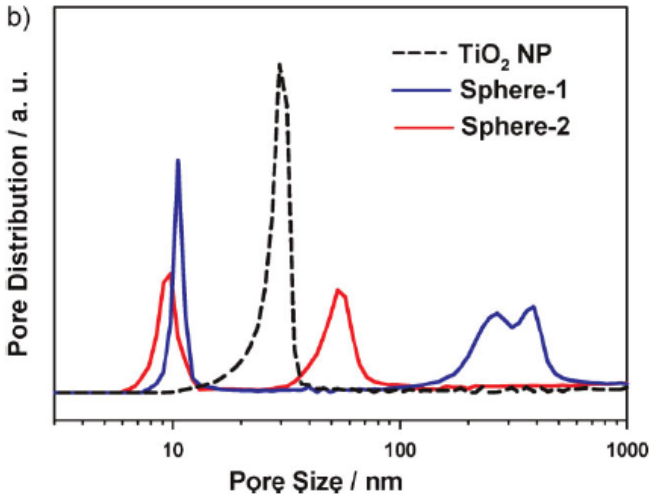

- hydrothermal treatment instead of calcination
- surface area > 100 m^2/g
- efficency > 8%

I.J. Kim et al., Adv. Mater. 2009, 21, 1–6

Hierarchical ZnO

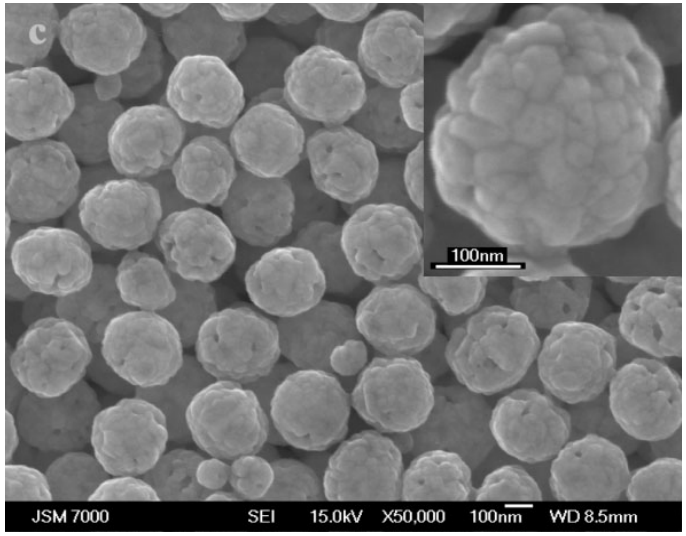

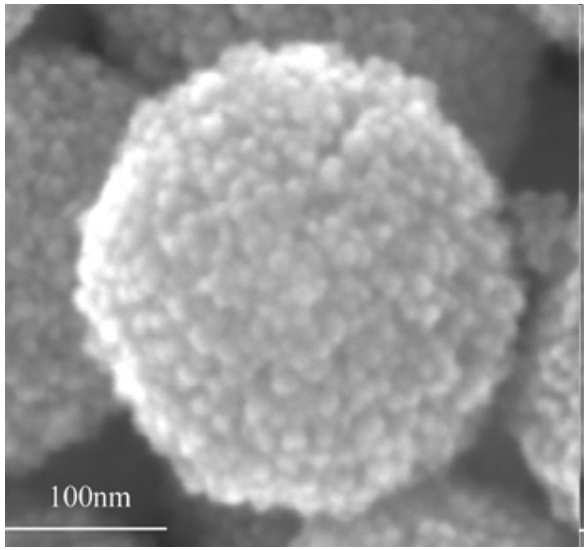

colloidal spheres

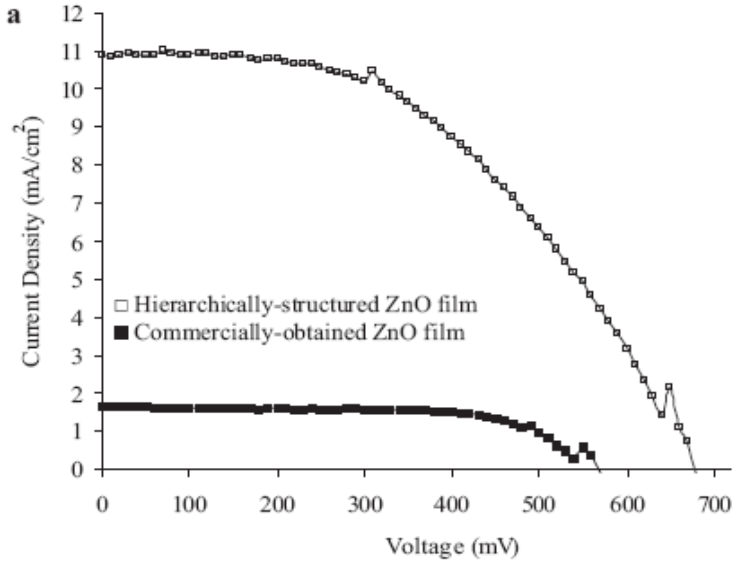

T. Chou, Q. Zhang, G.E. Fryxell, G. Cao
Adv. Mater. 2007, 19, 2588–2592

Advanced semiconductor photoanodes

Bicontinuous Double Gyroid Hybrid Solar Cell

from block copolymer templates

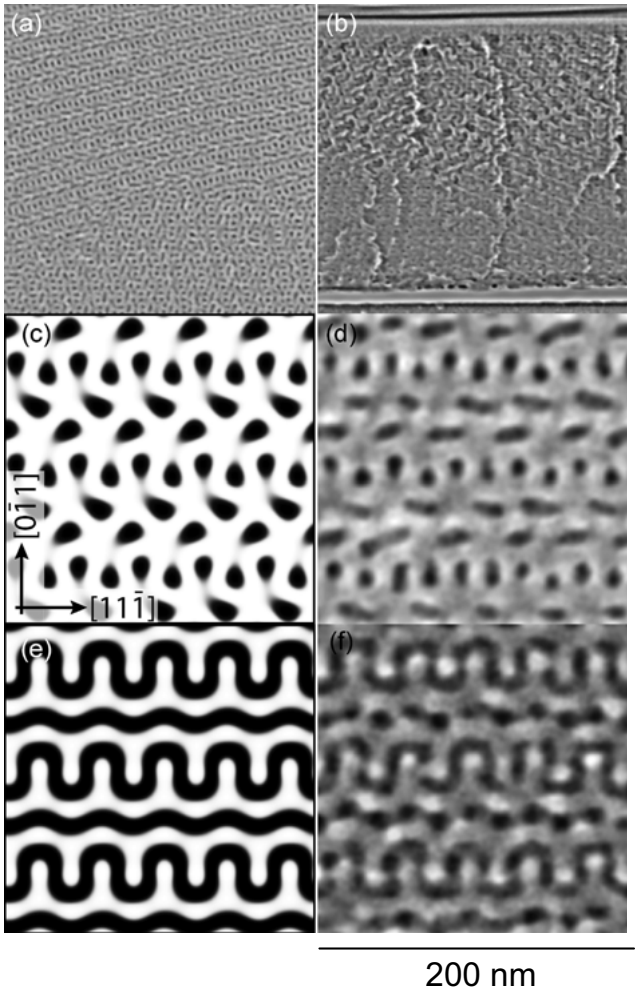

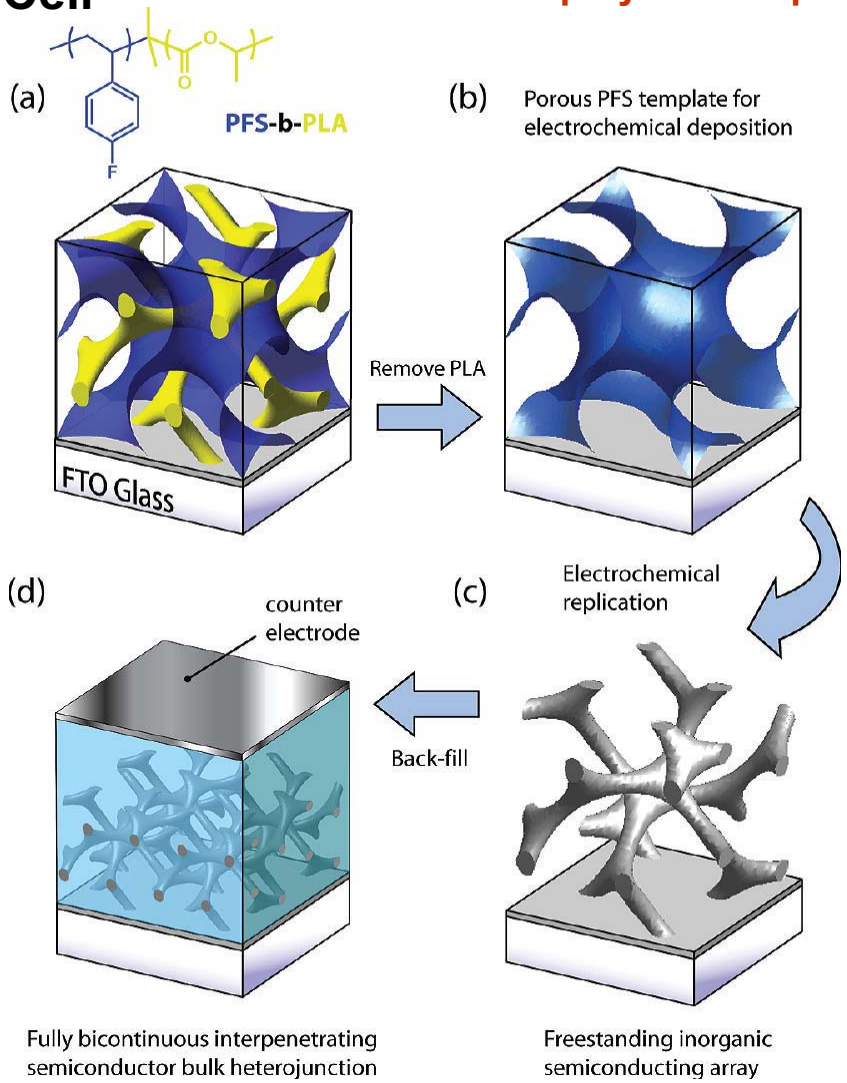

E.J.W. Crossland et al. (Snaith), Nano Letters 9, 2807 (2009)

Advanced semiconductor photoanodes

Bicontinuous Double Gyroid Hybrid Solar Cell

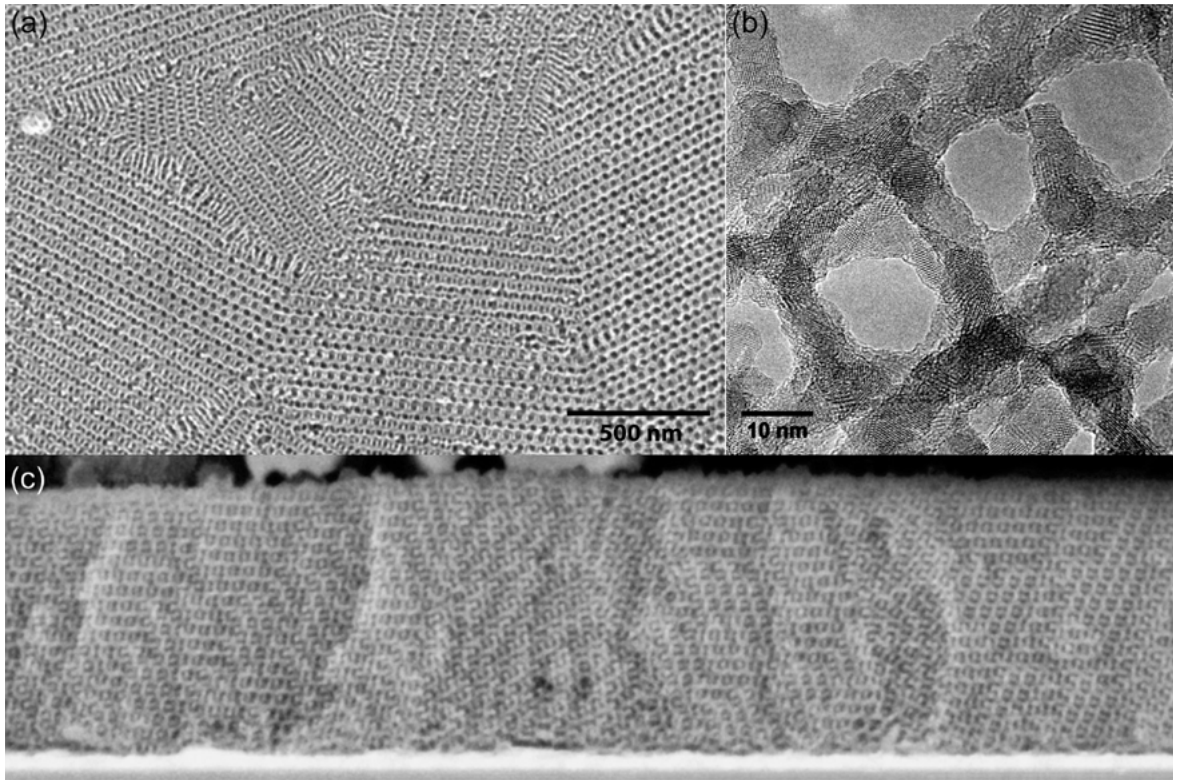

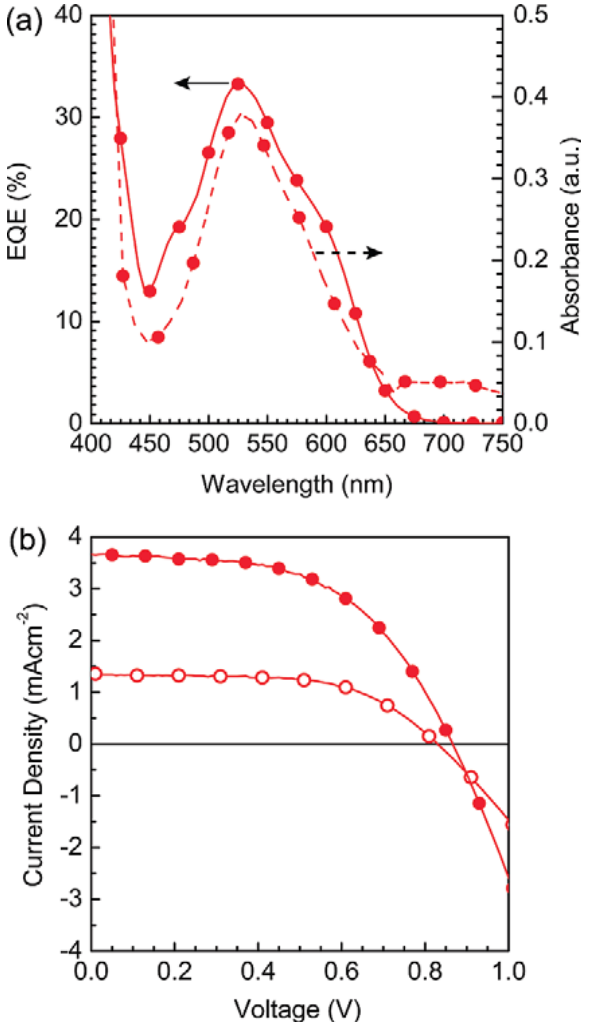

- anodic oxidative hydrolysis of aqueous $TiCl_4$ in electrochemical cell
- filled with spiro-MeOTAD
- efficiency 1.7% (comparable with nanoparticles, better than nanowires)

E.J.W. Crossland et al., Nano Letters 9, 2807 (2009)

Advanced semiconductor photoanodes

Core-shell nanoparticles

'blocking' layer for reduced recombination rate

Al_2O_3, ZrO_2, SiO_2, ZnO

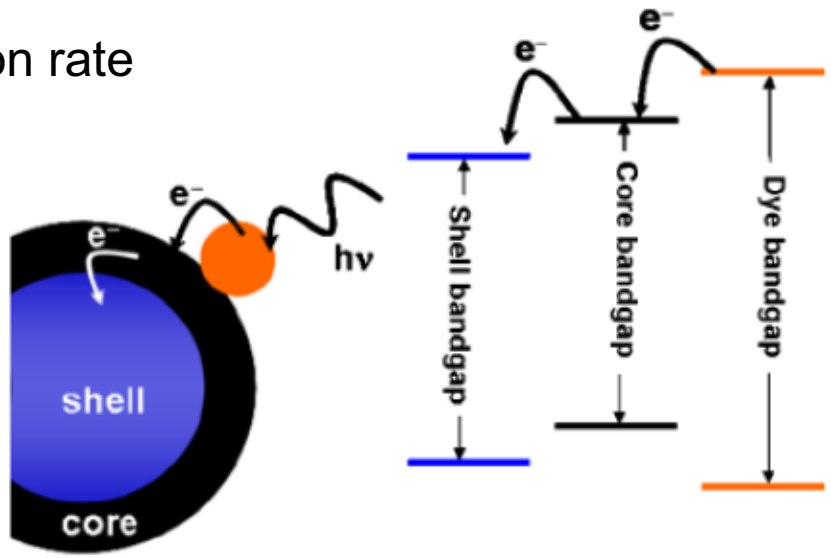

Fig. 7. Core/shell model and corresponding energy diagram. The shell induces potential barrier for electrons after injected into the core. This potential barrier prevent from electron to recombine with the electrolyte.

E. Palomares et al., J. Am. Ceram. Soc. 125, 475–82 (2003)

R. Jose et al., J. Am. Ceram. Soc. 92, 289–301 (2009)

Advanced semiconductor photoanodes

TiO_2-coated Multilayered SnO_2 Hollow Microspheres

- SnO_2 good conductivity but low dye absorption, fast recombination
- Chemical reaction from $SnCl_4$ + $TiCl_4$
- efficiency 5.6%

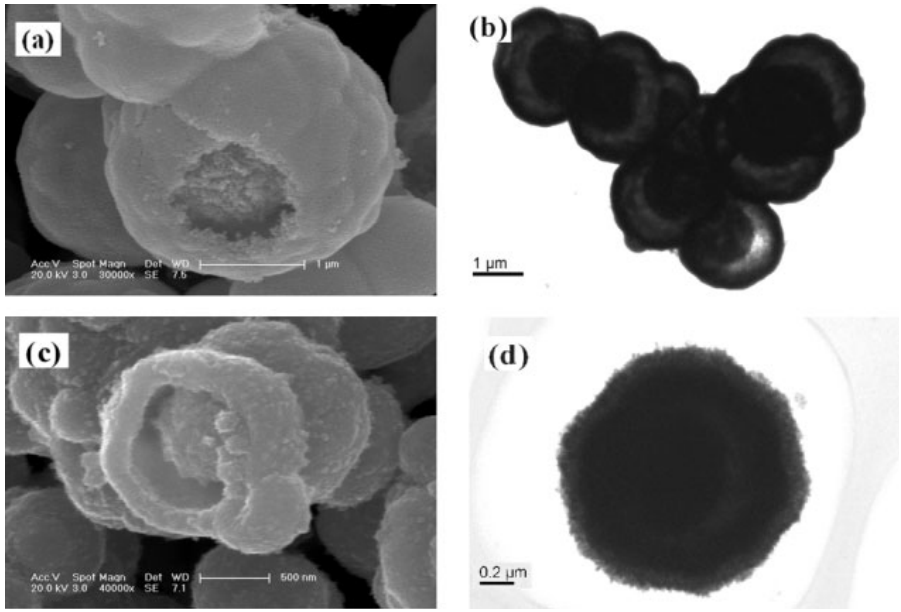

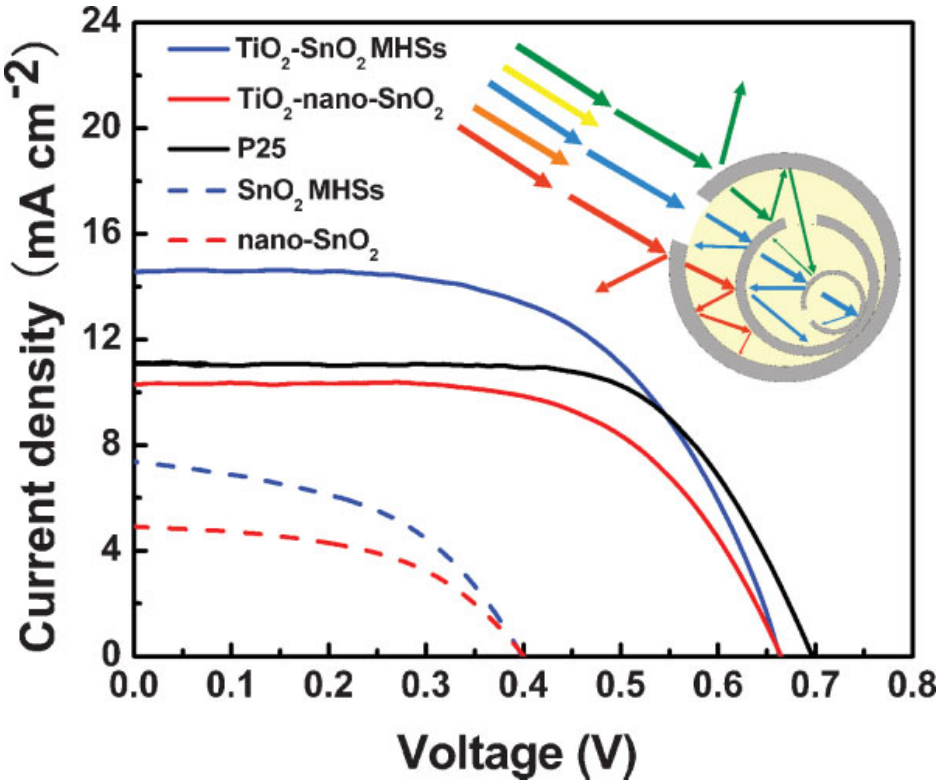

J. Qian et al., Adv. Mater. 2009, 21, 1–5

p-type oxides

NiO as p-type semiconductor:

PHOTOCATHODE

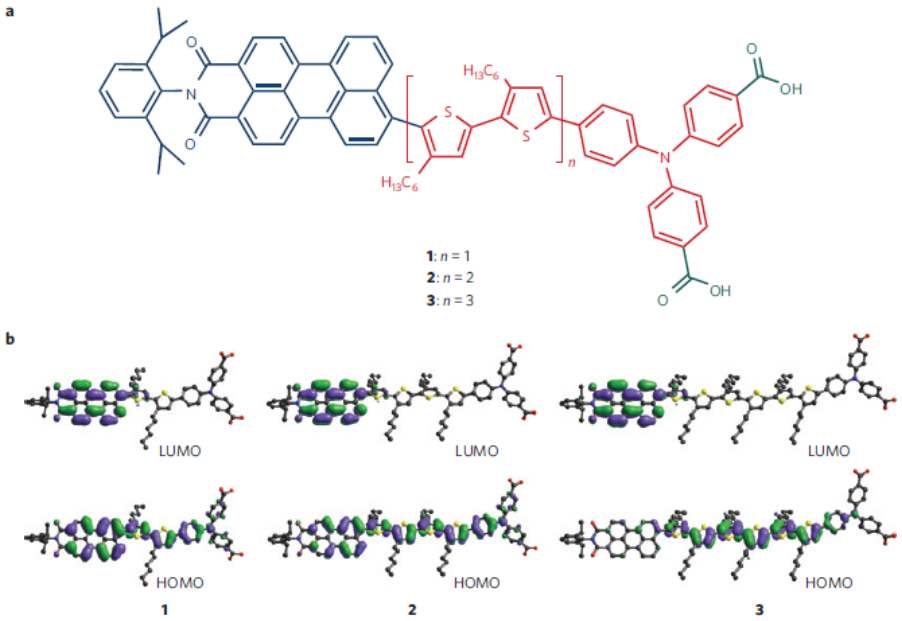

donor-acceptor dyes

Tandem cell

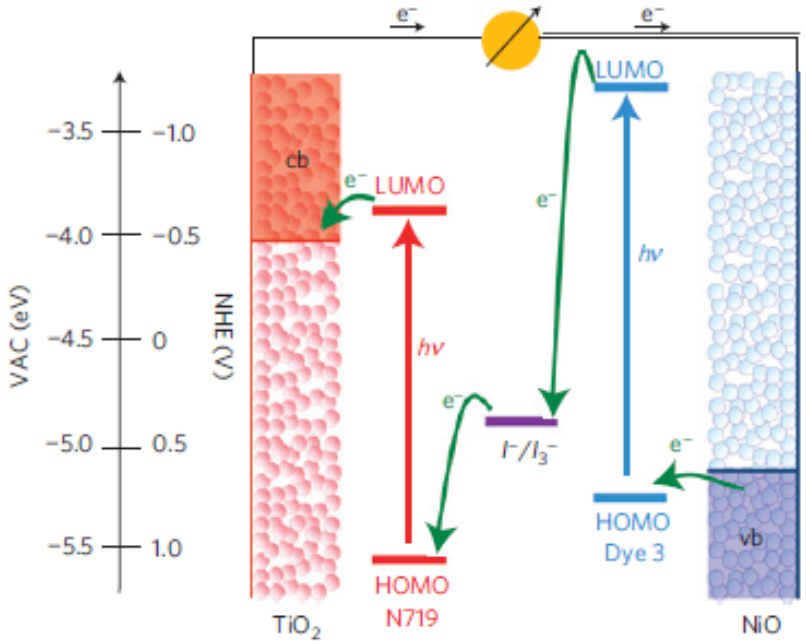

low efficiencies, max 1%

A. Nattestad et al., Nature Materials 2009

QD-based solar cells

see e.g. P.V. Kamat, *J. Phys. Chem. C*, **2008**, 112 (48), 18737-18753

Quantum dots in PV:

- **tunable band edge**, offers the possibility to harvest light energy over a wide range of visible-IR light with selectivity

- **hot carrier injection** from higher excited state (minimizing energy loss during thermalization of excited state)

- **multiple carrier generation** solar cells, utilization of high energy photon to multiple electron-hole pairs

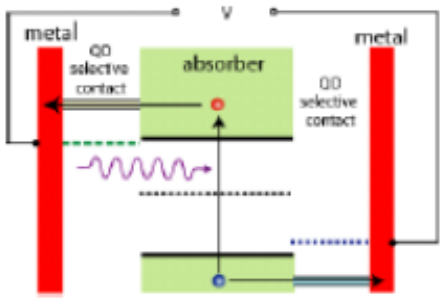

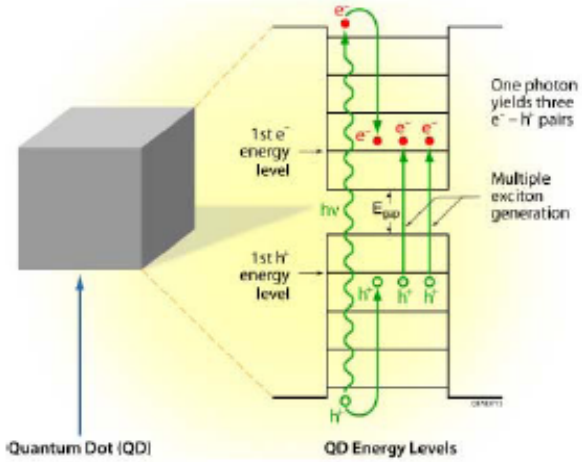

QD-sensitized solar cells

Polymer-s.c. nanocrystal/QD hybrids…

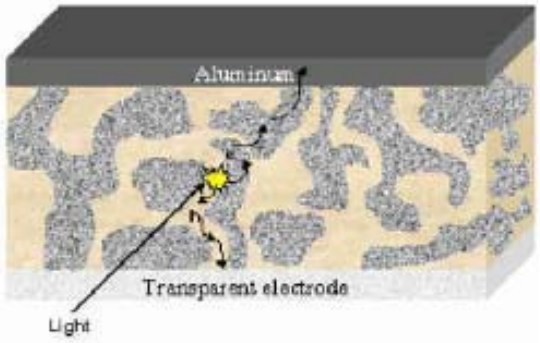

Adv. Mater. 2004, 16, 1009 (2004)

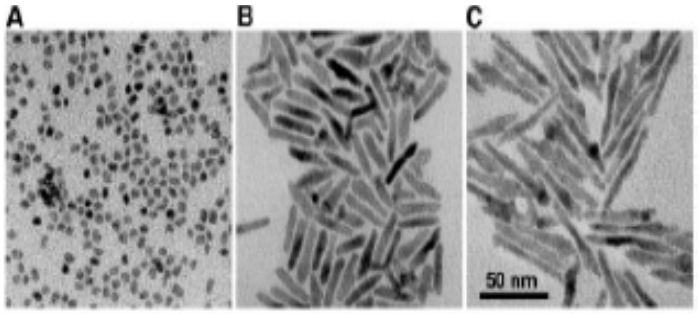

Science 295, 2425 (2002)

QDSSC

advantage of QD over conventional dyes as sensitisers is their very high extinction coefficients

→ thinner films of the mesoporous oxide can be used

→ reduce dark current, increase V_{OC} and efficiency

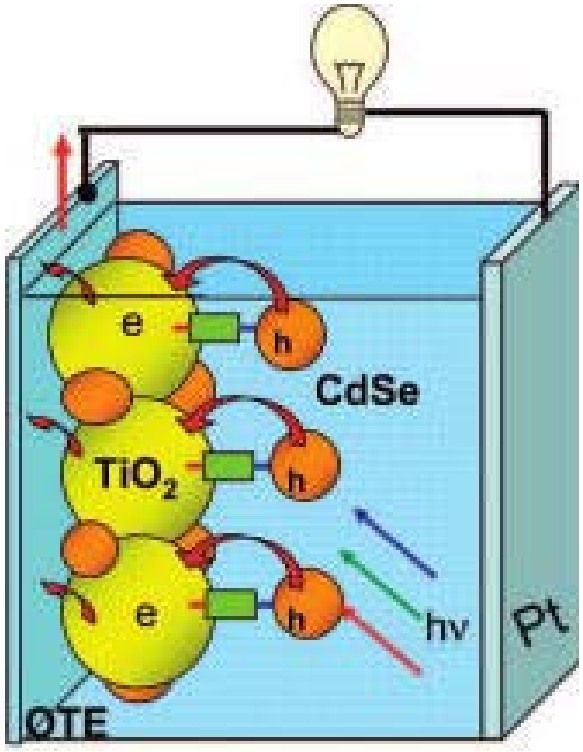

QD-sensitized solar cells

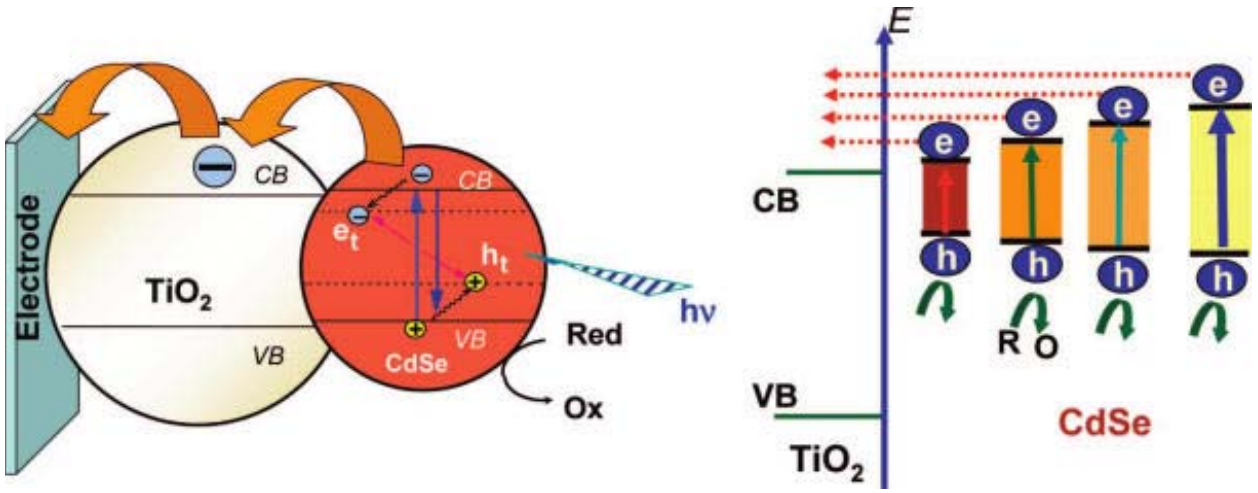

Modulation of the charge injection process by controlling the particle size?

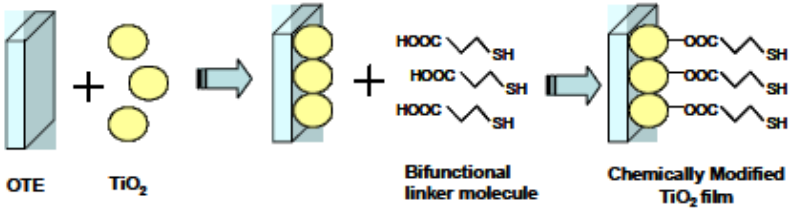

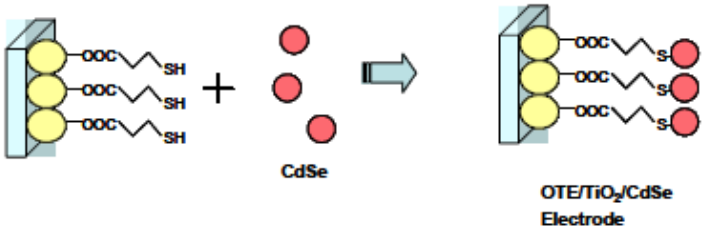

see e.g. P.V. Kamat, *J. Phys. Chem. C*, **2008**, 112 (48), 18737-18753

linking to TiO_2

J. Am. Chem. Soc. 2006,128, 2385-2393

QD-sensitized solar cells

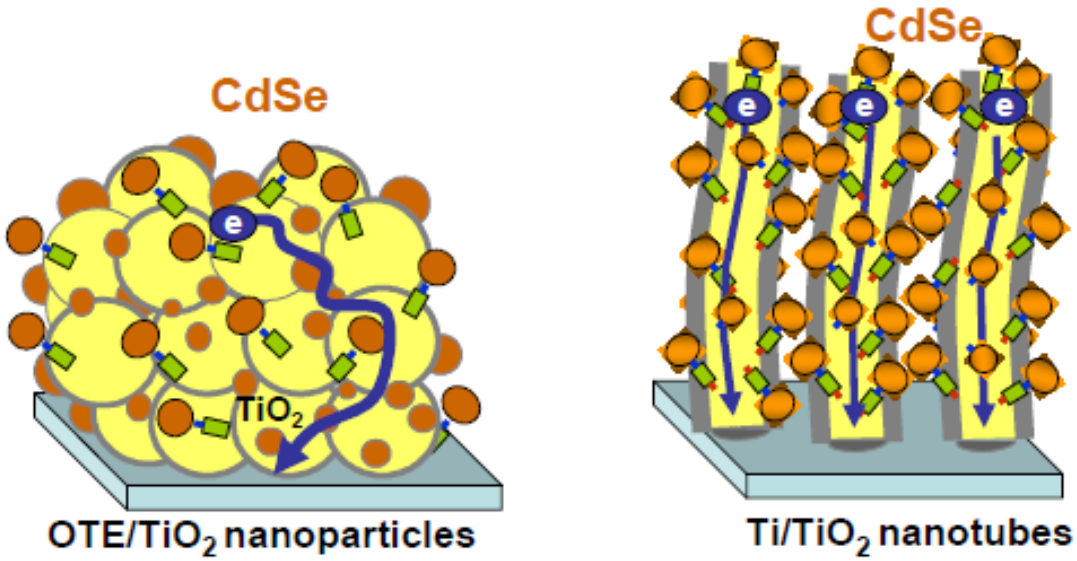

e.g. PbS, CdS, CdSe – sensitized solar cells

H.J. Lee et al., Langmuir 25, 7602 (2009)
H.J. Lee et al., Nano Lett. 9, 4221 (2009)

efficiency limited by surface area

QD surface decoration:

colloidal dispersion, chemical bath deposition, SILAR ('successive ionic layer adsorption and reaction') method

e.g. with polysulphide or Co-based electrolyte (QD corrosion problems)

Hybrid polymer / s.c. cells

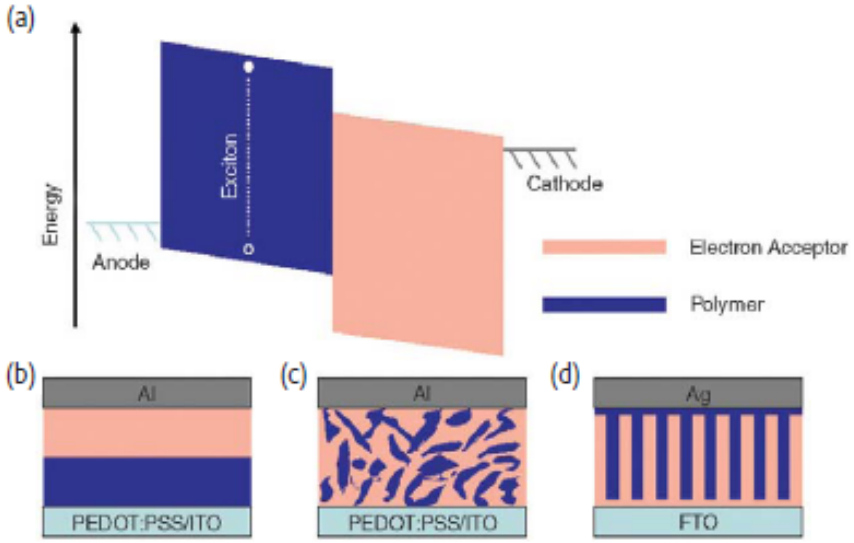

Similar to bulk heterojunction (BHJ), but electron-acceptor material replaced by a nanostructured n-type inorganic semiconductor (e.g. TiO_2, ZnO)

[W.U. Huynh et al., Science 295, 2425 (2002), K.M. Coakley and M.D. McGehee, Appl. Phys. Lett. 83, 3380 (2003), A.C. Mayer et al., Mater. Today 10 (11), 28 (2007), M.D. McGehee, MRS Bull. 34, 95 (2009)]

- problem of optimal infiltration of the polymer in the nano/mesostructured porosity of the oxide

[G.P. Bartholomew and A.J. Heeger, Adv. Funct. Mater 15, 677 (2005), K. M. Coakley and M. D. McGehee, Chem. Mater. 16, 4533 (2004), K.M. Coakley et al., Adv. Funct. Mater. 13, 301 (2003)]

- alternative architecture: ordered heterojunction with hole-transporting polymeric film infiltrated into a mesoporous ordered architecture or a nanowire/nanorod array of an *n*-type inorganic semiconductor, e.g. TiO_2

[G.K. Mor et al., Appl. Phys. Lett. 91, 152111 (2007), K. Shankar et al., Langmuir 23, 12445 (2007)].

Hierarchical mesoporous TiO_2 photoanode by Pulsed Laser Deposition (PLD)

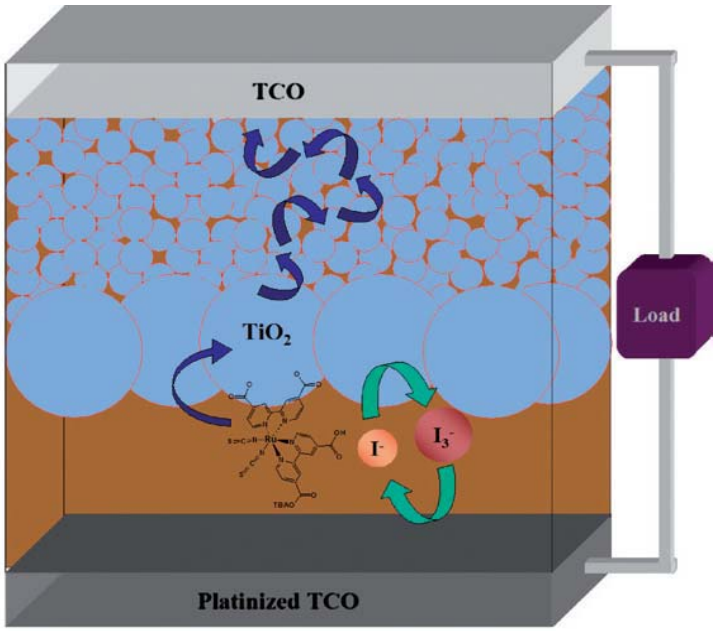

Hamann, Energy Environ. Sci., 2008, 1, 66–78 | 67

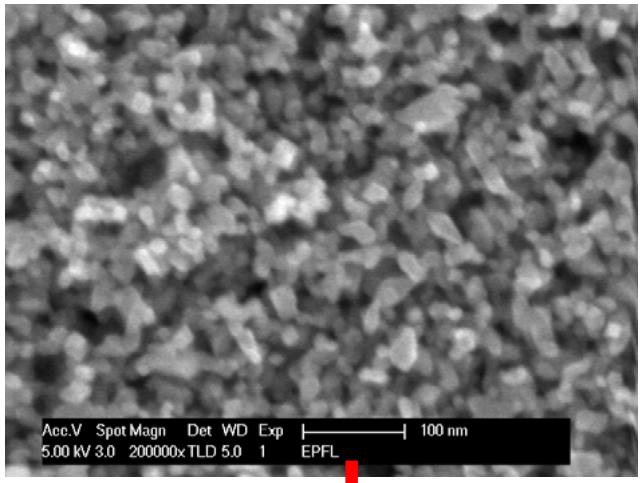

s-TiO_2

From isotropic to anisotropic photoanode

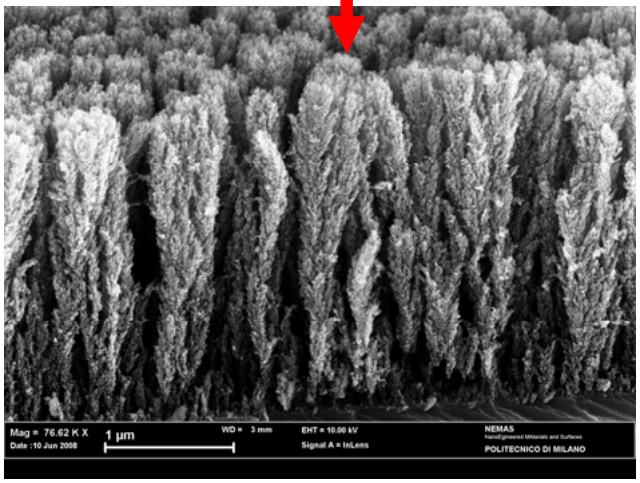

h-TiO_2

Some of the issues:

- Efficient electron transport
- High surface area
- Light trapping/harvesting
- Efficient mass transport for ILE
- Solid State DSC (polymer infiltration)

Pulsed Laser Deposition (PLD)

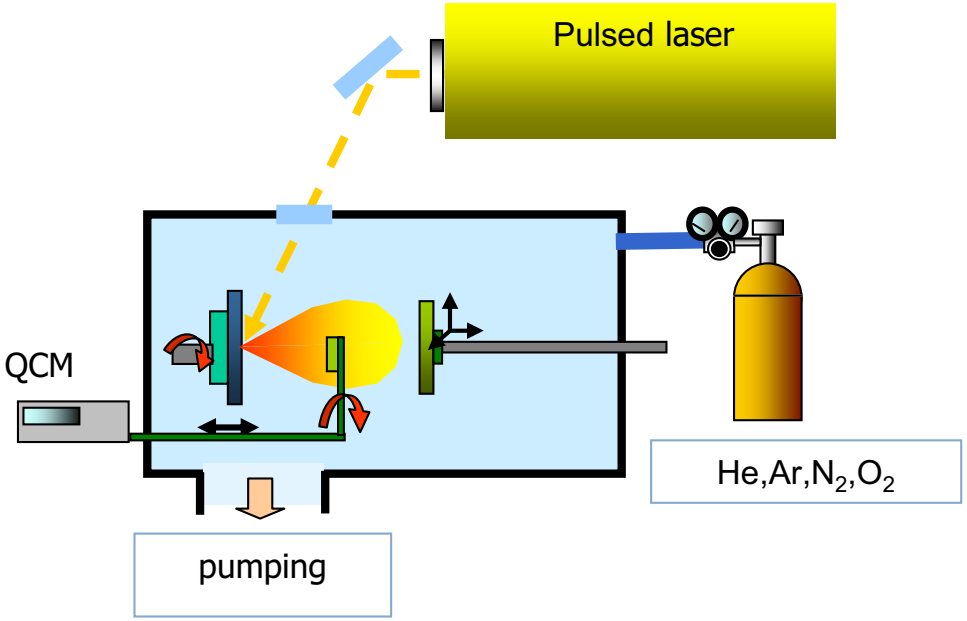

- Laser pulse (10 ns, 200 mJ)
- Target ablation
- Ablation plume expansion
- Deposition

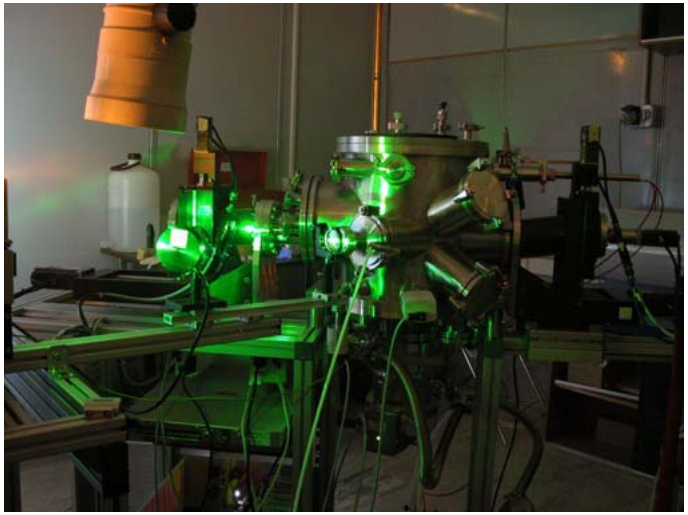

Control of:

- nanoscale/mesoscale morphology
- crystalline structure
- chemistry

Pulsed Laser Deposition (PLD)

Increasing background pressure

Vacuum

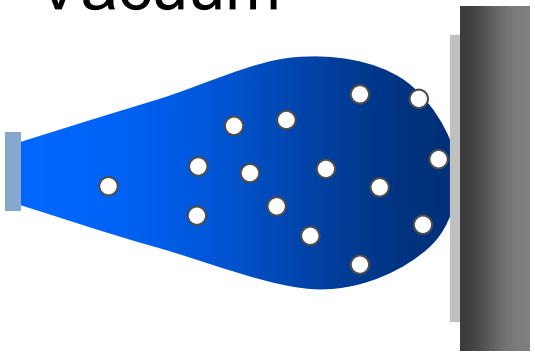

- High kinetic energy
- Atom by atom deposition

Inert gas

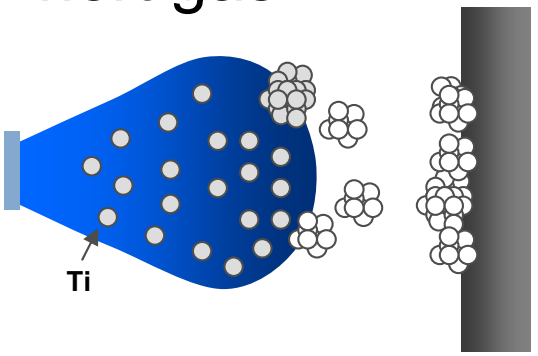

- Plume confinement
- Increasing collision rate
- Decreasing kinetic energy

Reactive gas

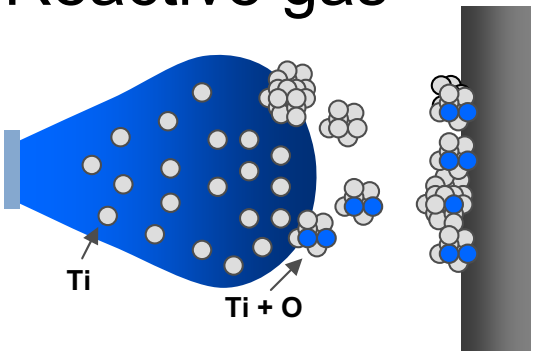

- Chemical reactions

TiO_2 - Tuning film mesostructure and density

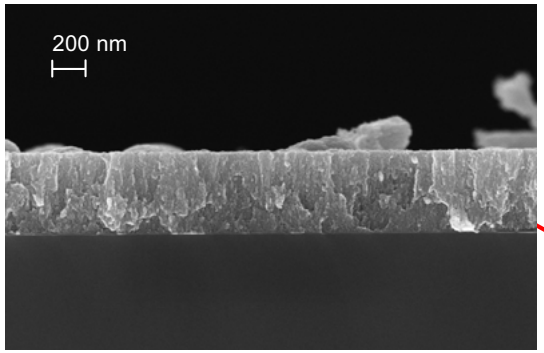

L<1: compact

Film density: 0.3 - 2.7 g/cm^3

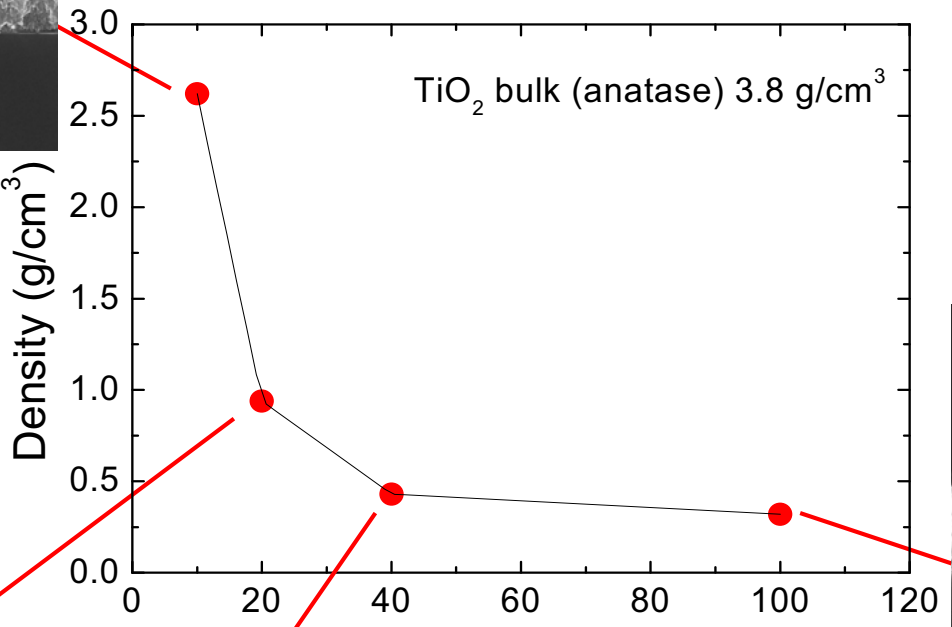

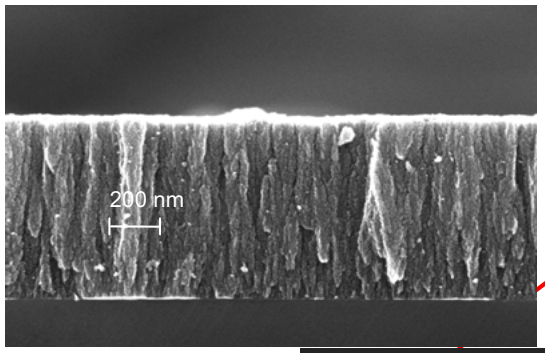

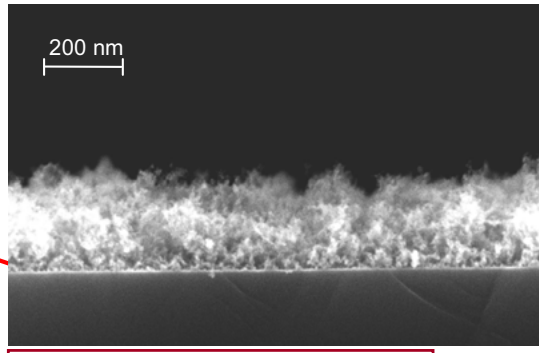

L>1: sponge-like

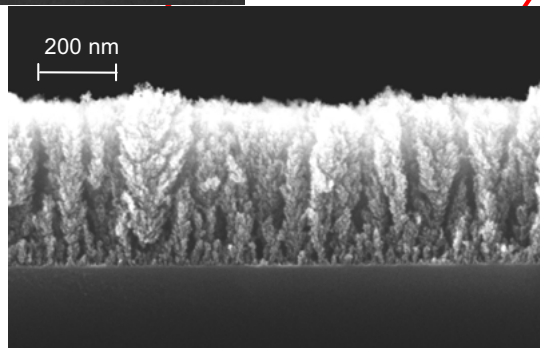

L≈1: columnar/hierarchical

TiO_2 - Tuning film nanostructure and density

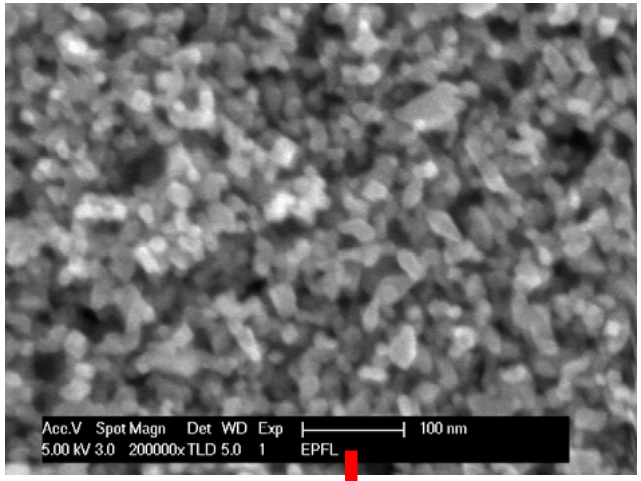

From isotropic to anisotropic photoanode

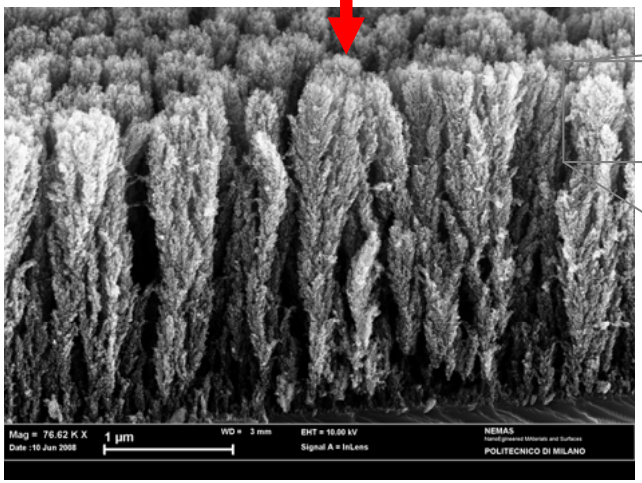

np - TiO_2

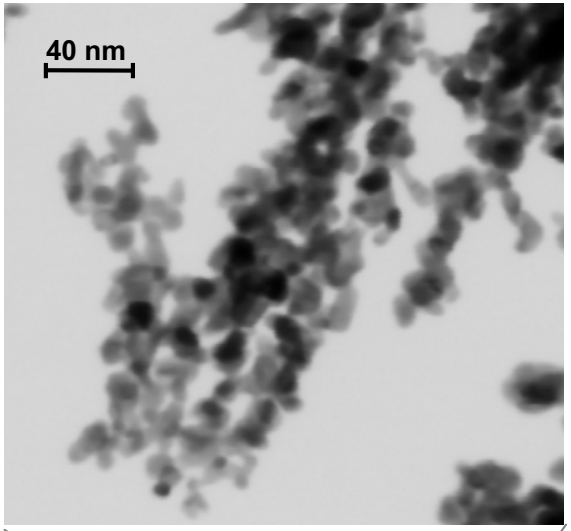

porosity 60-80%
surface area 40-100 m^2/g

Hierarchical TiO_2

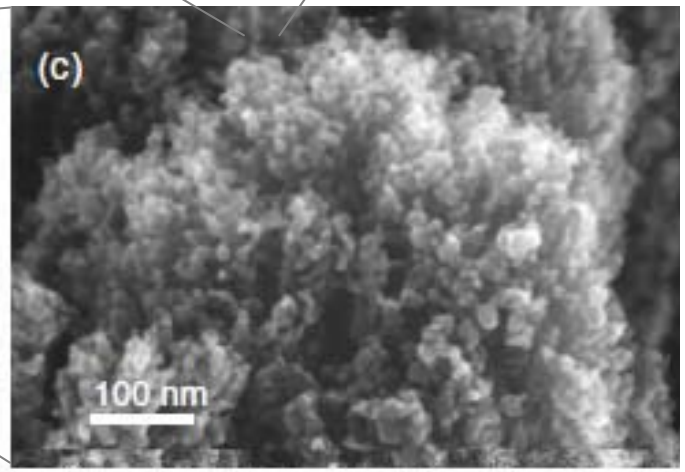

Tuning film crystalline structure

Annealing in air at 400 °C

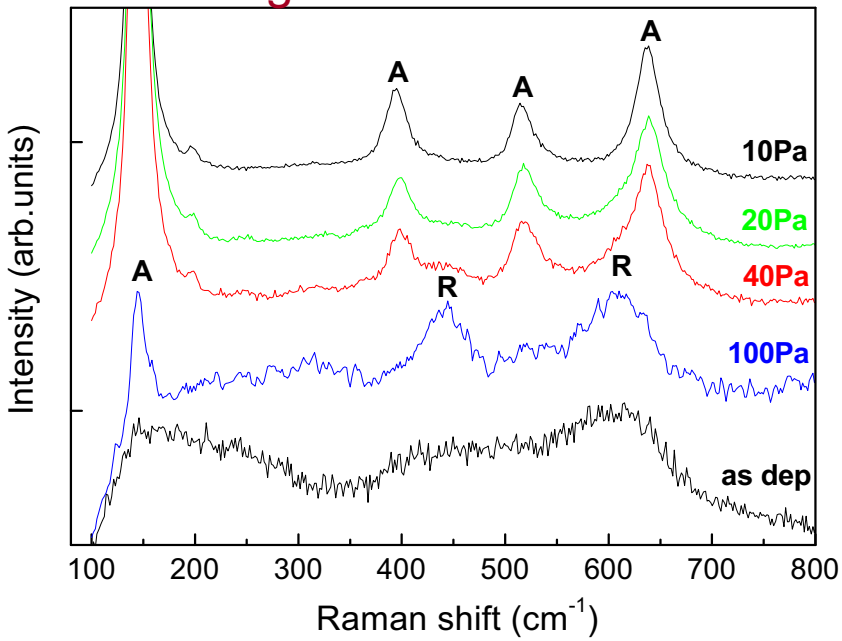

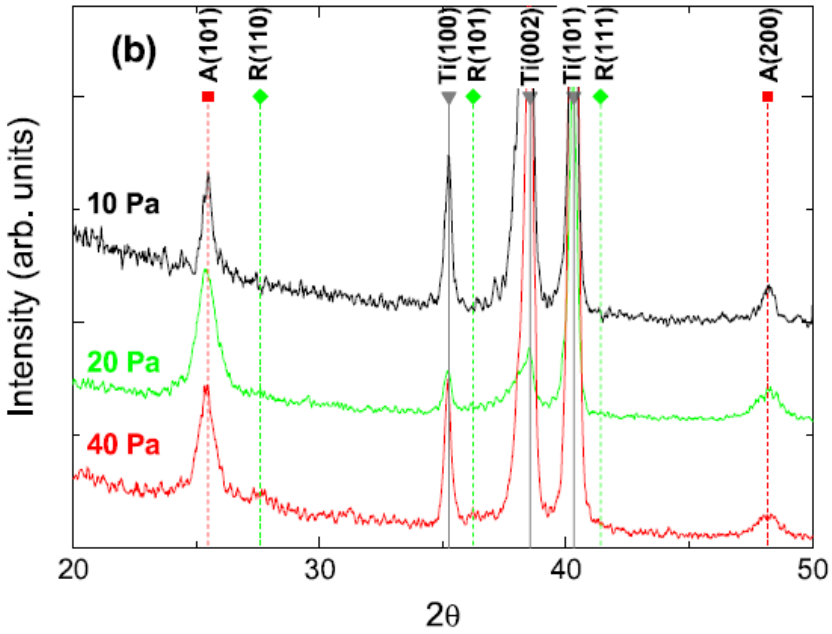

	A/R content	Anatase grain size	Rutile grain size
10 Pa	100%	~20 nm	-
20 Pa	90%	~10 nm	-
40 Pa	87%	~10 nm	~6 nm
100Pa	22%	-	-

- different anatase/rutile content
- reduced grain growth

F. Di Fonzo et al. Nanotechnology **20**, 015604 (2009)

Nanostructured TiO_2 for DSSC

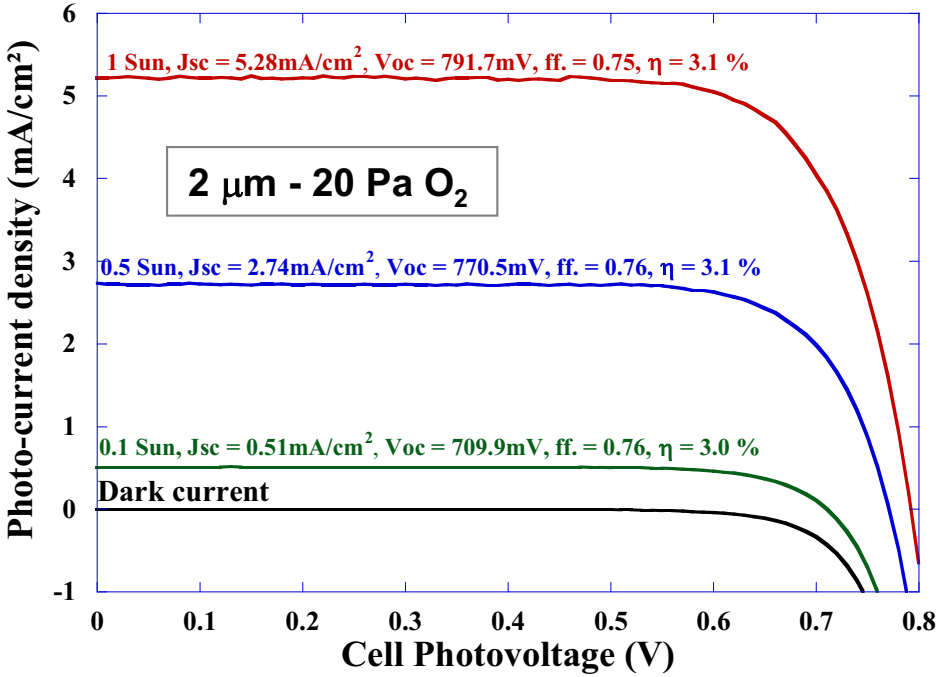

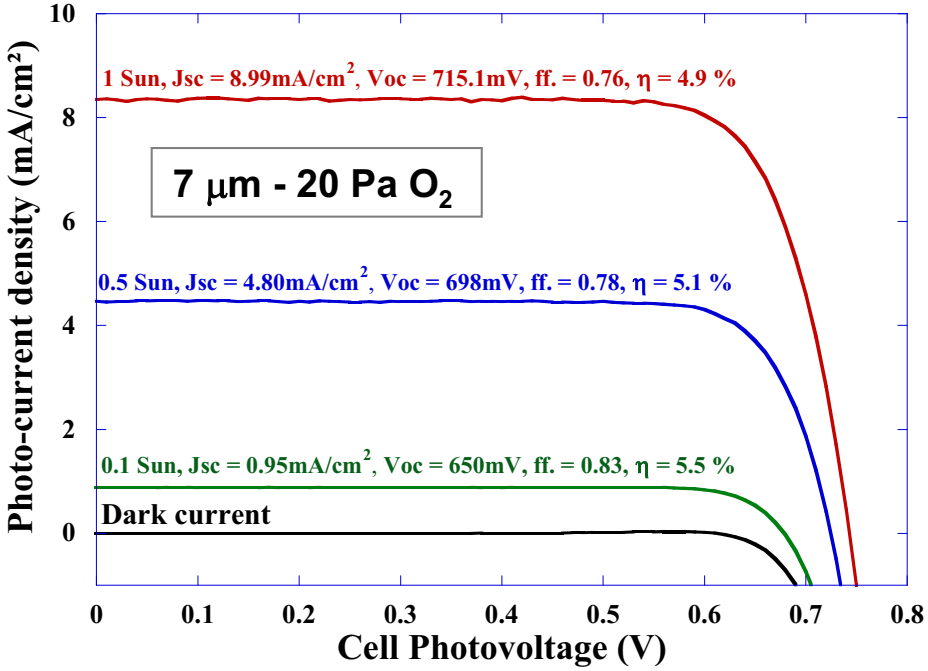

Efficiency up to 5% with C101 dye
(high extinction coefficient)

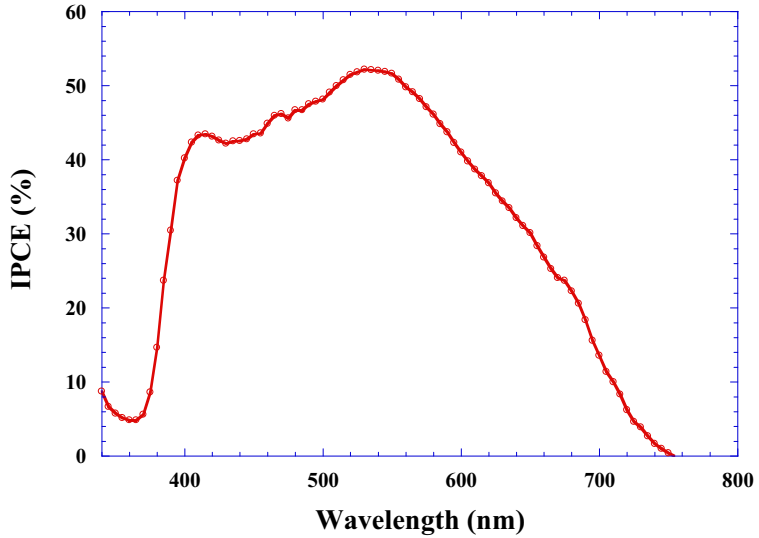

Useful reviews:

• M. Graetzel and J.R. Durrant, 'Dye-sensitized mesoscopic solar cells', in 'Nanostructured and photoelectrochemical systems for solar photon conversion', ed. M.D. Archer, A.J. Nozik, World Scientific, 2008

• M. Graetzel, MRS Bull 30, 23 (2005)

• M. Graetzel, Nature 414, 339 (2001)

• M. Graetzel, Journal of Photochemistry and Photobiology C: Photochemistry Reviews 4, 145 (2003)

• K. Hara and H. Arakawa, 'Dye-sensitized solar cells', in Handbook of Photovoltaic Science and Engineering, A. Luque and S. Hegedus ed., Wiley 2003

• H.J. Snaith and L. Schmidt-Mende, Adv. Mater. *19*, 3187 (2007)

• R. Jose et al., J. Am. Ceram. Soc. 92, 289 (2009)

• A.B.F. Martinson et al., Chem. Eur. J. 14, 4458 (2008)

• S. Gunes and N.S. Sariciftci, Inorganica Chimica Acta 361, 581 (2008)

• T.W. Hamann et al., Energy & Environ Sci. 1, 66 (2008)

• P.V. Kamat, J. Phys. Chem. C 112, 18737 (2008)